SOME USES OF POROUS NICKEL IN BIOTECHNOLOGY

by

MARCO FABIO CARDOSI

A dissertation submitted to the University of London in candidature for the degree of Doctor of Philosophy.

JULY 1984

Department of Bichemistry
Imperial College
University of London
London SW7 2AZ

ABSTRACT

M.F.Cardosi.

SOME USES OF POROUS NICKEL IN BIOTECHNOLOGY.

The work described in this dissertation was carried out in order to investigate the possibilities of using porous nickel, a sintered nickel preparation manufactured by INCO, both as an insoluble support to which enzymes could be covalently bound and as the base sensor in an amperometric enzyme electrode.

In the former case, techniques based around cyanuric chloride chemistry were developed by which enzymes were covalently attached to the support. This involved forming a stable oxide film on the surface of the porous nickel and then derivitizing the Ni/NiO phase with cyanuric chloride. The derivitized surface was characterized by Infra Red spectroscopy.

Three enzymes were successfuly immobilized to the porous nickel by this technique. Each was characterized in terms of its apparent kinetics and stability towards pH, temperature and storage.

In the latter case, it was found that shiny nickel was unsuitable as an electrode material. Consequently, the nickel was modified with the $Fe(CN)_6^{4-/3-}$ redox couple. The basis of this modification was a precipitation followed by a surface adsorption of the insoluble salt.

Direct electron transfer between the modified electrode and the redox site of glucose oxidase (FAD) was not observed. A mediated electron transfer however was achieved, using ferrocenes as the mediator.

The oxidation of the ferrocene at the modified electrode was investigated and a model was developed to explain the findings.

Working electrodes incorporating porous nickel were

constructed and used in the electrochemical experiments. Much larger steady state currents were recorded using these electrodes than with the bulk metal ones.

PREFACE

I should like to take this opportunity to thank my supervisor, Professor Brian Hartley, for his help in the form of encouragement, support and seemingly unshakeable optimism. I also wish to thank Dr. Minnie Rangarajan for introducting me to the delights of protein chemistry and for invaluable guidance and advice when the project was first initiated.

Thanks are also due to:

Mr. Richard Sweeny for his assistance with the XRD work.

Mr. Richard Chater for his help with the I.R. analysis.

Mr. Stephen Wiles for his rapid manufacture of the working electrode, and for coping patiently with my constant design changes.

Mr. Glyn Millhouse for an excellent photographic service.

Miss Deanne Eastwood for her patience and for a rapid and accurate typing of this dissertation.

Mr. Jim Brannigan for the proof reading.

I would also like to express particular thanks to Dr. A.G. Cass for his helpful advice, useful discussions and for teaching me the current techniques in electrochemistry and for outlining their potential as tools in biochemistry.

Finally, I would like to express my deepest thanks to my parents and my fiancee for their continuous support, encouragement and great patience.

TO OONAGH

Abbreviations

Most are standard, but attention is drawn to the following:-

Å	Angstrom
ATP	Adenosine triphosphate
BSA	Bovine serum albumin
Cp	Cyclopentane
DHE	Dynamic hydrogen electrode
EDTA	Ethylene diamine tetracetic acid
FAD	Flavin adenine dinucleotide
G°	Standard Gibbs free energy
G°	Standard Gibbs free energy
i_{ss}	Steady state current
j	Current flux
J.C.P.D.S.	Journal of Chemical Powder Diffraction Spectra
K_m	Michaelis constant
NAD^+	Nicotinamide adenine dinucleotide
NADH	Nicotinamide adenine dinucleotide reduced form
OD_n	Optical density at wavelength n
PMSF	phenylmethane sulphonyl fluoride
RDH	Ribitol dehydrogenase
SCE	Saturated calomel electrode
SDS	Sodium dodecyl sulphate
SEM	Scanning electron microscopy
TEMED	N,N,N',N' tetramethyl-ethylene-diamine
Tris	Tris (hydroxy-methyl) amino methane
UV	Ultra-violet
XRD	X-ray diffraction

V_{max}	Maximum specific velocity in the forward direction
1°	Primary
2°	Secondary

CONTENTS

LIST OF FIGURES

LIST OF TABLES

LIST OF PLATES

CHAPTER 1

AN INTRODUCTION TO BIOTECHNOLOGY

Biotechnology

Biotechnology is the general term which encompasses the various activities concerned with the application of living organisms, or components thereof, to industrial, analytical and environmental problems. As a result of improved enzyme isolation, immobilisation and modification the biotechnologist is now provided with specific biocatalysts which he can use under suitable conditions to tackle all of the above problems.

Enzymes, production and isolation

Enzymes are the proteinaceous catalysts found in all living cells. Their function is to accelerate the rate at which biochemical reactions occur. They possess a high degree of specificity in their reactions, showing both regio and stereo specificity. They function under mild aqueous conditions, usually around neutral pH and especially relevant to applications they maintain their activity when isolated from the cell.

With a few exceptions, such as papain and rennin, the majority of enzymes of biotechnological interest are microbial in origin. The reasons for this are outlined below:

i) Microorganisms can be cultivated rapidly and easily. Harvesting of the organisms is straightforward, usually requiring little more than a filtration or a centrifugation step.

ii) Suitable selective pressures can be applied to produce novel enzymes or enzymes with favourably altered kinetic

parameters such as a decreased K_M for a particular substrate.

iii) Advances in genetic engineering have meant that enzymes can be designed with specific amino acid changes. This may result in increased stability or favourable kinetics. Since these enzymes are expressed in microorganisms they can be produced in large quantities.

iv) Certain microorganisms produce interesting enzymes extracellularly. Consequently such enzymes can be obtained simply by recovering the supernatant.

At present industry mainly uses crude enzyme preparations. However, a significant increase in the use of purified enzymes can be anticipated as a result of the development of large scale purification techniques. Familiar laboratory techniques such as precipitation, gel permeation chromatography, ion exchange and affinity chromatography have all been scaled up. Furthermore, new techniques such as liquid/liquid extraction (Kula, M.R. (1979)) and membrane selective filtration are now being introduced. Such developments should eventually lead to greater availability and a reduction in the cost of enzymes used in industry. In some applications, however, e.g. analytical uses, enzymes of a higher purity must be used.

Enzymes in Industry

For thousands of years processes such as brewing, bread making and the production of cheese have involved the unrecognized use of enzymes. The association of enzymes with foodstuffs is still evident today with the food industry being one of the largest industrial consumers of enzymes. These are mainly hydrolytic enzymes such as α-amylase, glucoamylase, rennin, papain and bacterial proteases which are used to degrade large molecular weight substrates. A

summary of other industrial applications is shown in fig. 1.1.

The industrial usage of enzymes seems poised for a remarkable growth. In 1980 enzymes sales worldwide were reported to be $390 million, 25% up from 1979 (Katchalski-Katzir, E. and Freeman, A. (1982)). By 1985 it is predicted that enzyme sales in the USA and Western Europe will increase to around $500 million (O'Sullivan, D. (1981)).

The Reaction Step

Traditionally, industrial enzymes have been used in batch processes with soluble substrates and soluble enzymes. Under these conditions, recovery and reuse of the catalyst is extremely difficult. Furthermore, the inactivation of the processing enzyme(s) may be necessary at the conclusion of the reaction and the altered conditions required to effect this inactivation may cause undesirable effects on the products.

Despite these shortcomings, however, enzymes can still offer a number of operational advantages over "chemical" processes. These are:-

i) Because of their specificity, impure substrates can be used in reactor vessels.

ii) There are no wasteful side reactions since substrate is converted to product in usually 100% yield.

iii) The reactions are carried out under mild conditions, e.g. pH7, 30°C in aqueous buffer. No extremes in temperature or pressure are required.

Immobilized Enzymes

The problems outlined above associated with the use of soluble enzymes can be elegantly overcome by immobilizing the enzyme onto an inert support, in effect making the enzyme insoluble.

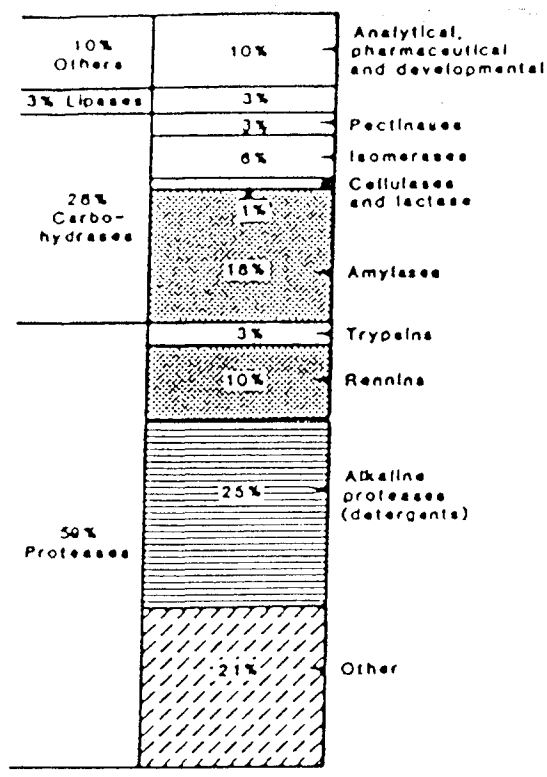

Fig 1.1. Diagram illustrating the main industrial applications of enzymes.

The major use of proteases is in detergents; rennins are used in making cheese, and other proteases are used to tenderize meat and in the production of pharmaceuticals. Amylases are used primarily to hydrolyze starch; other carbohydrases are used to produce invert sugar, to convert glucose to fructose, to hydrolyze pectic substances and to oxidize glucose to gluconic acid. Lipases are used primarily to hydrolyze fats and fatty acid esters. Catalases are used to decompose hydrogen peroxide.
(Diagram taken from Maugh,T.M. 1984)

An immobilized enzyme can be defined as an enzyme physically confined and localised in certain defined regions of space which retains its catalytic activity and can be used either repetitively or continuously.

Since the first report of an active water insoluble enzyme was published in the literature (Nelson, J.M. and Griffin, E.G. (1916)), enzymes have been immobilized to a wide range of substances ranging from paper, wood chips, crushed red brick, ion exchange resins, ceramic glass and stainless steel (Chibata, I. (1978)).

Immobilized enzymes can be subdivided into two major groups. This is shown schematically in fig. 1.2.

i) Matrix entrapped

Entrapment is carried out in polymeric gels such as polyacrylamide. The enzyme is usually added to the gelling solution just prior to polymerization so that the enzyme becomes entrapped in the gel volume. The technique is relatively inexpensive and easy to perform, although in some instances the polymerization may inactivate the enzyme. Furthermore substrates, cofactors, etc., can sometimes encounter diffusional problems in the gel matrix.

ii) Micro encapsulation

The enzyme is trapped in a membrane, e.g. a liposome or dialysis membrane, which permits the free diffusion of substrate, but retains the enzyme. This technique works well but can be expensive.

iii) Adsorption

This is by far the easiest form of immobilisation strategy and, as such, usually involves dipping the support into the enzyme solution. Such preparations, however, are

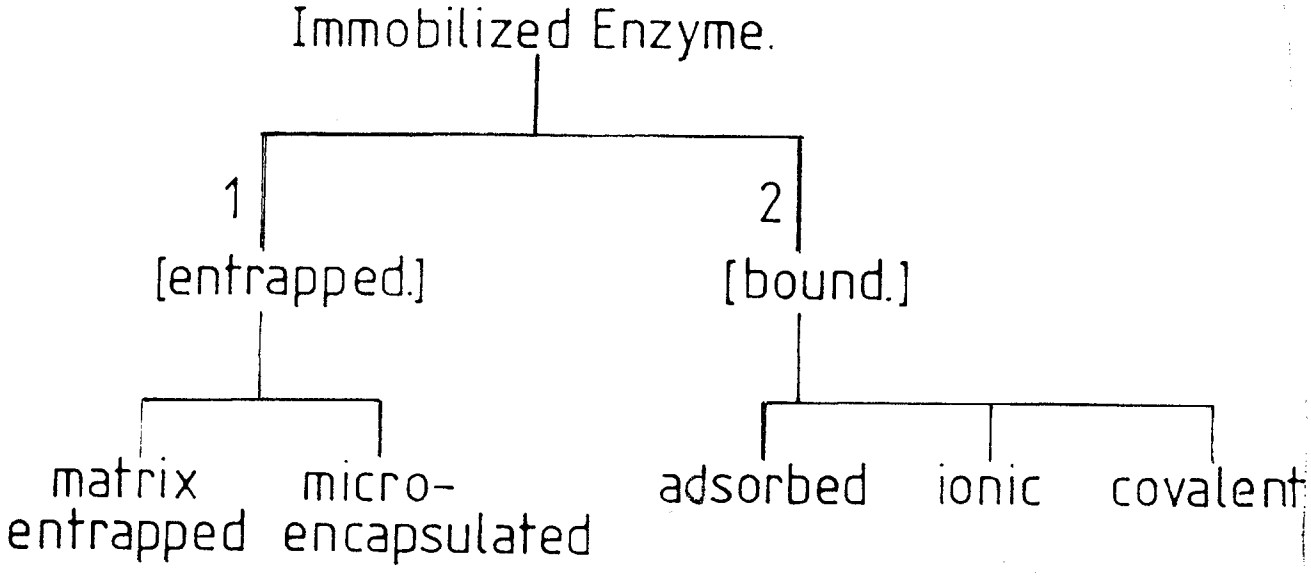

Fig 1.2. Diagrammatic representation of the two types of enzyme immobilization. The enzyme can either be entrapped in a suitable matrix or can be bound to the support material.

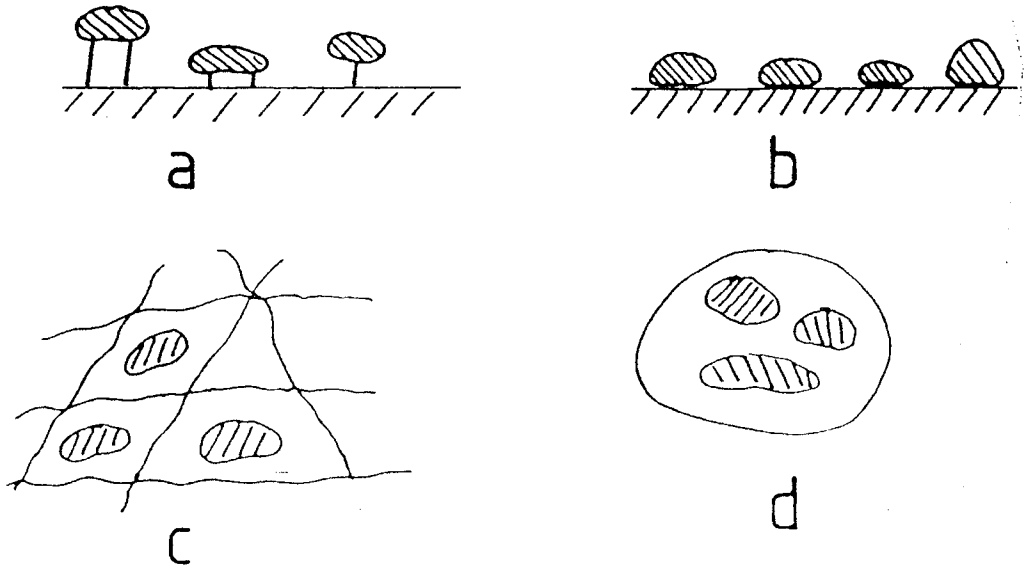

Schematic representation of the different types of immobilized enzyme preparations.

a Covalently bound. c Matrix entrapped.

b Adsorbed. d Micro-encapsulated.

often not stable with leakage of the enzyme from the support being the major problem.

iv) Ionic binding

This is another popular immobilization technique. The technique is based on the formation of salt bridges between the charged groups on the surface of the enzyme and the charged groups present on the support. Again, this type of preparation may not be very stable, with leakage being an appreciable problem, especially when the insoluble enzyme is used in solutions of high ionic strength.

v) Covalent attachment

This technique is based on the formation of stable covalent bonds between residues on the surface of the enzyme and functional groups present on the support. As such, it represents a very stable preparation which is suitable for continuous applications.

Many synthetic protocols for covalent attachment have been reported in the literature. Fig. 1.3 outlines two commonly used procedures employed to attach enzymes to glass and poly hydroxy resins such as Sephadex.

Unfortunately, the advantages of this technique must be balanced against factors such as;

(a) The chemistry required may be complex and time-consuming.

(b) Unless suitable precautions are taken, inactivation of the enzyme may occur because the essential amino acids, e.g. active site residues, are modified during the chemical reaction step.

Immobilized Enzymes in Biotechnology

In terms of industrial applications a stable insoluble

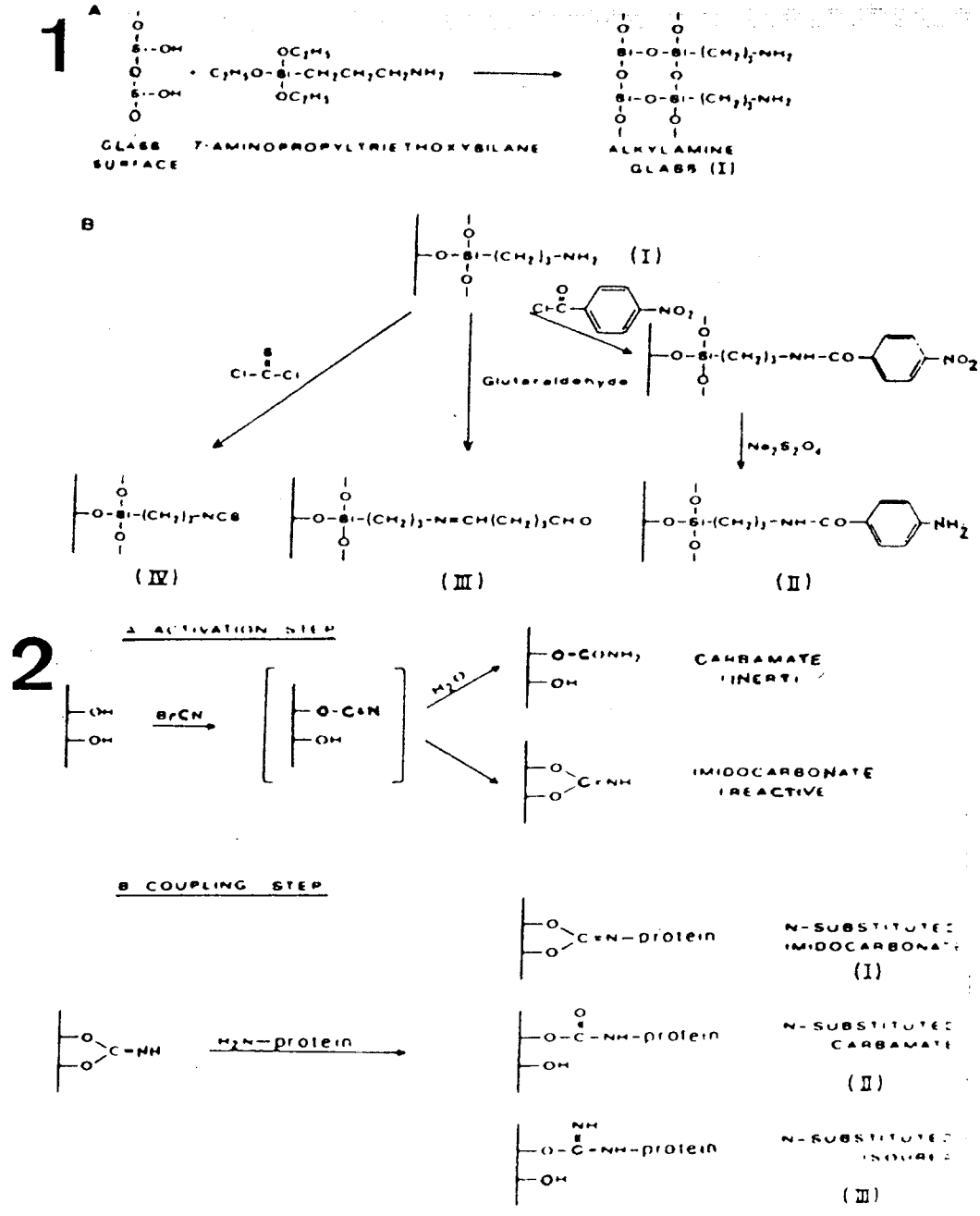

Fig 1.3. Diagram showing two methods commonly employed for the covalent attachment of enzymes to insoluble supports.

(1) shows the binding of enzymes to glass through the use of organo-silane chemistry.

(2) shows the binding of enzymes to polysaccharides via cyanogen bromide activation.

The available immobilization techniques have enabled a high degree of flexibility in reactor design since they have allowed enzyme immobilization on polymeric supports of different geometric structures such as powders, beads and tubes.

enzyme preparation can offer a number of operational advantages. These are summarized below.

i) The enzyme can be used continuously in a suitable reactor vessel. The same enzyme can be used more than once, thus making the process more cost effective.

ii) There is no contamination of the product with the enzyme. Consequently the product can be isolated fairly easily.

iii) Immobilisation of the enzyme may lead to enhanced stability and may even give rise to improved kinetic parameters.

The cost effectiveness of using immobilized enzymes can be clearly illustrated with reference to the industrial production of L-amino acids using immobilized aminoacylase, a process developed by the Tanabe Seiyaku company in Japan.

Chemically synthesized amino acids are racemic mixtures of the L- and D- isomers. The L-form is the biologically active form which is used by both the food and pharmaceutical industry. A process for resolving the mixture is therefore needed.

The reaction catalysed by aminoacylase is shown below.

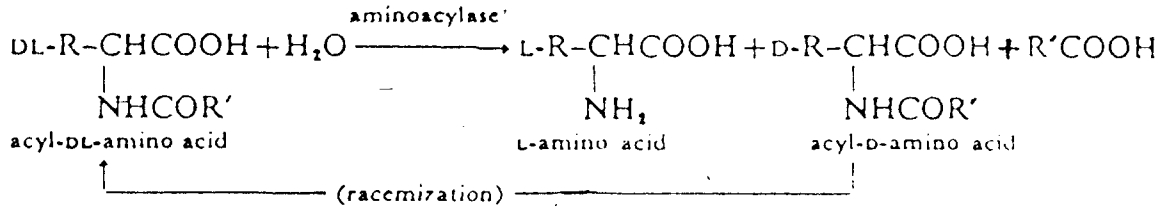

Chemically synthesized acyl-D-L-amino acids are asymmetrically hydrolyzed by the enzyme to give L-amino acid and acyl-D-amino acid. After concentration, both materials are easily separated on the basis of the difference in their solubilities. Acyl-D-

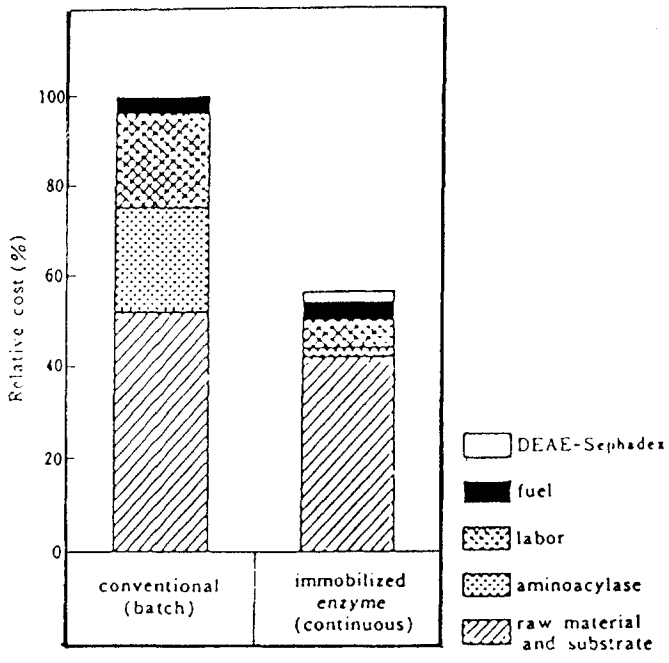

Fig 1.4. Diagram showing the comparison of production costs for the manufacture of L-amino acids by batch and continuous processes. In the immobilized enzyme process the overall cost is more than 40% lower than that of the conventional batch process using soluble enzyme. Savings of enzyme and labour costs are the main contributors, as well as the increase of product yield due to easy isolation of L-amino acids from the reaction mixture.
(Data adapted from Chibata,I. 1978.)

amino acid is racemized and reused in the ensuing resolution procedure (Chibata, I. (1978)). A break-down in the overall production costs using a batch process with soluble and insoluble enzyme is shown in fig. 1.4.

The most successful large scale industrial application employing immobilized enzyme technology is the production of high fructose corn syrup by the partial isomerization of glucose derived from starch. The enzyme employed is Glucose isomerase, immobilized by ionic binding to DEAE cellulose. The process yields a high fructose corn syrup which is used as a sweetener in the U.S.A., Japan and Europe (O'Sullivan, D. (1981)).

In other areas, immobilized enzymes have found particular application in analytical processes in which the availability of enzyme columns, enzyme membranes and enzyme tubes has facilitated the more extensive use of enzymes for analysis within the laboratory and the clinic. Enzyme columns, when inserted into suitable automatic analyzers, permit the continuous assay of substrates such as glucose, lactose, urea and uric acid (Penderson, H. and Horvath, C. (1981) and Carr, P.W. and Bowers, L.D. (1980)). A good example is the system based on immobilized glucose dehydrogenase which is used in the routine clinical analysis of glucose.

Glucose dehydrogenase catalyses the reaction;

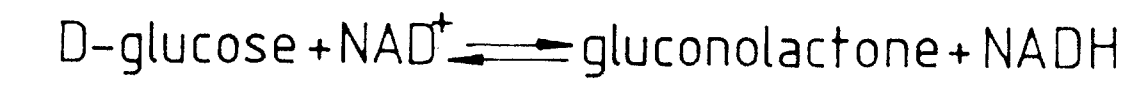

The enzyme is immobilized onto the inner surface of a nylon tube using the chemistry outlined in fig. 1.5(a). The enzyme tube is then incorporated into a Technicon AA1 flow system, as

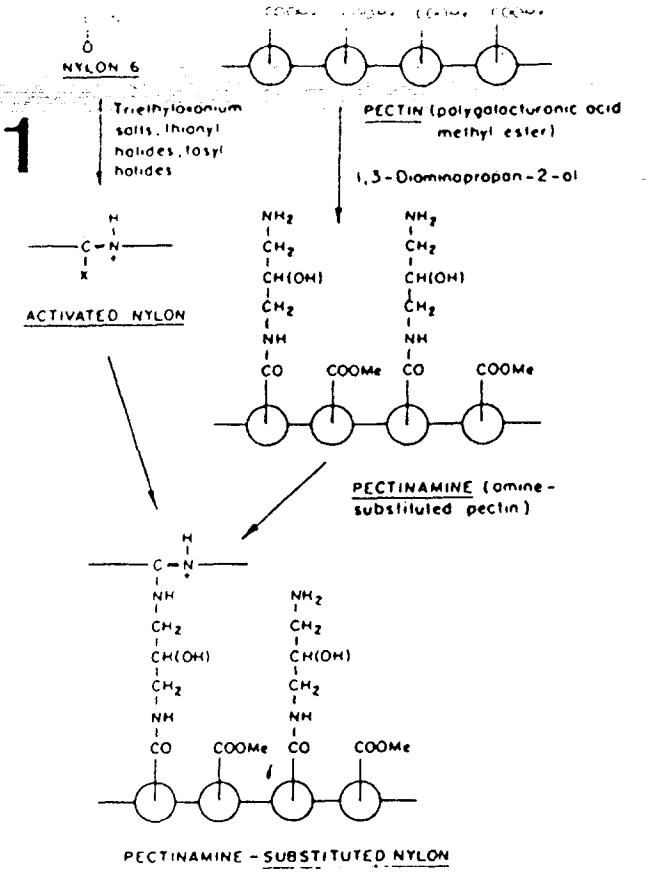

Fig 1.5(a). Diagram showing the covalent attachment of enzyme to the interior of a nylon tube.

(1) Nylon tubing is activated on its inside surface by the reaction some of its secondary amide linkages with triethyloxonium salts to form the corresponding imidate esters. Nylon which has been O-alkylated in this way is very reactive toward nucleophiles such as amines and hydrazides.

The activated nylon is then treated with a solution of an amine substituted pectin. In this way, the surface of the nylon is coated with a hydrophilic polysaccharide that contains a large number of primary amino groups.

Fig 1.5(a) cont'd.

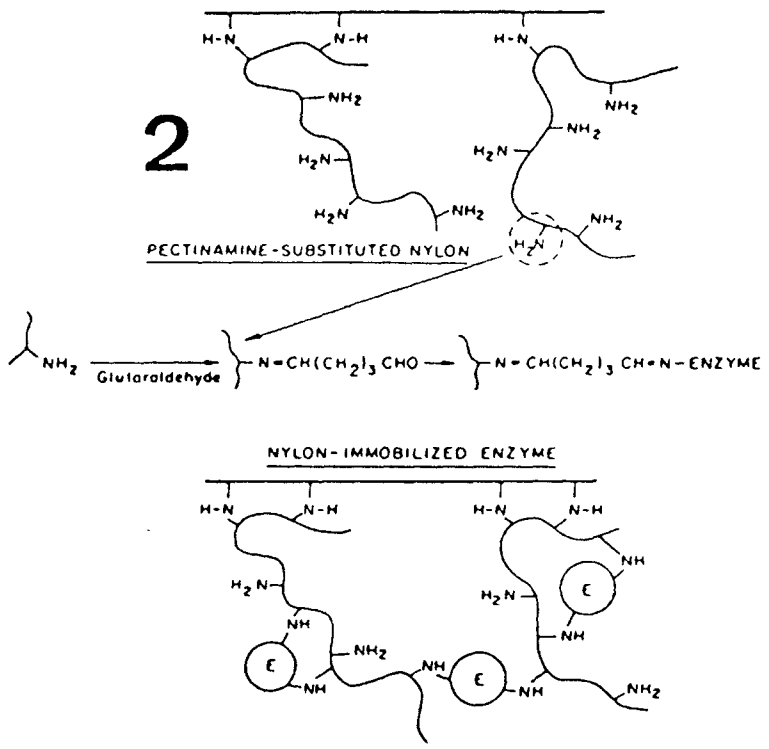

(2) The enzyme is coupled to the amine-substituted nylon through glutaraldehyde.

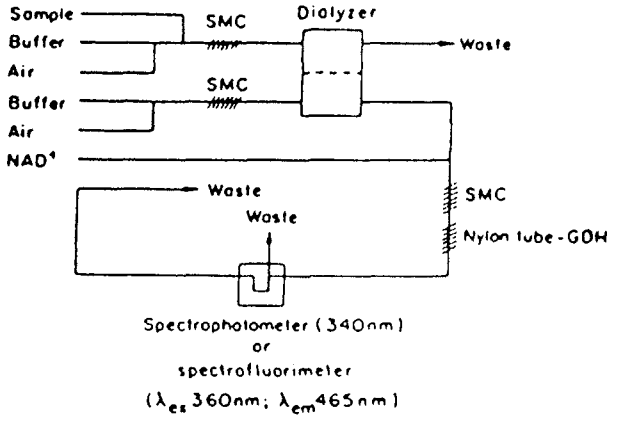

Fig 1.5(b). Diagram showing the flow system for the determination of glucose using nylon tube-immobilized glucose dehydrogenase.

(data adapted from Chibata I. 1978)

shown in fig. 1.5(b). A spectrophotometer is used to measure the production of NADH, which in turn is related to the concentration of glucose in the sample.

Another exciting development in terms of analytical techniques is the development of the biosensor electrode, a physico/chemical transducer which functions by combining a sensing procedure with immobilized enzyme activity. More will be said about a specific type of biosensor, the enzyme electrode, later.

Concluding Remarks

The great inherent potential of enzymes as biocatalysts in general, and of immobilized enzymes as heterogeneous catalysts in particular, seems to assure the extensions of the application of enzymes in the future. The ability of enzymes to catalyse the synthesis, degradation and modification of molecules under mild conditions will undoubtedly facilitate future developments in enzyme engineering. Further impetus will be gained from the growing need to transform biomass and other waste products into useful chemicals such as gas and liquid fuels.

It should be pointed out, however, that to date enzymes which require cofactors in order to carry out their reactions have not been used on a large scale. The high price of cofactors such as ATP, NAD(P)H and the lack of suitable methods for recycling them have prevented this development. Attempts to achieve this goal are currently under investigation.

In terms of the immediate future, there is tremendous interest in manufacturing "tailor made enzymes" either to introduce favourable properties, e.g. better operational stability, or more favourable kinetics. To this end, different

lines of investigation are being pursued.

Using classical mutagenesis techniques, the Cetus Corporation were able to alter the pH optimum of the enzymes used in the production of glycols with the result that they could be used simultaneously in the same reactor vessel (Maugh, T.H. (1984)).

Using modern genetic engineering techniques such as in vitro mutagenesis (Winter, G. et al (1982)), investigators are selecting specific amino acid residues they wish to replace, and at the same time selecting the residues they wish to replace them with. This approach requires a precise knowledge of the 3-D structure of the enzyme, and at the moment the major goals are simply academic, i.e. finding out more information about enzyme mechanisms and the dynamics of protein folding. For the near future, the major aims will simply be to improve the stability of enzymes so they can better tolerate the conditions found in industrial fermentors and also to improve their "immobilizability" so that less activity is lost when the enzyme is attached to the support (Maugh, T.H. (1984)).

Longer term goals include changes in substrate specificity, changes in catalytic activity and perhaps, eventually, the fusion of related enzymes so that multienzymic process may be carried out in one composite protein.

CHAPTER 2

POROUS NICKEL

Introduction

Porous nickel is a sheet metal material made by the International Nickel Company (INCO) which is used extensively for electrodes of sintered plate alkaline batteries (nickel/cadmium type) and for certain types of experimental low and medium temperature fuel cells (Giles, R.D. (1982), Dams, R.A.J. et al (1982) and Tracey, V.A. (1965)).

The main reason for this wide application is its resistance to corrosion by the potassium hydroxide electrolyte, but a further favourable factor is the availability of a range of carbonyl-nickel powders which provide the combination of properties needed in these applications.

In electrodes for nickel/cadmium batteries, high porosities (70-90%) are essential to permit accommodation of the maximum quantity of active mass in the pores of the sintered matrix. Furthermore, the porous electrode must contain a central support to provide strength and rigidity, enhance electrical conductivity and prevent shrinkage during the sintering process. In this particular case the support is a mesh of nickel plated iron, onto which the nickel powder is laid. Nickel plated iron is used because it is cheaper than pure nickel (Tracey, V.A. (1965)).

There are a number of various techniques available for the manufacture of porous materials which determine the porosity and thickness of the final preparation. Because of their needs, INCO exclusively use the Slurry technique for the manufacture of porous nickel (Tracey, V.A., pers. commun.).

The Slurry Technique

The slurry technique is used to coat a suitable support by dipping it into an appropriate solution (slurry). The stages are as follows:

1. Slurry prepared.
2. Support material coated by passing through a slurry bath.
3. Coated strip passed from slurry bath through thickness control stage, and thence
4. through a drying furnace.
5. The dried strip is passed through the sintering furnace.
6. The sintered strip is wound onto a coiler.

Fig. 2.1 shows a schematic drawing of the continuous process used by INCO.

Preparation and control of the slurry (stage 1) is essential, to ensure correct viscosity and, hence, consistent properties. Cellulose derivatives in water have been found to produce good slurries, to which the nickel powder is then added. To keep the powder in suspension the solution is agitated with a slowly moving impeller.

The nickel carbonyl powder used in the slurry technique is filamentary Type 225 with an average particle size of 2.6-3.4 μm (Tracey, V.A. (1965)).

Sintering of the dried strip (stage 6), the process by which the nickel powder is converted into a coherent solid, fig. 2.2, is carried out at 900°C in a controlled atmosphere which ranges from pure hydrogen to a nitrogen atmosphere containing a small percentage of hydrogen (~5% v/v). The sintered material is then allowed to cool and wound onto a coiler.

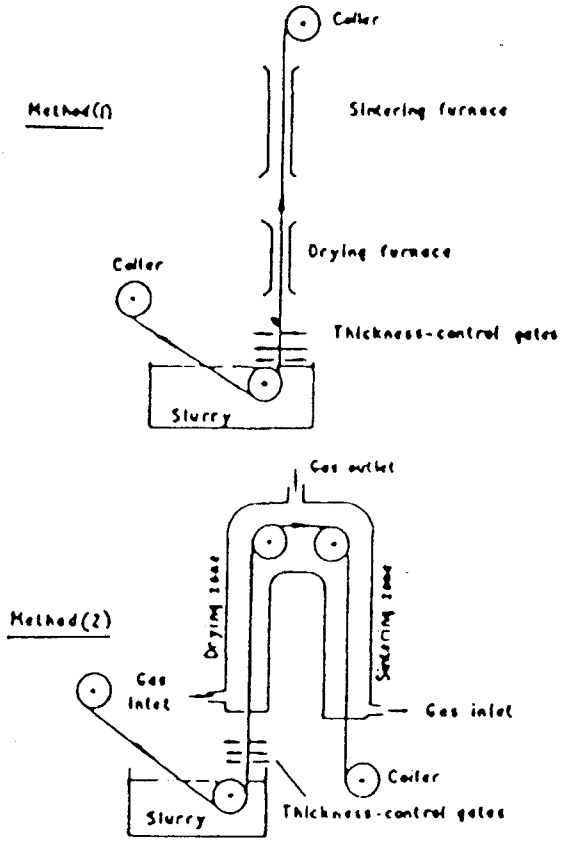

Fig 2.1. Diagram showing a typical layout for the slurry coating line used by INCO for the production of porous nickel.
(Data adapted from Tracey,V.A. 1965.)

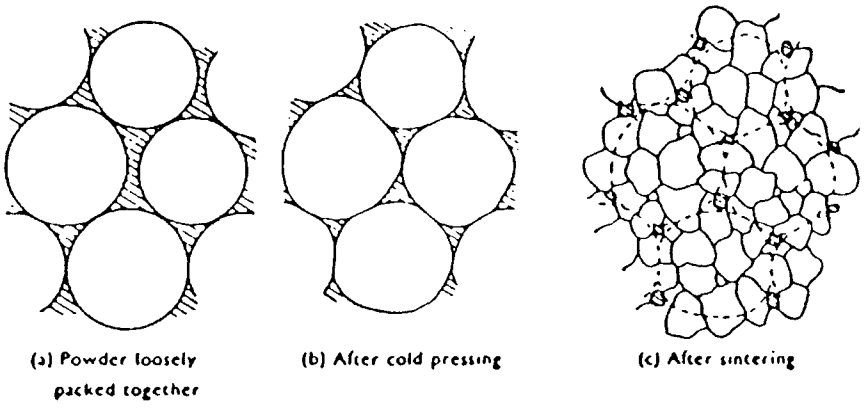

Fig 2.2. Diagram showing the stages in powder metallurgy operation. In this process fine metallic powder is agglomerated to form stock. The main process consists of cold pressing followed by heating. The temperature of the heating process is below the melting in the case of pure metals. Considerable contraction in volume and increase in density result from the heating. The bonding resulting from the heating is brought about by various atomic movements including recrystallisation crystal growth across the cold worked interfaces. During sintering, volatiles such as traces of lubricant are removed and oxides should be reduced or dissociated by the action of the sintering atmosphere.
The reduction of porosity usually associated with sintering is due in some way to the atomic movement and migration that takes place.
(Adapted from A Text-Book of Powder Metallurgy.)

The porous nickel supplied for this work was a gift from INCO. It was supplied in the form of sheets with dimensions 10 cm x 20 cm and a thickness of 0.5 mm. The following technical information was also supplied:-

i) Cost of manufacture - £11,400/tonne.

ii) Porosity 70-90%.

iii) Surface area of the porous matrix 0.15m^2/g.

iv) Support grid - nickel plated iron mesh.

v) Materials involved in the manufacture: nickel powder Type 225, slurry former (3% wt/wt methyl cellulose in water) and a support grid.

It was noted that the porous nickel sheet was flexible and could be cut into any desired shape, e.g. a 1 cm x 1 cm square with a pair of sharp scissors or a steel punch.

The high surface area and porosity of the porous nickel can be clearly seen under the electron microscope, plates 2.1 and 2.2. The electron micrographs were taken as described in Materials and Methods for section I.

Aims of the Project

The usefulness of porous nickel will obviously involve making use of its high surface area and structural properties. In this respect, there are two immediate applications which are worth investigating. The first of these, which will be dealt with in Section I, is using porous nickel as an insoluble support to which enzymes can be immobilized. The attractive features of the porous nickel in this respect are its large surface area which should ensure a high enzyme loading, and both its porous nature and mechanical strength, which would make the porous matrix ideal for continuous flow applications.

The other particularly attractive application is to use

Plate 2.1.

Scanning Electron Micrograph of the surface of porous nickel.

Magnification: X 1,500
Length of calibration bar: 10μm.
Accelerator Voltage: 25KV.
Microscope: Philips T 200.

Note the porous nature of the surface of the nickel sinter. Pores can be seen with different diameters. By inspection, an average pore diameter of about 10 m can be calculated. Note also the pitted appearance of the surface. This structure is lost following oxidation.

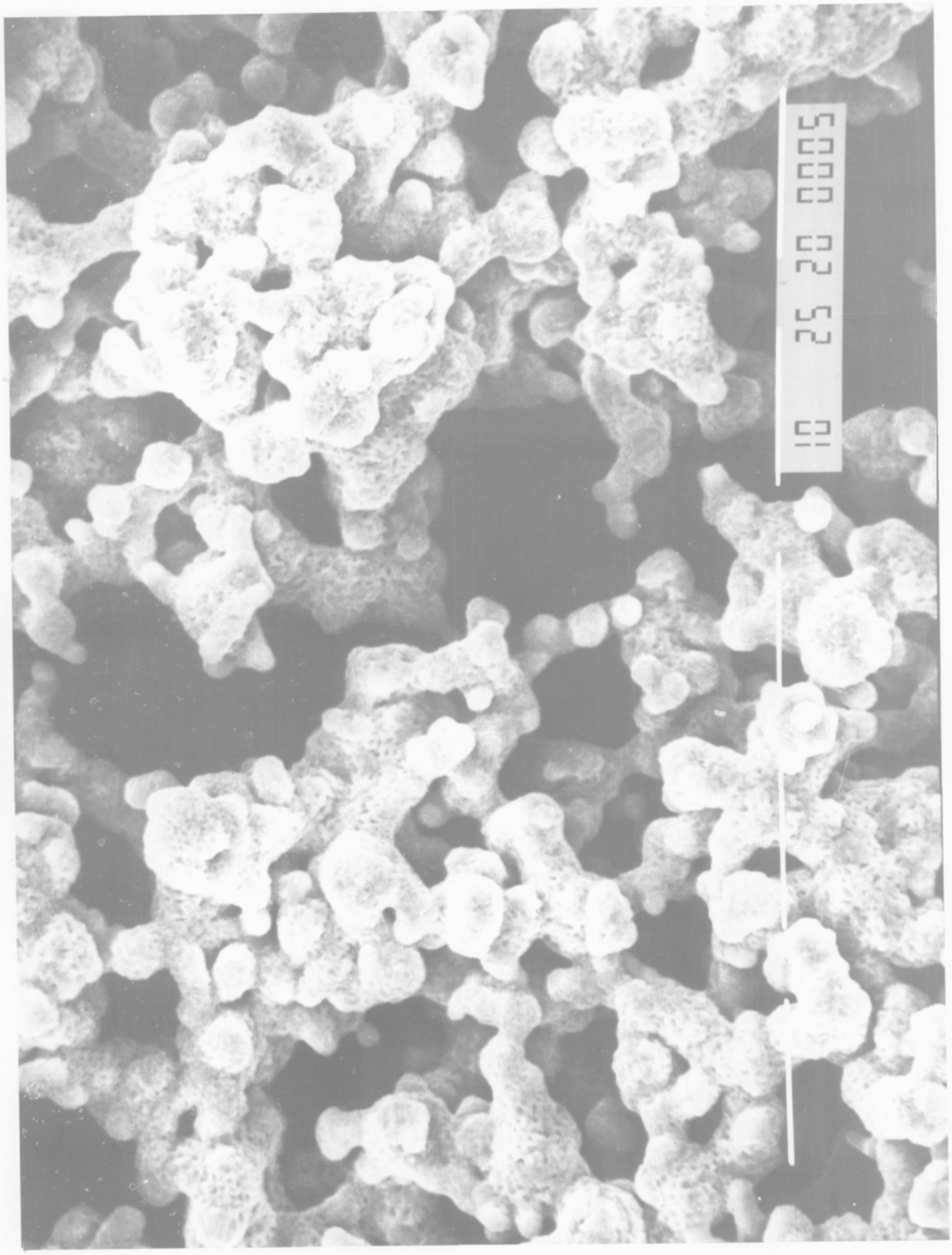
5000 22 52 01

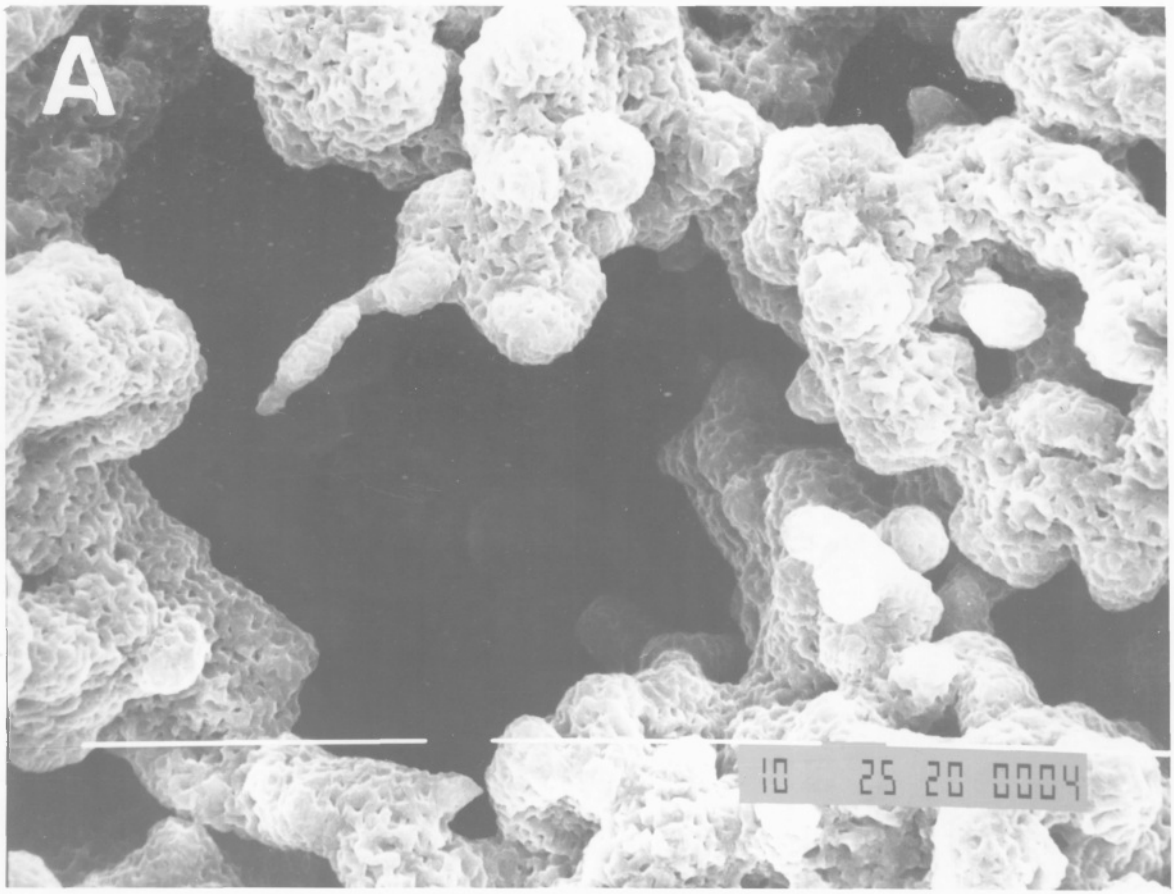
A
10 25 20 0004

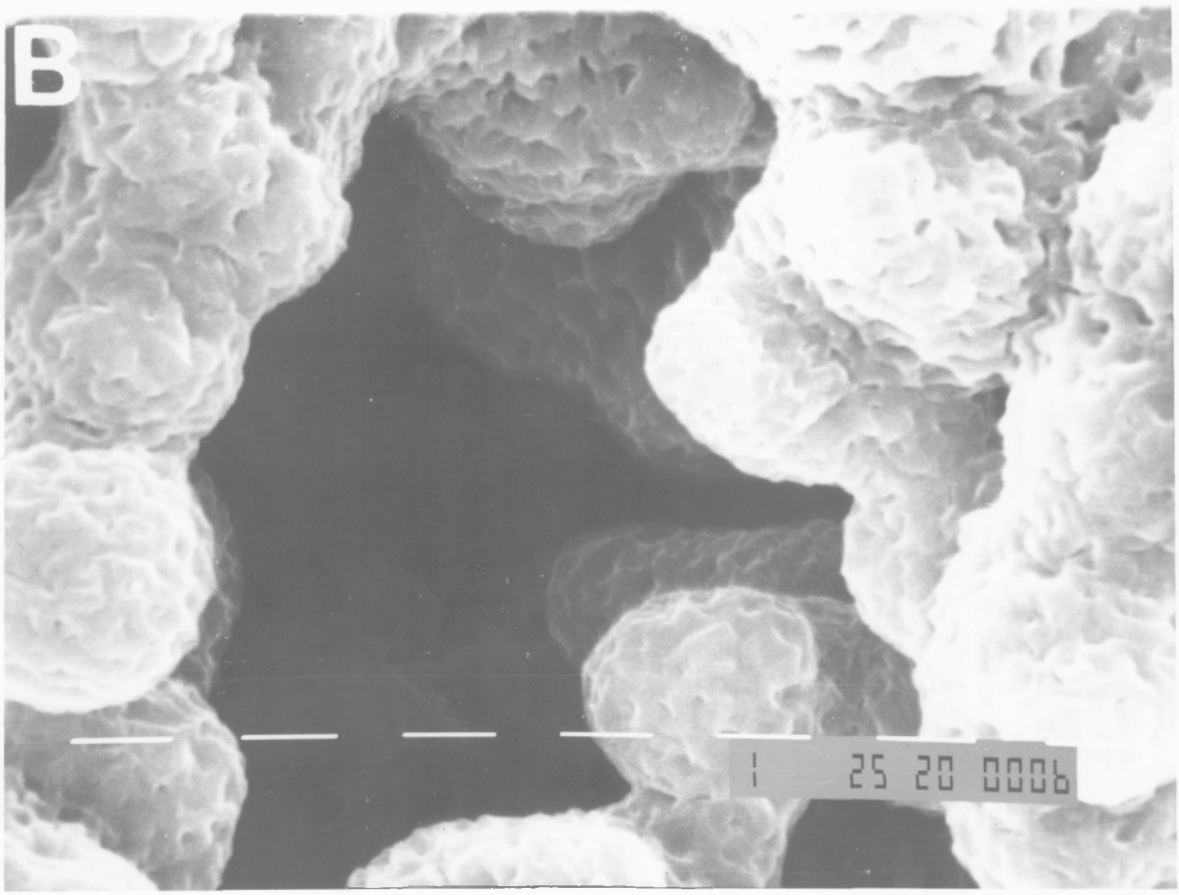
B
1 25 20 0006

the porous nickel as the base sensor around which an amperometric enzyme electrode can be constructed. Obviously, its metallic structure makes it a conductor. The high surface area of the nickel would mean that large currents would be passed during the electrochemical experiment. This would result in increased sensitivity and, furthermore, a porous nickel electrode would be cheaper to manufacture than the corresponding gold or platinum electrode. This work will be dealt with in Section II.

CHAPTER 3

INTRODUCTION TO SECTION I

An ideal enzyme support for use in reactor vessels or other applications should fulfil the following criteria:

i) Provide dimensional stability, density and a high surface area. The support must be stable and must not collapse at high flow rates.

ii) The porosity of the support should be as high as possible so as to allow free and rapid movement of the reaction solution.

iii) The support should represent an inert volume, in so far that after the immobilization is complete the support should play no further part in any chemical reaction.

iv) The support must be amenable to solution chemistry, if covalent attachment is the desired immobilization technique, and furthermore, regeneration of the "active" support should be efficient.

It is evident because of its inherent properties that porous nickel does indeed provide a matrix of good stability and high surface area. The porosity of the nickel matrix is high (70-90% porosity), an essential prerequisite for its successful application as a porous anode in both water electrolytes and Ni/Cd storage batteries.

In terms of its inertness it can be argued that being a metal, the porous nickel matrix would be susceptible to corrosion in aerated aqueous buffers. (The corrosion reaction can be represented as $M = M^{n+} + ne^{-}$). Such a situation would be unsuitable because not only would the corrosion process undermine the structural stability of the matrix, but the

accumulation of metal ions M^{n+}, in the solution could lead to the poisoning of the immobilized enzyme (Munro, P.A. et al (1977)).

In this respect nickel offers a particular advantage in so far as if nickel is covered by a surface oxide film the underlying metal is protected from further corrosion (passivated). The corrosion resistant properties of the surface oxide film is derived from the fact that the oxide film formed on the surface of the nickel is non porous and therefore forms a protective layer. Because of this property, nickel has found applications as an alloying and plating agent.

Although a surface oxide coating would protect the nickel from corrosion, it must be pointed out that the surface oxide can be reactive towards certain solution species (this will be discussed later), thus fulfilling criterion number (iv) overleaf.

Surface attachment of molecules to metals

To date, the main area of interest in attaching molecules to the surfaces of metals has been in the manufacture of modified electrodes. In the majority of cases, this has been carried out by a three step process.

(i) Activating the metal surface. This is usually achieved by forming an oxide film on the surface of the metal.

(ii) Derivitizing the surface oxide with a suitable chemical agent.

(iii) Functionalising the derivitized oxide surface with the molecule of interest.

Traditionally, largely as a result of the research carried out on "bonded phases", organo silane chemistry has been utilized for step (ii) (Murray, R. (1980)). Schematically the reaction of an organosilane with face hydroxy groups can be

represented as;

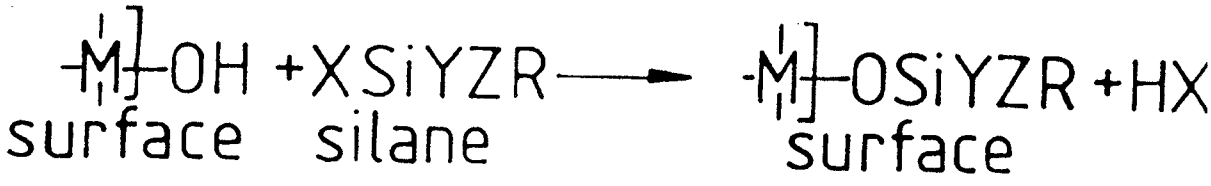

Further groups can now be added to the metal surface by using the appropriate chemistry, for example if R is an amino group through an amide coupling reaction.

The bond formed between the silane and the metal/metal oxide phase is a stable M-O-Si ether type linkage, which is resistant to both acid and alkali hydrolysis.

In 1977 Kuwana et al (Kuwana, T. et al (1977)) described the use of cyanuric chloride as a general linking agent in the preparation of modified electrodes. Cyanuric chloride was reacted with surface hydroxy groups on glassy carbon as shown below.

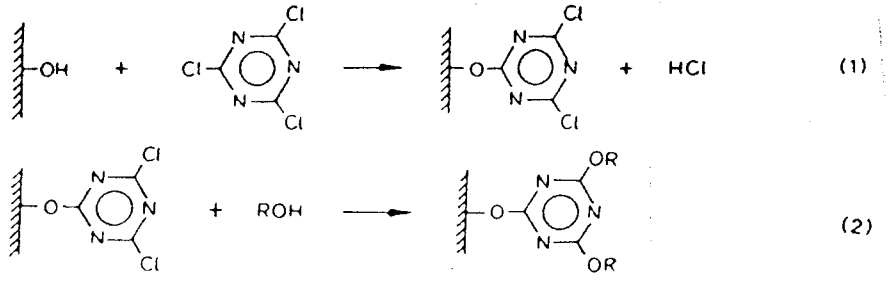

Other groups, e.g. hydroxyl, amino and Grignard reagents, can then react with the derivitized surface as shown. Furthermore, Kuwana showed that the bond formed between glassy carbon and cyanuric chloride, C-O-C, was extremely stable to hydrolysis by both acid and alkali. Although the research was aimed primarily at glassy carbon, Kuwana suggested that cyanuric chloride could be used equally effectively with metal oxide surfaces.

Research in covalently binding enzymes to metal surfaces has been extremely limited. In 1979 Halling and Dunnill (Halling, P.J. and Dunnill, P. (1979)) described the immobili-

zation of chymotrypsin to a variety of ferromagnetic powders, including nickel powder. Their interest was in the development of magnetic non porous supports for immobilized enzymes.

First, a surface oxide was formed on the nickel powder by heating in air at 350°C for 60 minutes. After this treatment, they found that the nickel powder did not corrode to any detectable level. They then employed traditional organo silane chemistry, using 3-aminopropyltriethoxysilane, as the derivitizing agent. This procedure, however, gave rise to an unstable surface link with desorption of the enzyme occurring within two hours. From this they concluded that the individual Ni-O-Si bonds were unstable.

A more stable linkage was produced by joining together many silane links in a layer of polyglutaraldehyde and then attaching the enzyme to the polyglutaraldehyde layer. This is shown schematically below.

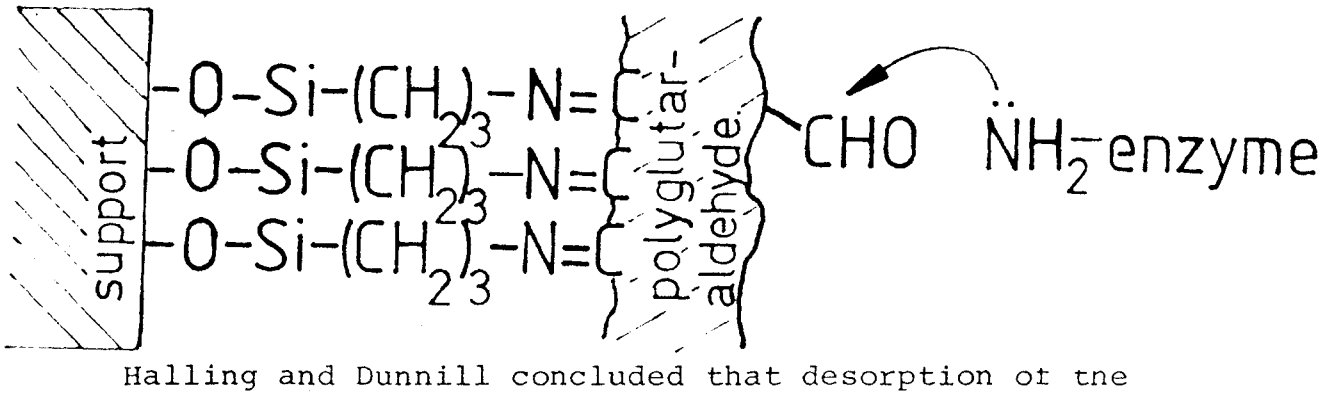

Halling and Dunnill concluded that desorption of the enzyme occurred because of the instability of the Ni-O-Si bond, suggesting that a hydrolysis reaction was taking place. They did not discuss, however, the possibility that an unstable surface oxide layer had been formed on the nickel powder, which in turn would account for the observed desorption of material.

The strategy in this investigation therefore was first to optimize the formation of the surface oxide layer to give the most stable coat possible. The linking chemistry presented

above is somewhat complicated and so an alternative and more straightforward approach was sought. From the work presented by Kuwana et al, cyanuric chloride seemed to be a good candidate. The aim of this work was to improve the stability of the linkage from the metal to the enzyme and so increase the useful operational time.

CHAPTER 4

MATERIALS AND METHODS FOR SECTION I

Reagents

Unless otherwise stated, all solutions were prepared from Aristar grade (BDH) chemicals in high purity water (Millipore). Phosphate buffers were adjusted to the correct pH by the dropwise addition of 1.0M NaOH. Tris buffer was adjusted to the correct pH with 0.1M HCl.

Glucose oxidase (EC 1.1.3.4 type 2) from Aspergillus niger, mol wt 186,000, was supplied from Boehringer Mannheim and had an activity of 247 I.U. mg^{-1}.

Alcohol dehydrogenase (EC 1.1.1.1) from yeast was purchased from Sigma (London) Ltd., Poole, Dorset, and had an activity of 230 I.U. mg^{-1}.

Ribitol dehydrogenase (EC) from Klebsiella aerogenes was prepared in the laboratory. This will be discussed later.

Caesin hydrolysate, dithiothreitol, Bromophenol Blue, acrylamide and NN'-methylene bis acrylamide (both specially purified for electrophoresis) were from BDH Ltd., Poole, Dorset.

D-ribitol and xylitol were from Cambrian Chemicals Ltd., Croydon. Purified agar was from Oxoid Ltd., Basingstoke, Hants. Ultrogel AcA44 was from LKB, South Croydon, Surrey. DE23 and DE52 were from Whatman.

PMSF (phenyl methane sulphonyl fluoride), Coomassie Brilliant Blue E250, bovine serum albumin, aldolase, pepsin, cymotrypsinogen and lysozyme, proteins used as molecular weight markers, and all other bio chemicals were from Sigma (London) Ltd.

Inorganic chemicals (AR grade) and solvents were obtained

from several suppliers.

General techniques

Spectrophotometry

All enzyme assays coupled to changes in optical absorbance were carried out in a Gilford 252 spectrophotometer fitted to a Unicam SP500 monochromator. The temperature of the cuvette compartment was controlled by circulating water from a Grant SE15 water bath. Quartz cuvettes of 1cm light path were used. Rates of change of absorbance were determined using a Gilford 600 chart recorder.

Constant absorbances were determined, either with a Gilford 252 or with a lambda 3 Perkin Elmer.

Conductivity Determination

The conductivity of buffers, resins, etc. were determined at room temperature using a Radiometer Conductivity Meter CDM3 fitted with a type CDC 314 cell.

Determination of pH

The pH values of solutions were routinely determined using a Radiometer type PHM 26 pH meter fitted with a GK 2302 combined electrode and reference cell.

Polyacrylamide Gel Electrophoresis

Polyacrylamide slab gels of 1.5mm thickness were used for the electrophoretic separation of proteins in the presence of SDS (sodium dodecyl sulphate). The resolving gels were approximately 15cm x 15cm and unless otherwise stated were prepared by the polymerization of 10% w/v acrylamide. The samples to be subjected to electrophoresis were applied in wells formed in a low percentage acrylamide stacking gel, at a pH value less than that of the resolving gel.

Resolving gels were prepared by polymerising a mixture

of acrylamide and bis-acrylamide (NN'-methylene bisacrylamide) by the addition of ammonium persulphate and the catalyst TEMED (tetramethylenediamine). A stock solution containing 30% w/v acrylamide and 0.8% w/v bis-acrylamide was stored in the dark at 4°C and discarded after a week's storage. Gels were prepared by mixing:

10% (SDS)

25 ml	750mM-Tris.HCl pH 8.8
16.5 ml	acrylamide/bisacrylamide solution
6.9 ml	high purity water
60 µl	TEMED
500 µl	10% w/v SDS
1 ml	1% w/v ammonium persulphate (freshly prepared)

For gels other than 10% the ratio of acrylamide/bisacrylamide was altered accordingly.

The buffer, acrylamide/bisacrylamide and water were mixed and thoroughly degassed before the addition of the TEMED, SDS and ammonium persulphate. The mixture was rapidly poured between two glass plates, separated by 1.5mm Perspex spacers (sealed with melted soft paraffin wax), and was over-laid with butan-1-ol to exclude air. The polymerisation was allowed to proceed at room temperature and was complete after about an hour.

The stacking gel was prepared as follows;

3.4 ml	750mM Tris.HCl pH6.5
2 ml	acrylamide/bis acrylamide
12.4 ml	high purity water
20 µl	TEMED
200 µl	10% SDS
2 ml	1% s/v ammonium persulphate

The components of the stacking gel were degassed as described above. The top of the polymerised resolving gel was washed free of butan-1-ol with distilled water and the stacking gel mixture was poured on. A perspex 'comb' with serrations of the same thickness as the spacers was introduced between the glass plates to form wells in the stacking gel. The wells had a depth of 1.5cm and a width of 8mm. The stacking gel was allowed to proceed at room temperature for about half an hour.

Samples for electrophoresis in the presence of SDS were dried in vacuo in Durham tubes, dissolved in 50µl SDS sample buffer and heated at 105°C for fifteen minutes to ensure complete denaturation. SDS sample buffer, which was kept at 4°C in a sealed vial, contained per 10ml:

200 µl	750 mM TRIS.HCl pH 6.5
1 ml	10% w/v SDS
1 ml	2-mercaptoethanol
5 ml	50% v/v glycerol
10 mg	Bromophenol blue
2.8 ml	distilled water

Using sample wells of 8mm width, suitable loadings of protein per well were found to be 100µg ⟶ 200µg of crude cell extracts or 1µg ⟶ 10µg of any single protein species.

After the polymerisation of the stacking gel, the comb and the bottom spacer were removed and the gel fitted to a gel tower. The upper and lower compartments were filled with electrode buffer which contained 3g/l Tris base, 1.45g/l glycene and 1g/l SDS. The samples were introduced into the wells in the stacking gel using a 50µl Hamilton microsyringe. A Shandon Southern SAE 2761 power-pack was used. Gels were run at room temperature at a current of 8mA until the dye front

had reached the bottom of the gel.

Prior to staining for protein gels were fixed by soaking in 25% w/v trichloroacetic acid for 15 minutes, washed for 10 minutes by soaking in 10% v/v acetic acid and then rinsed with distilled water. The gels were then incubated in staining solution for 45 minutes at 60°C. The staining solution was prepared by mixing equal volumes of 20% v/v acetic acid and 0.6% w/v Coomassie Brilliant Blue R 250 in methanol. The background was destained overnight with several changes of a 1:2:7 (by volumes) glacial acetic acid, methanol, water mixture.

Microbiological techniques

Unless otherwise stated, all media and solutions used in the microbiological work were sterilized by autoclaving at 123°C for 30 minutes. Solutions of sugars were normally autoclaved at low pH values, obtained by the addition of dilute phosphoric acid. Glassware and pipettes were autoclaved for 60 minutes and then dried in vacuo for 20 minutes.

Solid Media

Sterilin disposable Petri dishes of 9cm diameter were used.

M9 Plates

5.8 g/l Na_2HPO_4
3.0 g/l KH_2PO_4
0.5 g/l NaCl
1.0 g/l NH_4Cl
1 ml/l 1M Mg SO_4
2 ml/l trace elements solution.

The agar, $MgSO_4$, and trace elements were autoclaved together in 90% of the final volume of the medium and cooled to 60°C before the addition of the other salts as freshly autoclaved ten fold concentrate. The carbon source was either autoclaved

with the agar or added as a sterile concentrate.

Trace Elements Concentrate

500 mg/l	$FeSO_4.7H_2O$
70 mg/l	$CuSO_4.5H_2O$
45 mg/l	$MnCl_2.4H_2O$
50 mg/l	$ZnSO_4.7H_2O$
1.32 g/l	$CaCl_2.6H_2O$
100 mg/l	$CoCl_2.6H_2O$
7 mg/l	H_3BO_3
100 mg/l	$Na_2MoO_4.2H_2O$

Isolation and characterisation of ribitol dehydrogenase from a super producing strain of K aerogenes

Isolation of a super producing organism

Various strains of K aerogenes (A111M, A111, FG112 and A112) were grown on agar plates containing M9 salts and 0.2% xylitol as the only carbon source. After an overnight incubation at 37°C the largest single colonies were picked from each plate and then streaked on fresh agar plates of the same composition. The procedure was repeated until the organisms were firmly established at which stage the largest single colonies were again picked, but this time transferred onto "low xylitol" plates (0.05% xylitol). Each day the largest single colonies were picked and transferred to fresh "low xylitol plates". After 10 days, the largest single colonies were seen from strains FG112, A112 and A111M. It was therefore decided to grow these as liquid cultures.

Liquid cultures

The culture medium used was 200 mls of M9 salts supplemented with 2% casamino acids. The flasks were inoculated with the various organisms and then incubated in a Gallenkamp orbital incubator overnight at 37°C with the shaker speed set at

160 r.p.m.

Cell lysis

The cells were harvested by centrifugation in Sorvall GSA 250 mls buckets at 5875 g for 10 minutes at 4°C. The supernatants were discarded and the pellets were resuspended in 20 mls of buffer made by mixing together the following ingredients:

20 mls potassium phosphate pH7

2 mls 1M MgCl solution

1.6 mls 0.25M EDTA pH7

0.28 mls 2-mercapto ethanol

4 mls .01M PMSF

372 mls high purity water.

The resultant suspensions were transferred to 45 mls polycarbonate tubes and the cells were pelleted at 5000 g for 5 minutes at 4°C. The pellets were resuspended in the above buffer and the procedure was repeated. Finally, the cells were suspended in 5 mls of potassium phosphate pH 7 and then ruptured by sonication.

Enzyme assay

Ribitol dehydrogenase activity was measured by following the production of NADH + H^+ at 340 nm in the presence of D-ribitol spectrophotometrically. The assay mix was prepared as follows.

9 mls 0.3M potassium phosphate pH 7.0

2.25 mls 10mH NAD^+ solution

1.35 mls 1M ribitol

14.4 mls distilled water.

All assays were performed within 4 hours of the extraction.

Protein estimation

To determine the total protein in the supernatant the

technique of Bradford (Bradford, M. 1976) was used. The assay mix was prepared as follows;

100 mg of Coomassie Blue G250 was dissolved in 50 mls of 95% EtOH. To this, 100 mls of 85% (v/v) were added. The resultant solution was then diluted with high purity water to give a final volume of 1l.

The unknown was added to a test tube and the volume was made up to 1 ml with water. 4 mls of the Bradford reagent was then added and the absorbance read at 595 nm after 2 minutes.

Results:

Bacterial strain:	A112	A111M	FG112
Specific activity:	6.726	4.062	9.012

(Specific activity = μmoles NADH formed/hour/mg of protein).

From these results it was decided to use K aerogenes strain FG112 for large scale culture and isolation of ribitol dehydrogenase.

Purification of ribitol dehydrogenase

Essentially the same procedure as that reported by Rigby et al (Rigby, P.W.J. et al 1974) was followed.

Large scale cultures of strain FG112 were grown by the Imperial College Pilot Plant for 24 hours at 37°C in medium containing casamino acids (12.0g/l), Na_2HPO_4 (2.0g/l), K_2HPO_4 (2.0g/l) and $MgSO_4$ (1.2g/l). The cells were harvested by centrifugation and stored as a frozen cell paste at -20°C.

The cell paste was thawed into 2 litres of potassium phosphate buffer pH7 containing 10mM 2-mercapto ethanol and 1mM PMSF. The suspension was disrupted by two successive passages through a Menton Gaulin homogeniser. The passate was centrifuged in a Sorvall RS at 600 rpm for 30 minutes. The supernatant was pooled and cold distilled water containing

0.1mM PMSF and 1.0mM 2-mercapto ethanol was added to lower the conductivity to below 1 mS. The solution was then added to 900g of DE23 ion exchange resin equilibrated in 10mM potassium phosphate pH 7. The supernatant was shown to contain no ribitol dehydrogenase activity and was subsequently discarded. The resin was then washed with 100mM potassium phosphate pH7, and this time the supernatant did have the desired enzymic activity. 1,252g of Ammonium Sulphate were slowly added with stirring to give 50% saturation. After 30 minutes the resultant precipitate was removed by centrifugation and dissolved in 2 litres of 10mM potassium phosphate pH7. The resultant solution, which was shown to possess ribitol dehydrogenase activity, was dialyzed against 64 litres of 5mM potassium phosphate pH7 containing 1mM PMSF and 10mM 2-mercapto ethanol. The dialysate was pooled and loaded onto a glass column (25cm x 6cm) containing DE 52 ion exchange resin equilibrated with 10mM potassium phosphate pH7 gradient containing 1mM PMSF and 10mM 2-mercapto ethanol. The column was eluted with a 10mM-80mM potassium phosphate pH7 gradient containing 1mM PMSF and 10mM 2-mercapto ethanol. The fractions showing ribitol dehydrogenase activity were pooled and concentrated by Amicon filtration using a PM30 membrane and operating at 50 psi. Final purification was achieved by chromatography using an Ultrogel AcA44 column (75cm x 5cm). The purification procedure is summarized in fig. 4.1.

Notes

The flow rates of columns were controlled with an LKB 12000 Varioperspex peristaltic pump. The UV absorbance of the column effluent was monitored with an LKB Uvicord II system and the fractions were collected using an LKB 7000 Ultrorac system fitted with a drop counter.

Summary of the purification of ribitol dehydrogenase from Klebsiella aerogenes.

Purification Step.	Total enzyme Activity. (Units)	Specific Activity. (Units/mg prot).	Purification Factor.	Yield.
Crude Extract.	1.30×10^6	41.33	1	100%
DE 23 Batch adsorption.	3.91×10^5	51.95	1.26	30%
28-50% $(NH_4)_2SO_4$ cut.	2.57×10^5	83.5	2.02	19%
DE 52 column. Gradient elution.	2.10×10^5	90.0	2.2	16%
ACA44 column.	1.3×10^5	93.2	2.26	10%

Fig 4.1.

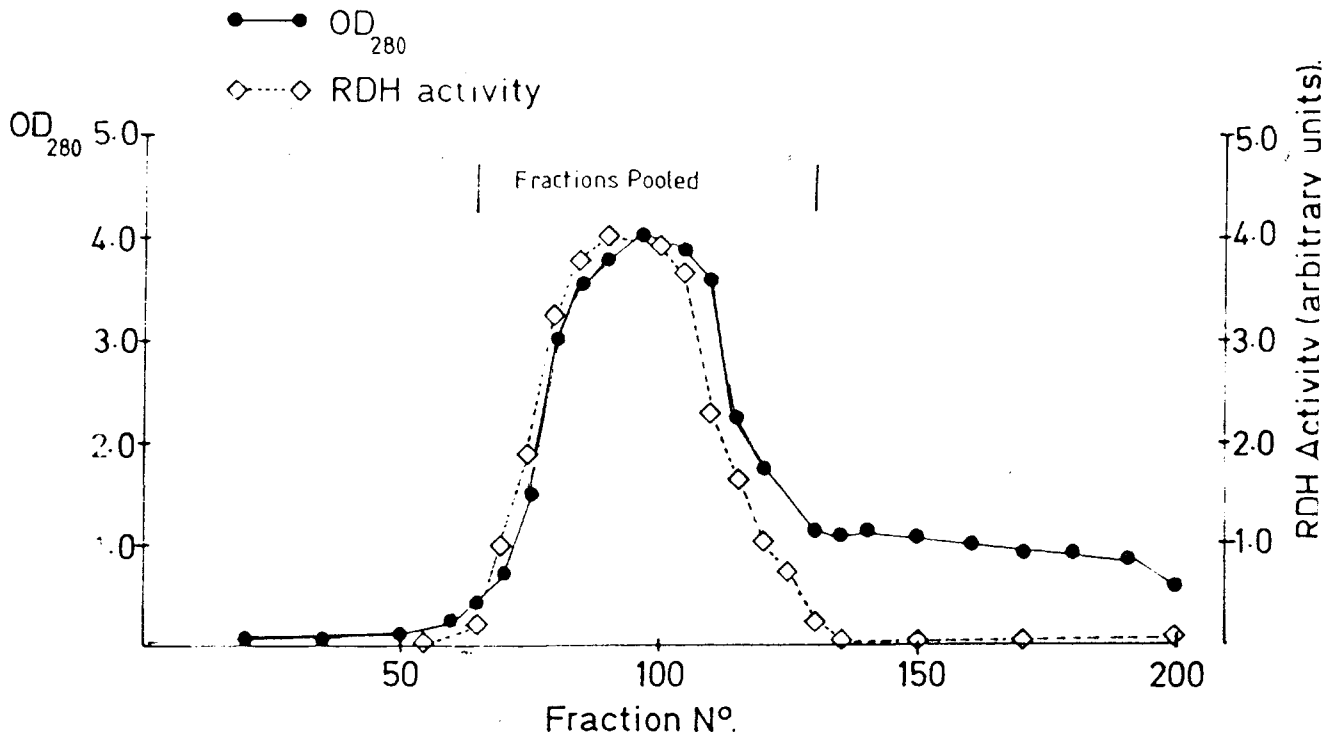

Fig 4.1 cont'd. Elution profile of the DE 52 column.

Operating conditions.

Column Dimensions:	25cm X 6cm.
Temperature:	4° C.
Mobile Phase:	10-80mM potassium phosphate pH 7.0 gradient.
Pressure:	Peristaltic pump.
Mode of Detection:	E_{280} and Enzyme assay.
Volume of fractions collected:	10mls.
Bed volume:	700mls.

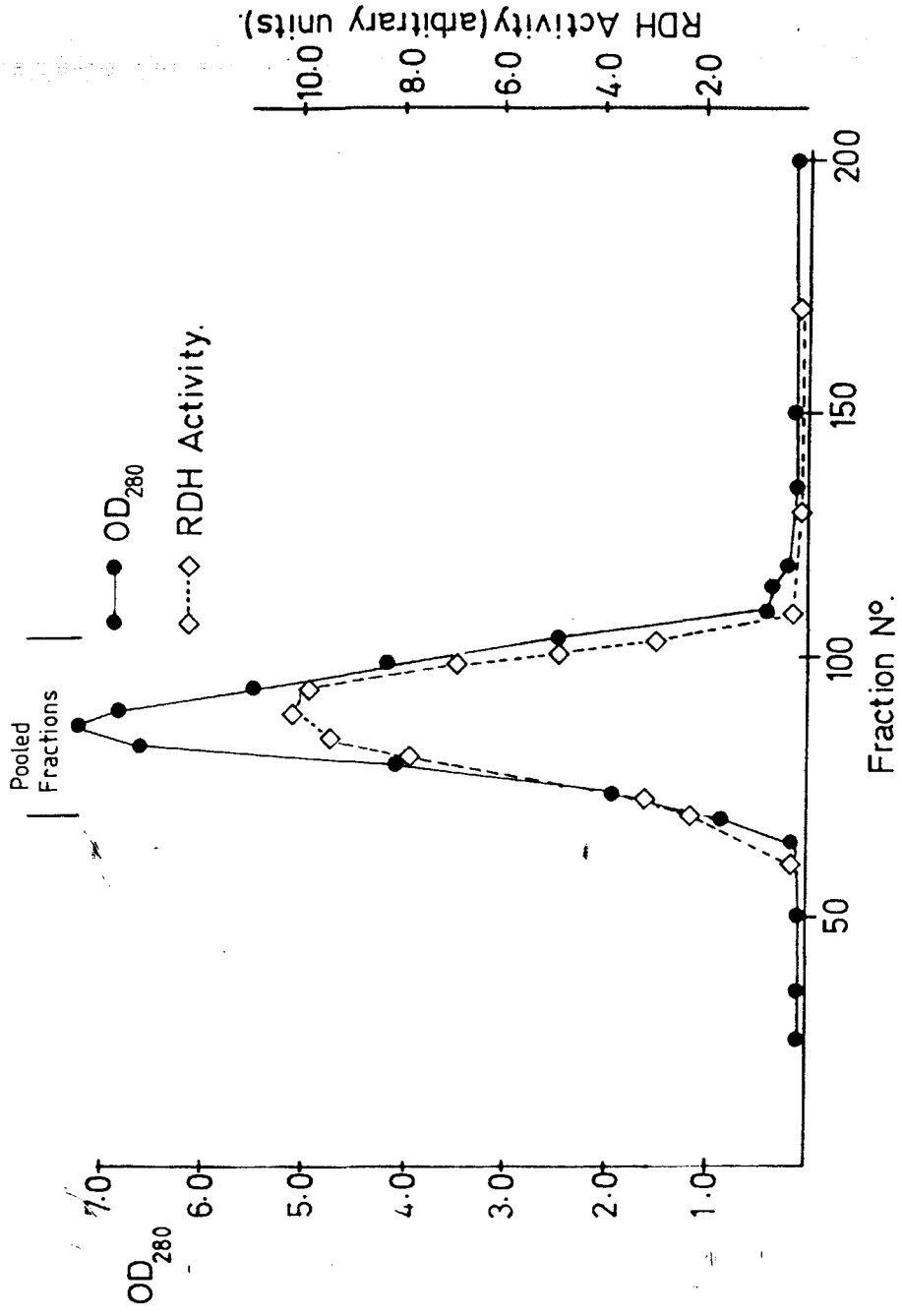

Fig 4.1 cont'd. Elution profile of Ac A44 column.

Operating conditions.

Column Dimensions:	75cm X 5cm.
Temperature:	4° C.
Mobile Phase:	10mM potassium phosphate pH 7.0
Pressure.	Peristaltic Pump.
Detection:	E_{280} and enzyme assay.
Volume of fractions:	10mls.
Bed Volume:	1,450mls.

DE 52 was supplied in a pre swollen form and so did not require precycling. However, before packing columns the resin was equilibrated to the pH and ionic strength of the loading buffer by repetitive washing until the pH of the buffer remained constant. Columns were packed at high flow rates, as recommended by the manufacturers and then washed overnight with the loading buffer before the application of the sample.

Ultragel AcA44, which is supplied pre swollen, was packed by pumping at the flow rate recommended by the manufacturers and was equilibrated with at least two column volumes of buffer. Columns were loaded by pumping the sample directly into the gel.

DE 23 was precycled prior to use as recommended by the manufacturers.

Characterisation of ribitol dehydrogenase

The peak fractions from the AcA44 column were pooled giving a final volume of 300 mls. This pool was concentrated by Amicon filtrating, giving a final volume of 50 mls. The enzyme was shown to be pure by polyacrylamide gel electrophoresis and was then dialyzed into 50% glycerol containing 0.1mM PMSF, 0.1mM EDTA and 10mM 2-mercaptoethanol. The enzyme was stored at a concentration of 20 mg/ml at -20°C. The specific activity of the purified enzyme was 93.2 units/mg protein.

The subunit molecular weight of ribitol dehydrogenase was determined by SDS polyacrylamide gel electrophoresis. The markers used were as follows;

Marker	M.Wt.
BSA	68,000
Aldolase	40,000
Pepsin	35,000
Chymotrypsinogen	27,700
Lysozyme	14,300

The M.Wt. was determined on both 12.5% and 15% gels. The values obtained were,

12.5% gel	21,900	(See fig. 4.2)
15% gel	22,000	

The Michaelis constant and maximal rate for both ribitol and xylitol were determined for ribitol dehydrogenase. The results are presented below.

Substrate	V_{max}	K_m
Ribitol	46.5 units	15.4 mM
Xylitol	8.6 units	153.8 mM

Furthermore, it was shown that the K_m for NAD^+ was 0.4 mM. These values, together with the subunit M.Wt. determinations, are consistent with what has been published in the literature.

Other techniques

SEM analysis of porous nickel

Scanning electron micrographs were produced using a Philips T200 electron microscope. The sample of interest was mounted onto a steel stage using epoxy resin. A small globule of silver was used to earth the nickel sample, thereby preventing the build-up of any static electricity. The sample was shadowed with gold by placing it into an evacuated vessel into which vaporized gold was introduced. To ensure even shadowing the sample was rotated. Technical data, e.g. magnification, acceleration voltage, etc., is given in the text.

Powder X-ray diffraction patterns

Samples were pulverized by grinding with a pestle and mortar and then loaded into a glass capillary tube which was then mounted in a Debye-Scherrer camera. The source of the radiation was a Cu anode tube with a Ni filter, monochromated to give CuK_α radiation (λ 1.542 A). The radiation was

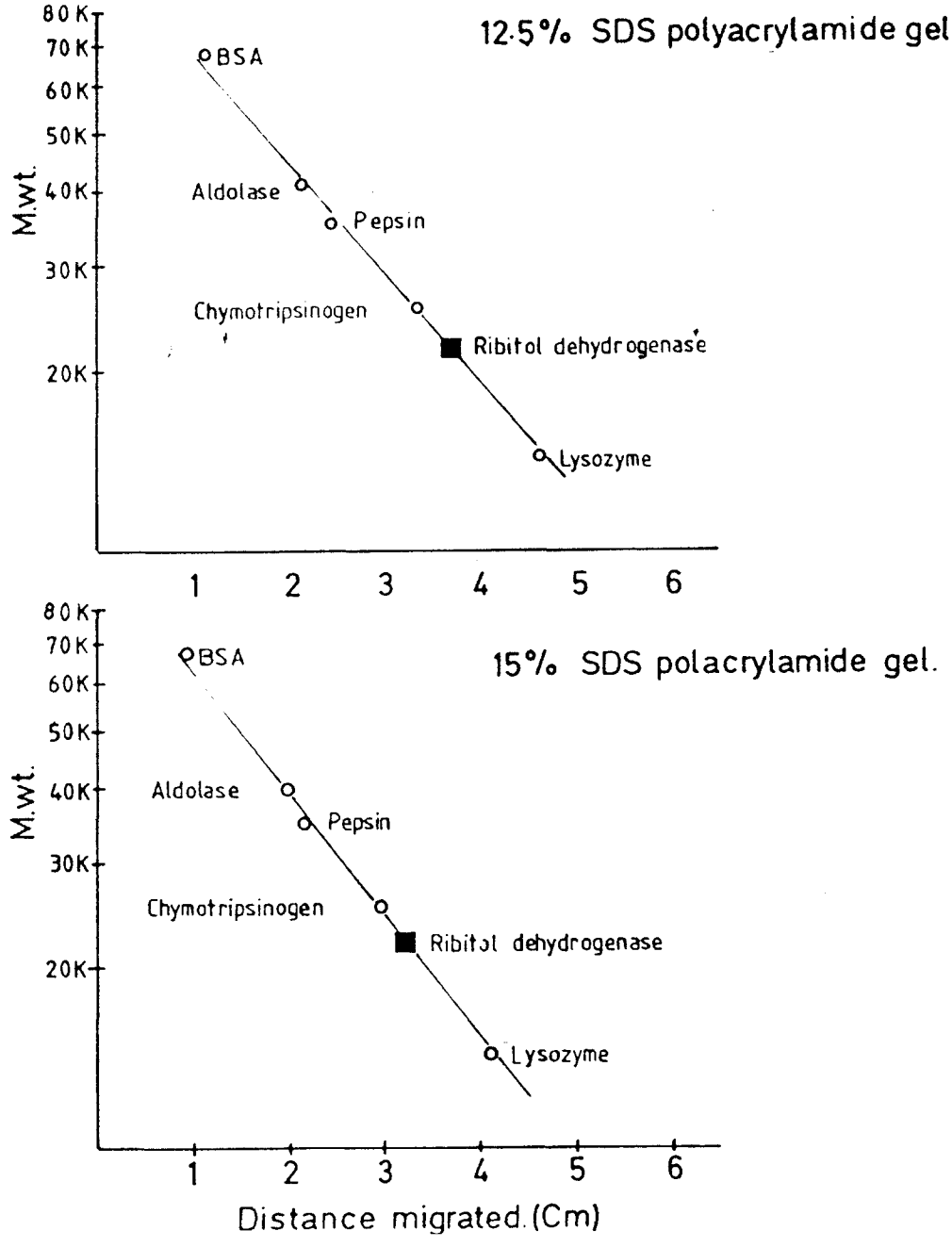

Fig 4.2. Subunit molecular weight determination by SDS polyacrylamide gel electrophoresis.

Subunit molecular weight.	Gel.
21,900	12.5%
22,000	15.0%

produced by a Philips 1310 X-ray generator operating at 35 kV and 32 mA. The film used to record the diffraction pattern was Kodak, NS 392T No Screen film. The film was exposed for 45 minutes.

Preparation of Sample for Infra Red Spectroscopy

In order to prepare a sample with sufficient I.R. active material and acceptable light scattering properties, the samples were prepared as follows.

The nickel oxide film was scraped off the surface of the porous nickel and then pulverized using a pestle and mortar. The powder was mixed with potassium bromide in the ratio 1 part nickel oxide to 5 parts potassium bromide. The sample was then subjected to 4000lbs of pressure in a hydraulic press, giving a potassium bromide/nickel oxide disc with the above properties. Prior to determining the I.R. Spectrum, the disc was dessicated under vacuum to remove all traces of moisture.

Assaying Immobilized Enzyme Activities

The assay procedure for soluble ribitol dehydrogenase has already been discussed. In a similar fashion, soluble alcohol dehydrogenase was assayed spectrophotometrically by following the production of NADH, in the presence of alcohol, at 340 nm. Soluble glucose oxidase activity was assayed by monitoring the decrease in dissolved oxygen tension in the presence of glucose by using a Clark type oxygen electrode operating at -0.6 V vs SCE. For maximal sensitivity, a teflon membrane was always employed.

The activities of the immobilized dehydrogenases were assayed using the apparatus shown in fig. 4.2. (An explanation of the apparatus together with its modus operandi is also presented).

Immobilized glucose oxidase was assayed by adapting the

Clark type oxygen electrode so that the porous nickel disc could be suspended in the assay buffer (fig. 4.3). The enzyme was assayed by measuring the decrease in dissolved oxygen tension in the presence of glucose.

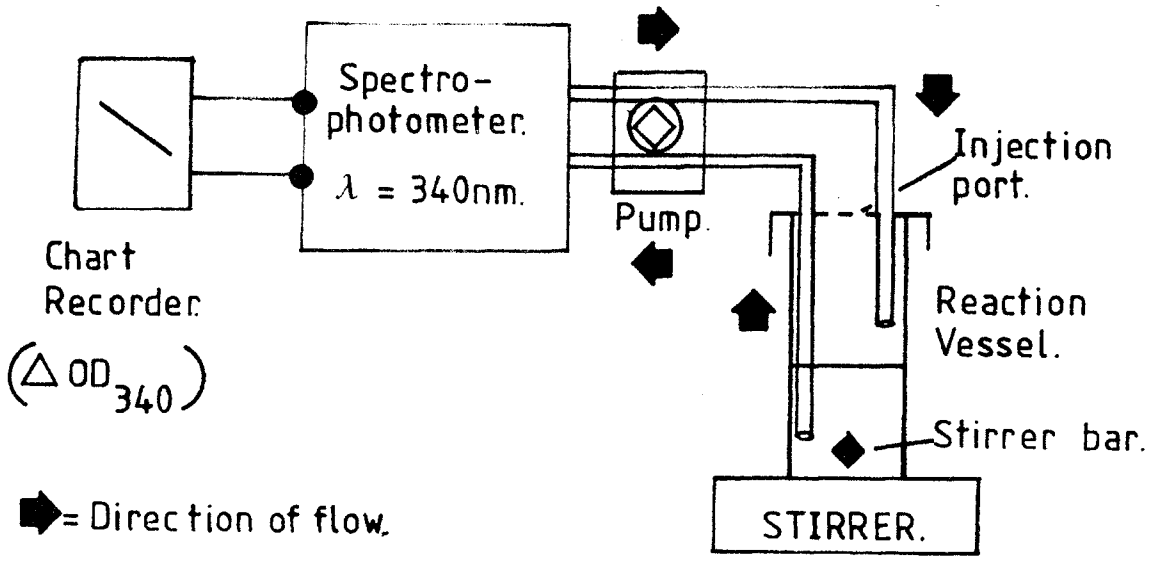

Apparatus for determining immobilized enzyme activity.

Fig 4.3. The apparatus shown above was used to determine immobilized dehydrogenase activity. The basic operational features of the apparatus are as follows.

1, The enzyme catalysed reaction takes place in the reaction vessel. The reaction is started by adding substrate to the vessel via the injection port. The immobilized enzyme is suspended in the vessel where it is bathed by the assay solution. A magnetic stirring bar ensures efficient mixing of the solution.

2, When the pump is switched on, a small portion of the reaction solution is drawn into the spectrophotometer. (The solution passes through a quartz flow cell with a working volume of 100μl.) The spectrophotometer monitors the change in absorbance at 340nm, i.e. the production of NADH from the enzyme catalysed reaction. The sampled aliquot is then returned to the bulk assay solution.

3, The reaction can be stopped at any given time simply

by removing the immobilized enzyme from the reaction solution.

4, With this apparatus, immobilized activities can be expressed in terms of ΔOD_{340} /unit time. It is thus possible to compare rates under different experimental conditions e.g. temperature and pH.

5, The reaction vessel can be fitted with a water jacket where temperature control is necessary.

Notes:

The variable parameters of the apparatus were standardised as follows;

1. Flow rate. 1ml min^{-1}.
2. Recording wavelength. λ = 340nm.
3. Stirrer speed. Maximum.

Operational Notes;

Because of the magnetic nature of the porous nickel care had to be taken to ensure that the nickel support did not get too close to the magnetic stirring bar.

Early experiments showed that rapid stirring was needed to obtain linear traces from the chart recorder.

When the immobilized enzyme was removed from the reaction mixture a lag of 2 to 5 seconds was commonly observed before ΔOD_{340} became zero.

Instrumentation.

The change in optical absorbance was monitored using a Gilford 252 spectrophotometer, fitted to a Unicam SP500 monochromator. Rates of change of absorbance were determined using a Gilford 600 chart recorder. The temperature of the reaction vessel was controlled by circulating water from a Grant SE15 water bath.

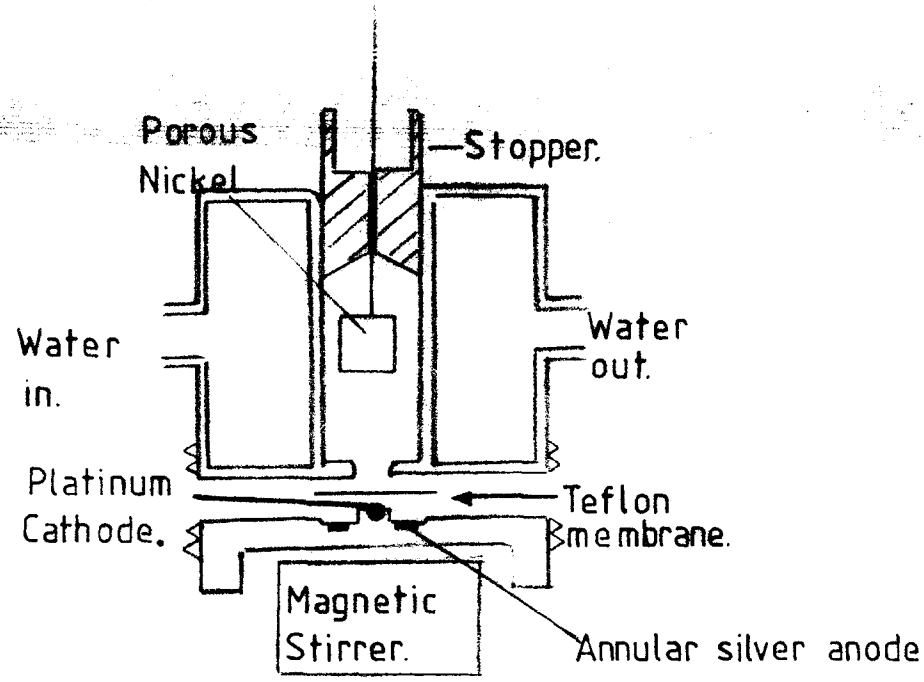

Fig 4.3. cont'd.

Diagram of oxygen electrode adapted for measuring immobilized glucose oxidase activity.

The glucose oxidase immobilized onto porous nickel was immersed in the cell as indicated above. The reacion was started by injecting an aliquot of glucose into the cell. The immobilized activity was monitored by following the decrease in the concentration of dissolved oxygen. Immobilized glucose oxidase activity was expressed in terms of ΔO_2/unit of time.

Operational notes:

The potential was maintained at -0.6 volts.

By selecting a suitable volume of assay buffer, the nickel square could be removed from the solution without having to remove the stopper.

To increase the sensitivity, a Teflon membrane was always used.

The immobilized enzyme was monitored in 0.1M sodium phosphate buffer pH 7.0. The temperature of the cell was controlled by circulating water from a Grant SE15 water bath.

The electrode apparatus was a Rank O_2 electrode.

Rates of change of dissolved O_2 were determined using a [illegible] recorder.

CHAPTER 5

RESULTS

SURFACE OXIDATION OF THE POROUS NICKEL

In general terms there are two ways in which an oxide film can be formed on the surface of a metal. The first of these, dry corrosion, involves heating the metal at high temperatures in an oxidizing atmosphere. The second procedure, wet corrosion, involves placing the metal in contact with an aerated aqueous electrolyte so that it dissolves, i.e. $M \longrightarrow M^{n+} + ne^-$. The tendency of the metal to dissolve will be related to its standard electrode potential in so far that the higher the potential, the lower the driving force behind the process of dissolution.

In general, the surface films formed during dry corrosion tend to be thicker and more stable than those formed during the wet process. The importance of obtaining a stable oxide layer has already been mentioned in the introduction. It was therefore decided to oxidize the surface of the porous nickel by the dry corrosion technique.

The Ellingham diagram for oxides, fig. 5.1, shows that most metal oxides have a $-\Delta G^\circ$ value, which indicates that a metal will tend to react spontaneously with oxygen under normal conditions to form an oxide. If the metal is heated in the presence of oxygen, thicker films will be formed. The temperature, however, cannot be increased indefinitely, since at very high temperatures the surface oxide may blister and crack, or even decompose.

The oxide films formed on the surfaces of metals during dry corrosion can be divided into three main types.

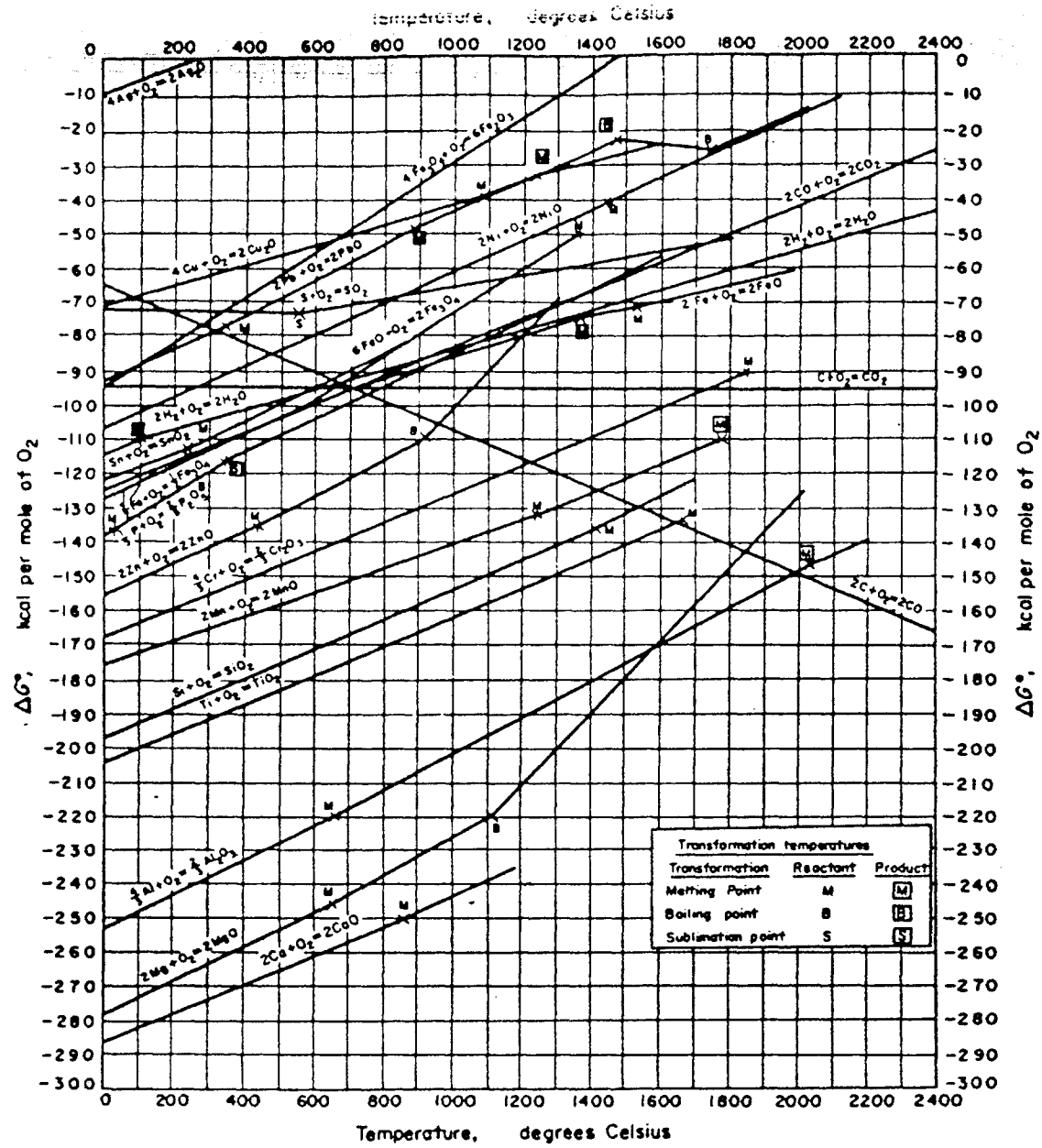

Fig 5.1. Ellingham diagram for oxides.

1. Those films which offer no protection to the metal and consequently the oxide grows linearly with time.

2. Those films which offer intermediate protection, in the sense that the rate of oxidation decreases with time.

3. Those films which entirely protect the metal after they have grown to a definite thickness. For such a film it is expected that as y, the thickness of the film, increases, the rate of increase of y will decrease with time.

It has been shown (Hill R.E. 1964) that the oxide film formed by heating nickel at 900°C in the presence of oxygen grows to a thickness of 50Å.

Description and formation of the NiO film

NiO films are cation deficient, and growth of the NiO layer takes place by the diffusion of Ni^{2+} ions via the vacant lattice sites in the $Ni^{2+}O^{2-}$ crystal lattice outwards from the metal-oxide interface to the oxide-gas interface. (A schematic representation of this is shown in fig. 5.2). Furthermore, NiO is a p type semiconductor, so the electrons produced by the reaction $Ni \longrightarrow Ni^{2+} + 2e^-$ are conducted to the oxide-gas interface by +ve hole conduction. This can be represented as $Ni^{3+} + 1e^- \longrightarrow Ni^{2+}$. At the oxide gas interface the oxygen is adsorbed on the surface of the film where the reaction $\frac{1}{2}O_2 + 2e^- \longrightarrow O^{2-}$ takes place. Thus, dry corrosion of nickel can be thought of as a 2 step process;

1. Cationic diffusion.

2. p-type electronic conduction.

Mass transport through the film will be the major factor affecting the growth rate of the film. When this becomes limiting, film growth will stop.

Experimental

1 cm^2 pieces of porous nickel were cut from the main

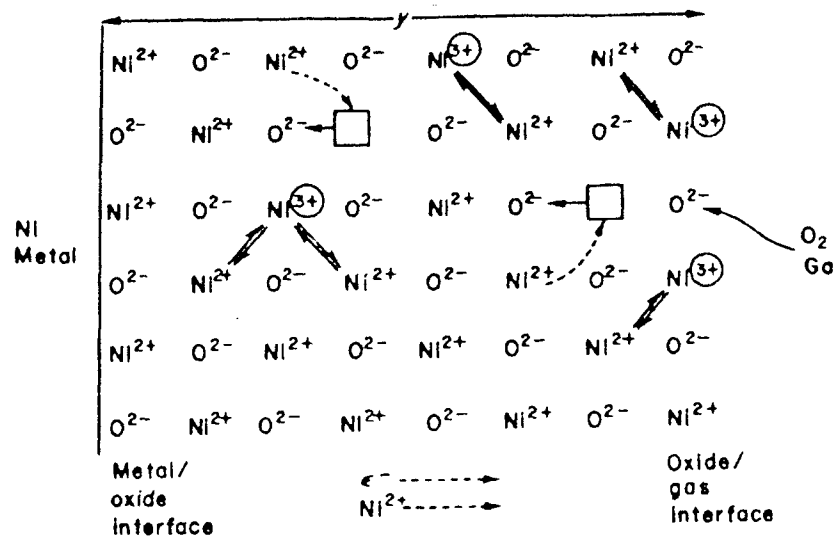

Fig 5.2. Representation of the growth of the oxide film on the surface of nickel. The oxide film grows by a two step process.

1 Cationic diffusion.

2 p-type electronic conduction.

(Data adapted from Hill, R.E. (1964)).

sheet, with a sharp pair of scissors and placed into heat resistant clay boats. At this stage the nickel squares had a dull grey appearance. The boat was then placed into a Griffin electric oven, preheated to 900°C. Dry oxygen was passed into the furnace, at a flow rate of 5 mls min^{-1}, and the reaction $Ni + \frac{1}{2}O_2 \longrightarrow NiO$ was allowed to proceed. When the consumption of oxygen had ceased the reaction was considered complete.

The boat was removed and allowed to cool. On inspection it was observed that the nickel squares had taken on a green colour. Furthermore, it was found that the porous matrix had become extremely brittle and could no longer be cut with scissors as before.

Powder x-ray diffraction analysis of the surface layer from the oxidized material indicated that the only phase present was NiO (plate 5.1). S.E.M. photographs obtained from the oxidized porous nickel showed that the porous structure of the matrix was still intact (plate 5.2).

DERIVITIZATION OF THE POROUS NICKEL

The reasons for using cyanuric chloride as the derivitizing agent have already been discussed.

Cyanuric chloride (2,4,6-trichloro-1,3,5-triazine) is a colourless solid which crystallises from carbon tetrachloride as large monoclinic crystals. Cyanuric chloride is a trichloro—substituted derivative of the parent sym triazine.

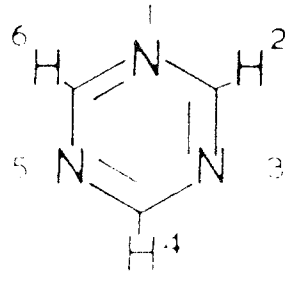

Parent triazine

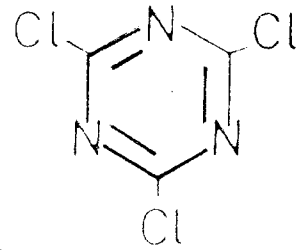

2,4,6 trichloro-s-triazine

Plate 5.1.

1. Powder diffraction photograph of nickel.

2. Powder diffraction photograph of nickel oxide.

Each sample was exposed to Cu K_{α} radiation ($\lambda = 1.542\text{Å}$) 35KV, 32mA for 45 minutes, to produce the diffraction patterns. In each case the camera diameter was 114.83mm with the film mounted in the Straumanis position.

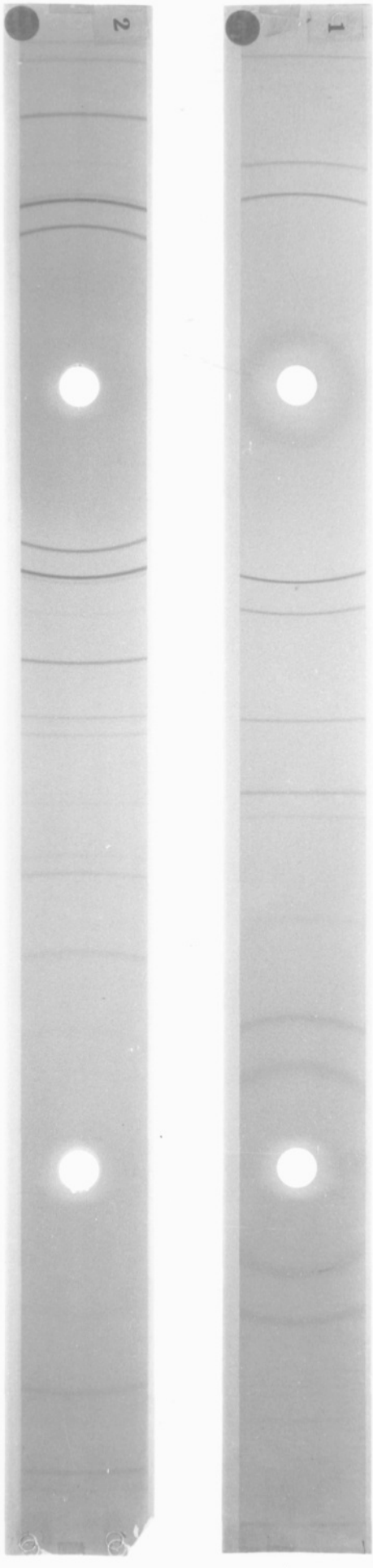
2
1

Identification of two powders by X.R.D.

Each sample was pulverized and loaded into a glass capilliary tube, which was then mounted in a Debye-Scherrer camera. The samples were exposed to Cu K_α radiation (λ = 1.542 Å) 35kV, 32mA for 45 mins, to produce their diffraction patterns. In each case the camera diameter was 114.83mm with the film loaded in the Straumanis position.

1. Untreated Porous Nickel

2	d/(Å)	Rel I
44.5	2.036	V.S.
51.85	1.763	S
76.35	1.247	M
93.5	1.058	M
98.9	1.014	W
122.25	0.880	V.W
145.0	0.808	D
156.0	0.788	D

This corresponds to J.C.P.D.S. file No. 4-850 Ni phase.

2. High temperature treated porous nickel

2	d/(Å)	Rel I
37.15	2.420	S
43.2	2.094	V.S.
44.6	2.032	W *
51.9	1.762	V.W. *
62.8	1.480	S
75.4	1.261	M
79.4	1.207	M
93.8	1.055	V.V.W *
95.8	1.038	V.W.
107.25	0.957	V.W.
111.4	0.932	M
129.5	0.852	W
147.25	0.803	V.V.W

* These lines are attributable to the Ni phase (4-850)

This pattern corresponds to J.C.P.D.S. file No. 4-835 NiO phase. There is, however, a very small amount of Ni phase also present.

Key: S-strong, M-medium, W-weak, V-very, D-diffuse.

Plate 5.2.

Scanning Electron Micrographs of the surface of porous nickel after it has been oxidized under the conditions described in the text.

A.

Magnification: X 3,500

Length of calibration bar: 10μm.

Accelerator voltage: 25KV.

Microscope: Philips T 200.

B.

Magnification: X 2,000

Length of calibration bar: 10μm.

Accelerator voltage: 25KV.

Microscope: Philips T 200.

There are two important points to note in these photographs.

(1) The porous structure of the matrix has remained intact under the oxidizing conditions. This is indicative of the fact that fusion and/or atomic migration have not occured to any great extent under these conditions.

(2) The pitted surface present in the untreated nickel is no longer present. Presumably the smooth surface is attributeable to the formation of a smooth surface oxide layer.

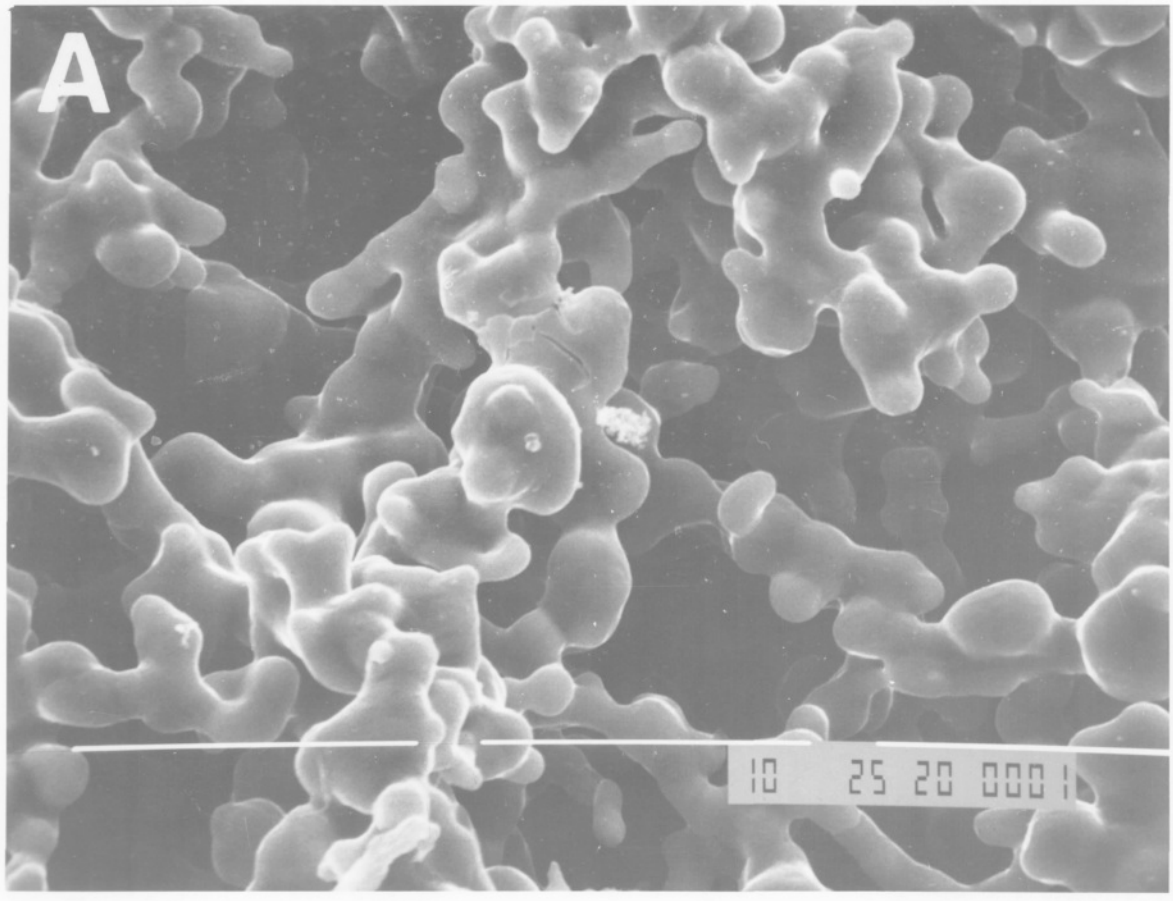
A
10 25 20 0001

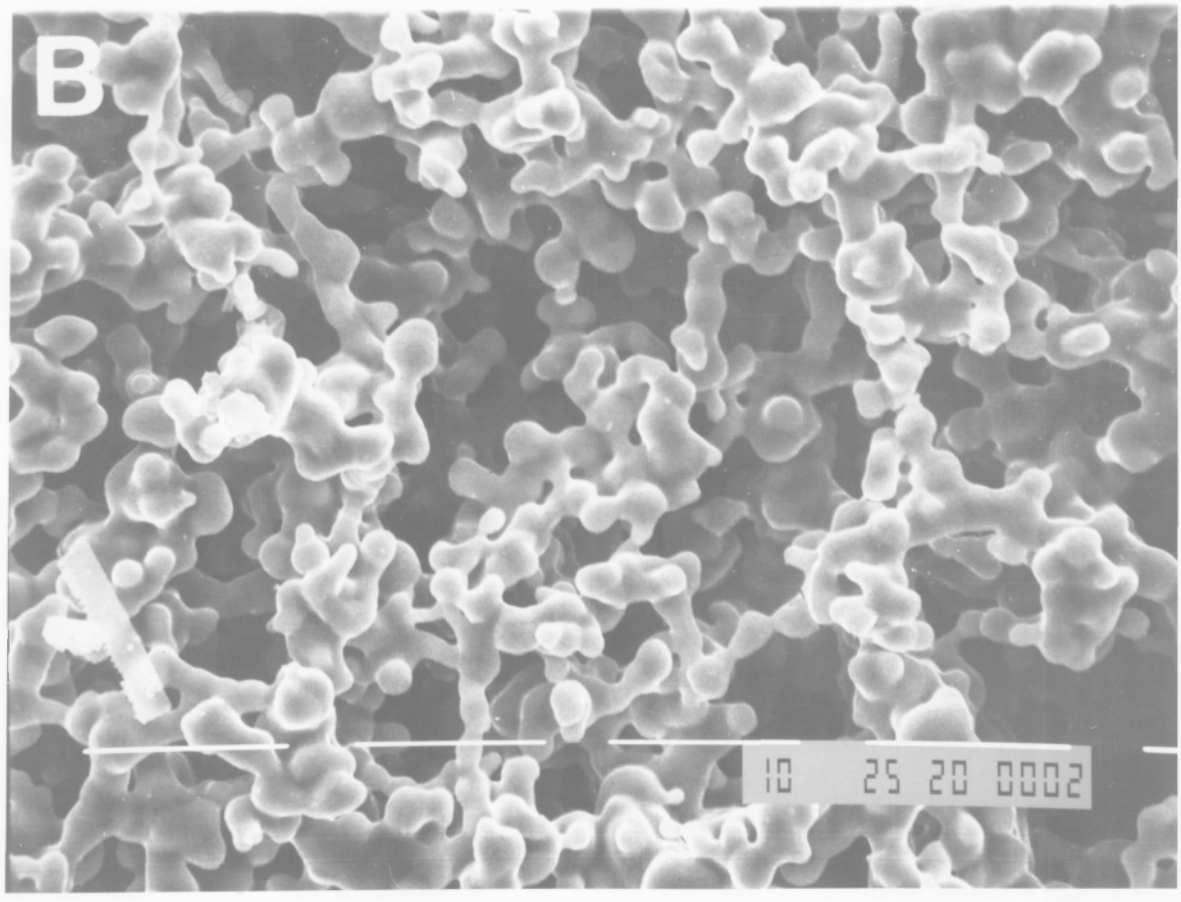
B
10 25 20 0002

Although structurally similar to trichloro benzene, cyanuric chloride is not chemically inert. As a rule, the Cl atoms of cyanuric chloride are more reactive than those of an alkyl chloride but less active than those of an acyl chloride.

Cyanuric chloride has been used to covalently attach enzymes onto water insoluble supports (Kay, G. and Crook, E.M. (1967)) for use in affinity chromatography. The two reactions which make this possible are; (1) the reaction of cyanuric chloride with hydroxy compounds, and (2) the reaction of cyanuric chloride with amino groups. The reactions are summarized below.

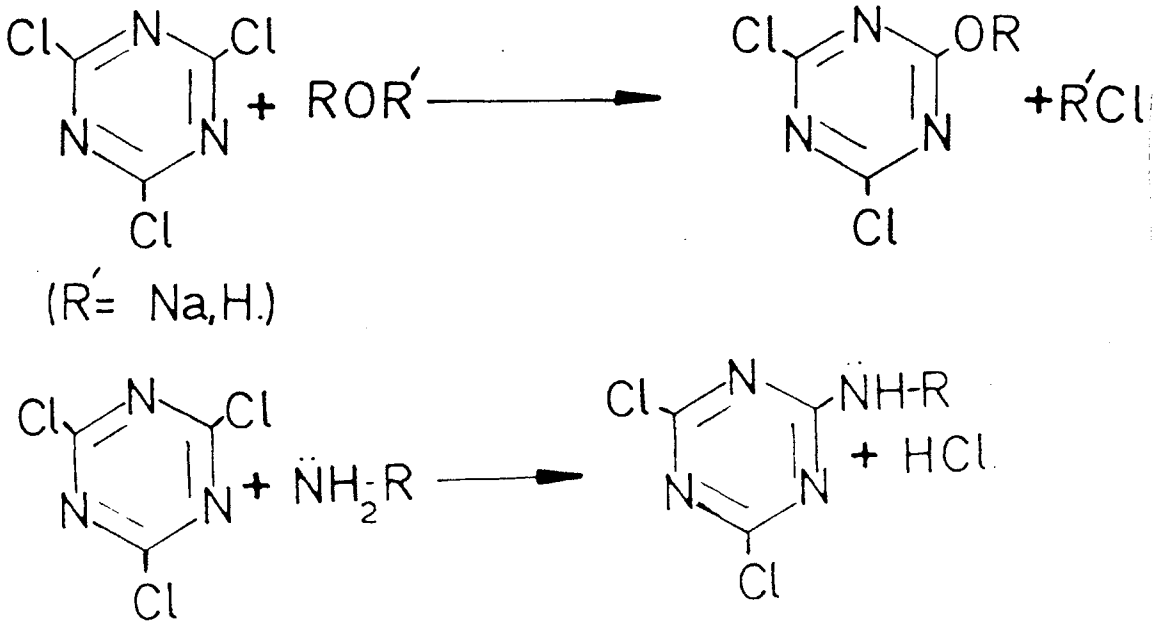

Experimental

i) Maximizing the number of surface reactive hydroxy groups.

In order to maximize the number of surface reactive hydroxy groups the surface was converted to the alkali earth alkoxide species, Ni-ONa. This was achieved simply by refluxing the oxidized porous nickel square in a saturated

alcoholic solution of sodium hydroxide for a period of 6 hours after which time the reaction was considered complete. It is important to note that the analogous reaction with mineral acid, i.e. Ni-o^{-} ⟶ Ni-OH (surface hydroxyl formation) is not suitable in this case, since nickel oxide dissolves in acidic conditions. However, as indicated by reaction scheme 1 above, cyanuric chloride can react with both hydroxyl and earth alkoxide groups. Following this treatment, the nickel square was removed from the reaction vessel and washed thoroughly in ethanol. The square was then stored dessicated in the presence of sodium hydroxide.

ii) Reaction with cyanuric chloride.

Acetone was chosen as the reaction solvent for the following reasons:

(i) Acetone is inert towards cyanuric chloride.

(ii) Acetone is safe and easy to distil.

(iii) The solubility of cyanuric chloride in acetone is 25g/100g of solvent.

Prior to use, the acetone was distilled over molecular sieve (4Å). The distilled acetone was then stored in the presence of molecular sieve to ensure it remained dry.

Cyanuric chloride (99% Aldrich Chemical Co.) was used without further purification. The porous nickel square was reacted with 5g of cyanuric chloride in 20ml dry acetone for 3 hours with refluxing. After this period, the derivitization reaction was considered complete. The porous nickel square was quickly removed from the reaction flask and washed in 100mls of dry acetone to remove any adsorbed reagent. The square was then removed and stored in a dessicator in the presence of silica gel to prevent hydrolysis of the surface

immobilized C-Cl bonds by surface moisture. The derivitized squares were stored under vacuum until needed.

CHARACTERIZATION OF THE DERIVITIZED SURFACE

The types of techniques which are available for the characterization of surface bound species are summarized below. The technique is presented together with the type of information that is obtained from the experiment.

	Technique	Information obtained
i)	Scanning Electron Microscopy (SEM)	Structure
ii)	Photoacoustic Spectroscopy	Molecules.
iii)	Secondary Ion Mass Spectrometry (SIM)	Molecular fragments.
iv)	Infrared)	Bonds
v)	Laser Raman)	
vi)	X-Ray Photoelectron Spectroscopy)	Atoms
vii)	Auger)	

The choice of technique that was used in this investigation was determined by two factors.

(1) The nature of the sample.

(2) Availability of instrumentation.

Infra Red Spectroscopy

Infrared spectroscopy will yield information about the groups present on the porous nickel. The application of this technique to the study of modified electrodes has been pioneered by Dubois (Dubois, J.E. et al (1981)). In order to obtain sufficient signal Dubois employed a multiple pass technique in which the beam was reflected between two metallic mirrors, one of which was also the electrode to be studied. Because of the non reflective nature of the porous nickel, such a technique was not applicable and so other techniques

had to be investigated. These will be described later.

The experimental strategy was to compare the I.R. spectrum of the NiO before and after derivitization with cyanuric chloride by difference spectroscopy and to see if any differences could be detected corresponding to the derivitizing agent.

It should be noted that the spectrum of any surface molecule would be superimposed on that of the NiO and so could only be detected in regions (windows) where the NiO was not absorbing too strongly. Analysis of the spectrum obtained from NiO revealed that there was only one suitable window through which any cyanuric chloride fine structure could be detected (fig. 5.3). This was between 1100 and 600 cm^{-1}.

Description of triazine I.R. spectra

The I.R. spectrum of the parent triazine molecule (1,3,5-triazine), fig. 5.4(a), can be divided into two distinct regions.

1. 1666-1428 cm^{-1} region

Clearly, however, this is outside the window and therefore not suitable for the needs of this work.

2. >833 cm^{-1} region

This region is within the window and therefore suitable for analysis.

In the >833 cm^{-1} region there is a strong band at 735 cm^{-1} and a medium strong band at 676 cm^{-1}. These bands have been respectively assigned as C-H wagging and ring bending (Goubeau, J. et al (1954), (Lancaster, J.E. (1954)).

Derivitization of the parent molecule causes changes to occur in the sym-triazine spectrum. The I.R. spectrum of

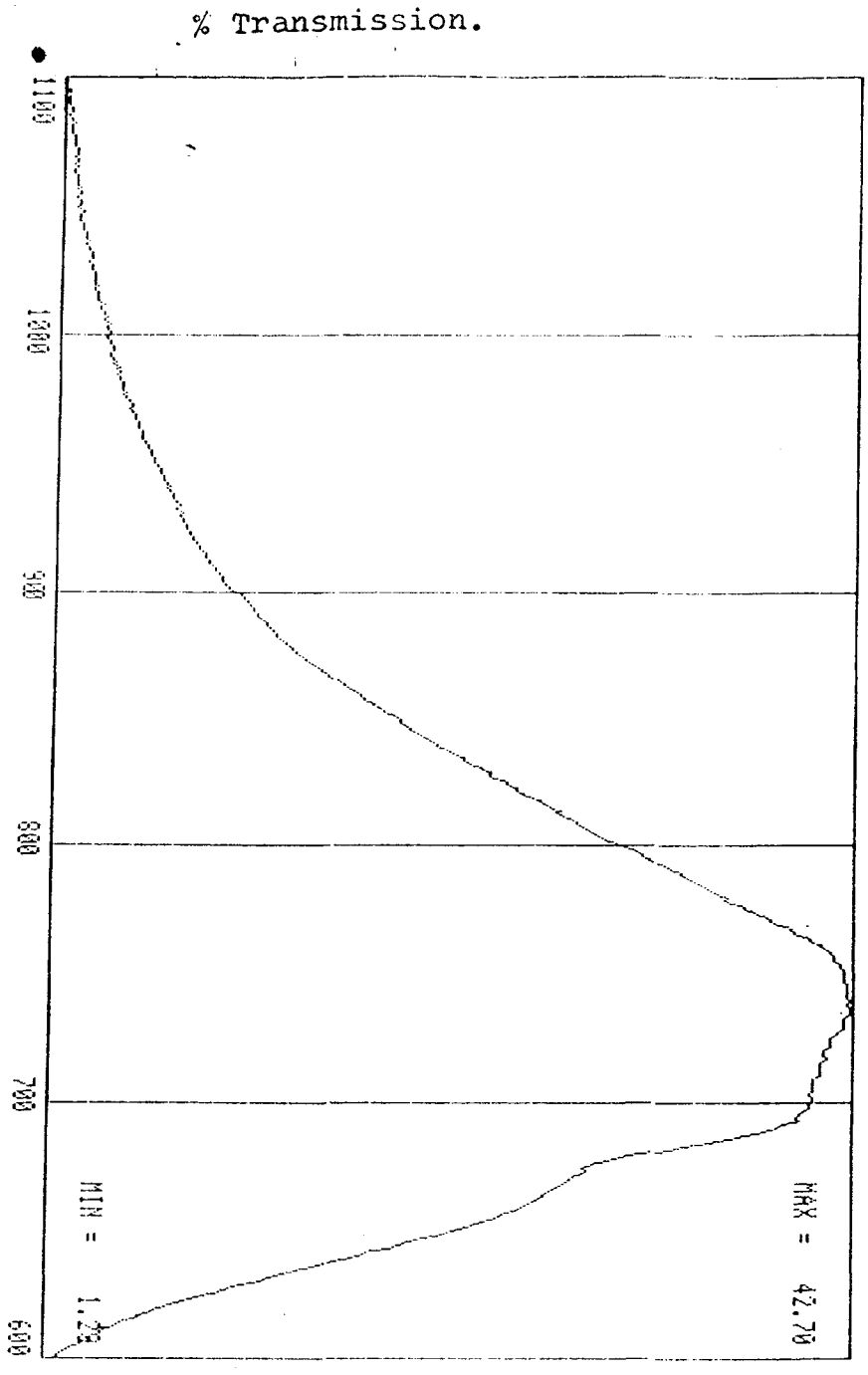

Fig 5.3. Infra Red spectrum of NiO showing the window region. (1,100 to 600 cm^{-1}).

Because of the insolubility of NiO in solvents suitable for Infrared work the material was studied as a KBr disc. Background absorption due to water was eliminated by drying the discs in a dessicator over NaOH.

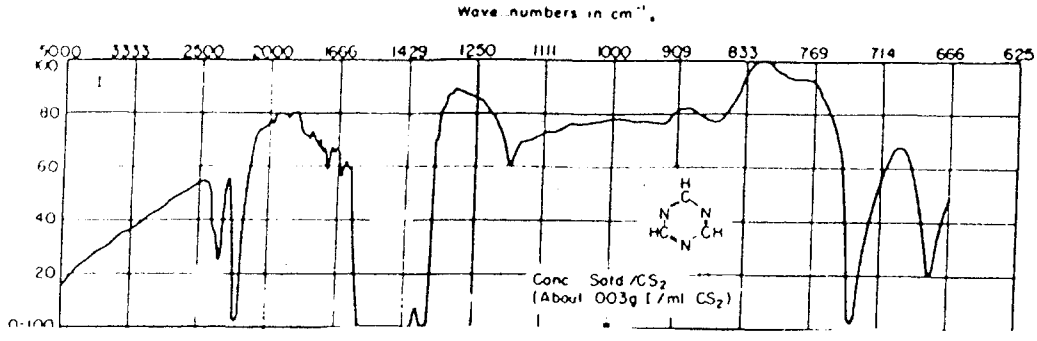

Fig 5.4(a). Infrared spectrum of 1,3,5,-triazine. The spectrum was determined in a solution of carbon disulphide. The broad absorption band between 1400-1600 cm^{-1} is attributable to the solvent. The bands in the 833 cm^{-1} region are clearly visible.

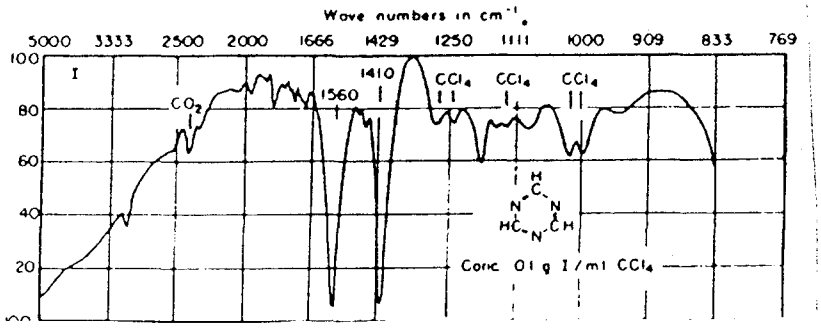

Infrared spectrum of 1,3,5,-triazine in CCl_4 . This time the bands in the region 1666-1428 cm^{-1} region are clearly defined.

(Data adapted from Goubeau et al 1954).

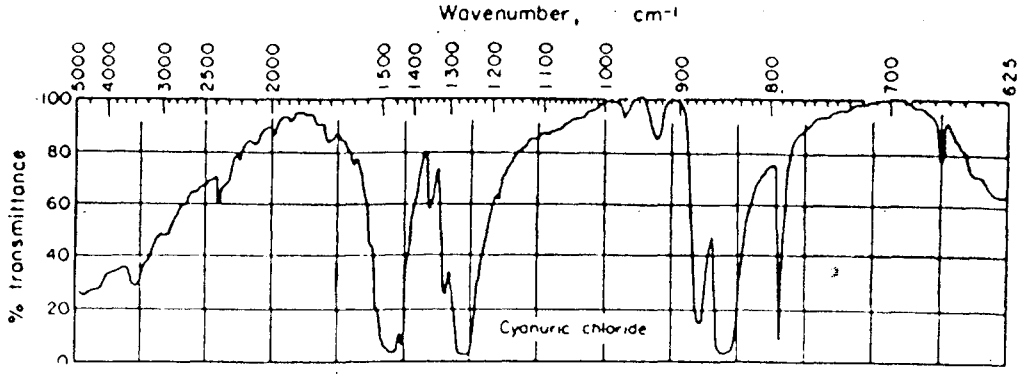

Fig 5.4(b). Infrared spectrum of cyanuric chloride, (2,4,6,-trichloro-1,3,5,-triazine). The sample was prepared as a KBr disc. Note the strong bands occuring at; 1504 cm^{-1}, 1266 cm^{-1}, 855 cm^{-1} and 800 cm^{-1}. An assignment of these bands is given in the text. The spectra of triazines which contain two or three chlorine atoms bonded directly to the ring carbons differ characteristically from those with fewer chlorine atoms by the presence of a strong absorption band at 885 cm^{-1}. This strong band is an especially useful analytical feature of the spectra of dichlorotriazines and permits rapid identification of this class of compounds. The band probably arises primarily from the in-plane asymmetric carbon-chlorine stretching vibration a more complicated description involving part of the ring is probably more accurate. (Adapted from Heckle et al 1961.)

cyanuric chloride, for example, differs from the parent molecule in all absorption bands (fig. 5.4(b)). Strong bands are found at 1504 cm^{-1}, 1266 cm^{-1}, 855 cm^{-1} and 800 cm^{-1}. These bands have been assigned as follows.

Band	Assignment
1504 cm^{-1}	In plane vibration of the substituted ring system.
885 cm^{-1}	C-Cl stretching vibration. This band is diagnostic of dichloro substituted triazines and is often used as a means of rapid identification.
800 cm^{-1}	Ring bending mode analagous to the 14.8μ band in the parent molecule.

(Heckle, W.A. et al (1961))

Only two bands fall within the window region, i.e. 885 cm^{-1} and 800 cm^{-1}.

Groups which are I.R. active in the window region are methoxy (CH_3O- groups). Consequently, a compound such as

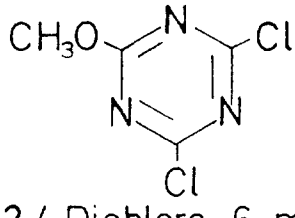

2,4 Dichloro-6-methoxy-s-triazine

would prove useful in this investigation for the following reasons.

(1) The methoxy group would provide extra bands in the window region.

(2) The 885 cm^{-1} band, which is diagnostic of dichloro substituted triazines, is present in 2,4,dichloro-6-methoxy-triazine but would be expected to disappear, following the reaction with the porous nickel.

(3) The chlorine atoms of 2,4,dichloro-6-methoxy-sym-triazine are as reactive as those in cyanuric chloride, and therefore the compound would react in the same way as cyanuric chloride. (SMOLIN, E.M. and Rapoport, L. (1959)).

The I.R. spectrum of 2,4,dichloro-6-methoxy-sym-triazine is shown in fig. 5.5. (Only the region between 1100 and 600 cm^{-1}) was recorded. The bands in this region have been assigned as follows.

Band	Assignment
1030 cm^{-1}	Rotational mode of the methyl group in the $-OCH_3$ moiety.
855 cm^{-1}	Diagnostic C-Cl stretch.
800 cm^{-1}	Ring bending mode.

The remaining two bands have not been assigned directly, however it has been suggested that they are representative of the structure as a whole (Heckle, W.A. et al (1961)). Further support for this comes from the finding that these two bands disappear if the structure is further derivitized (Heckle, W.A. et al (1961)).

Figure 5.6(a) shows the infra red spectrum of the underivitized nickel, showing the window region. Figure 5.6(b) shows the difference spectrum obtained following the derivitization reaction.

Analysis of the difference spectrum reveals that the band corresponding to the $-CH_3$ rotational mode (1030 cm^{-1}) is still present. Furthermore, the band corresponding to the ring bending mode (800 cm^{-1}) is also present, although it has been broadened. The broadening of the band is indicative of many closely spaced absorption modes.

As was expected, the C-Cl stretching band at 855 cm^{-1} has disappeared, suggesting that the reaction has taken place as

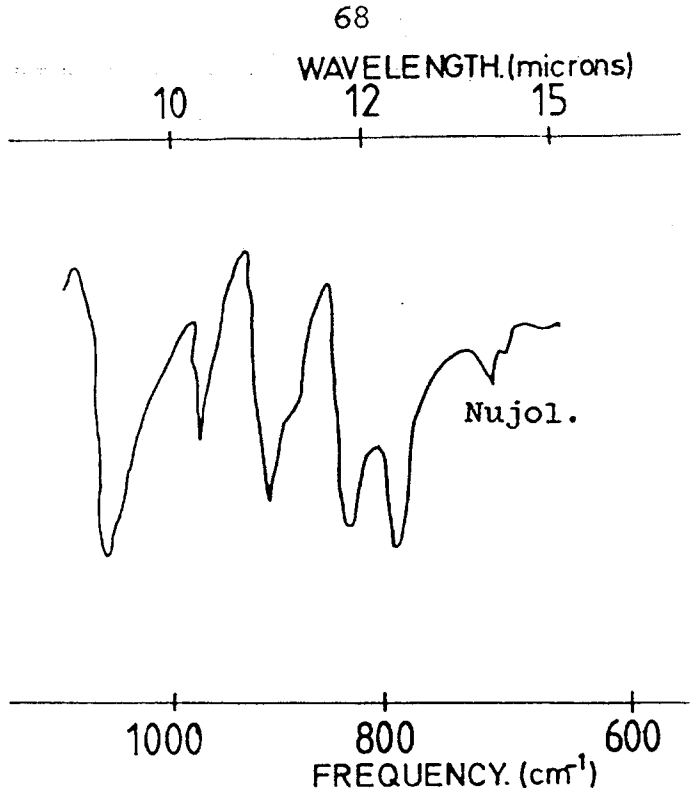

Fig 5.5. Infrared spectrum of 2,4,-dichloro-6-methoxy-1,3,5,-triazine taken in Nujol.(The bands attributable to Nujol have been indicated.) Note the appearance of an extra band at 1030 cm^{-1} in the I.R. spectrum. This band clearly lies within the window region and can therefore be used diagnostically. Note also the presence of the C-Cl stretching band at 855 cm^{-1}.

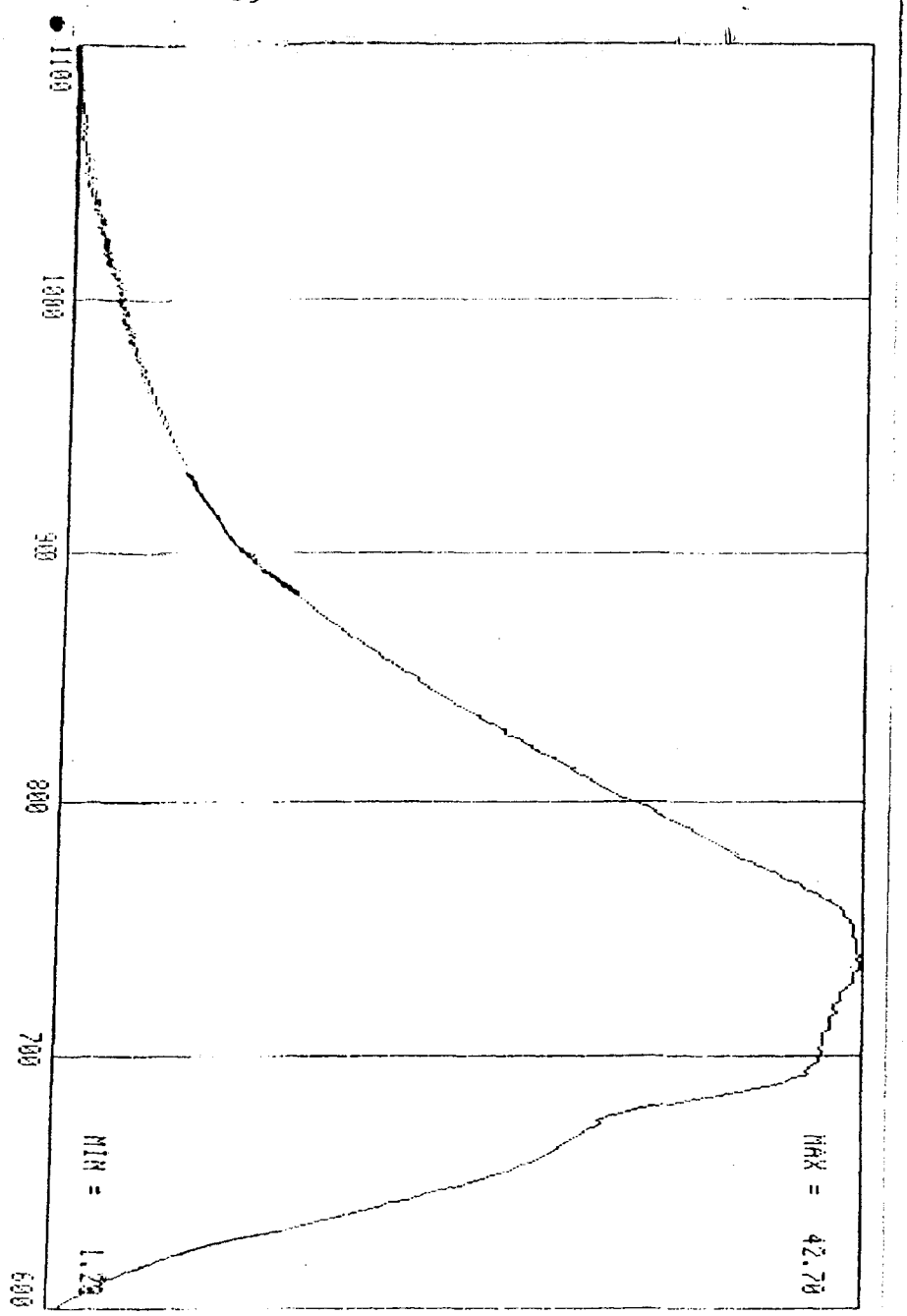

Fig 5.6(a). Infrared spectrum of untreated nickel oxide.

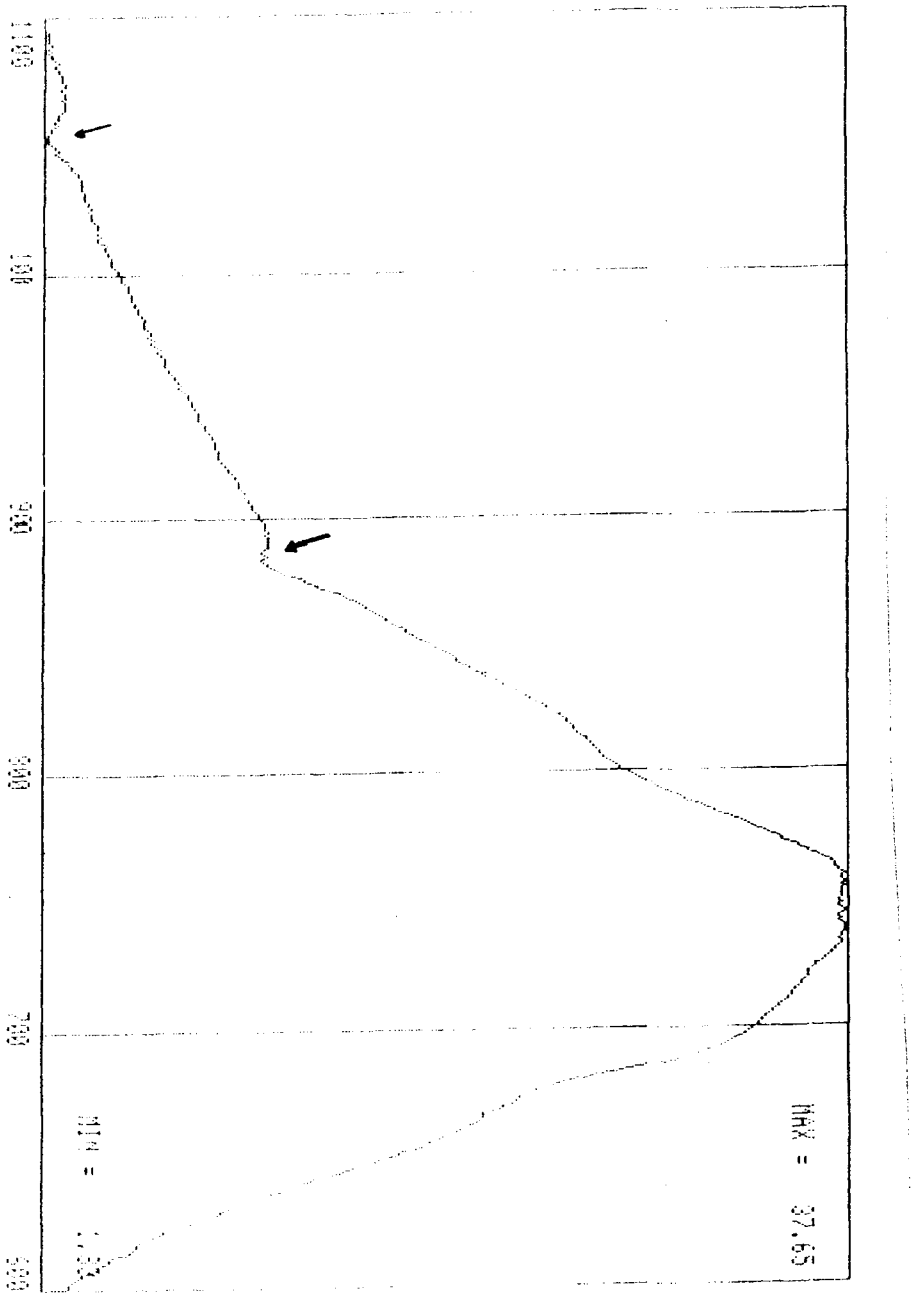

Fig 5.6(a). cont'd. Infrared spectrum of derivitized nickel oxide.

Novel bands are arrowed.

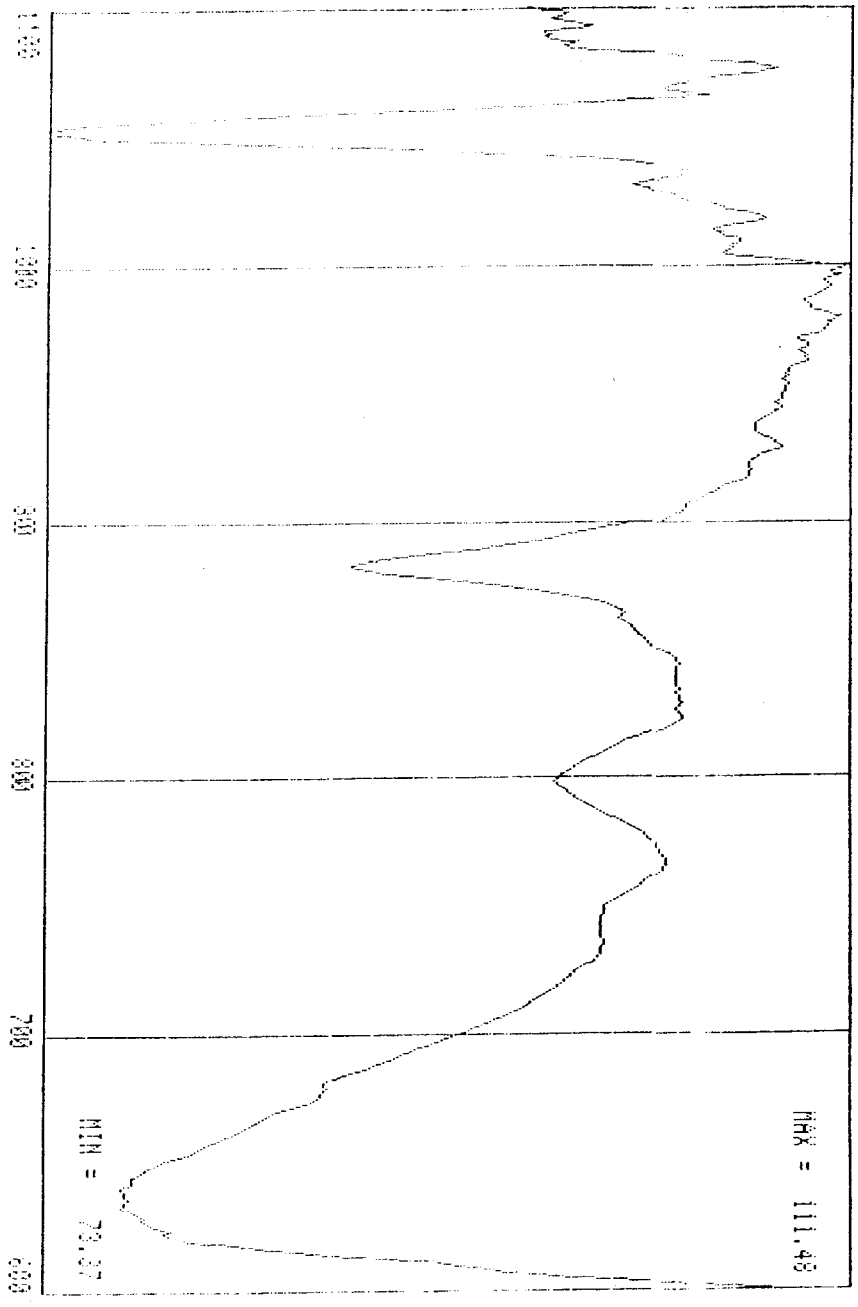

Fig 5.6(b). Computer generated difference spectrum of the derivitized nickel oxide.

follows.

The disappearance of the band at 980 cm^{-1} and the apparent weakening and shifting of the band at 920 cm^{-1} is more difficult to rationalize. Recalling, however, that these bands were sensitive to further substitution, it is suggestive of the fact that the reaction has taken place. In this context, it is interesting to note that the spectrum of the compound 2-Cl,4-cyclohexylamino-6-methoxy-triazine shows the disappearance of the band at 10.9μ and a broadening of the band at 10.3μ. Furthermore, a new band is found at 11.2μ. (Heckle, W.A. et al (1961)). This band at 11.2μ is found in many mono chlorinated-triazines.

The results presented above can be summarized as follows.

1. A compound with a triazine ring structure and methoxy group is present on the porous nickel. The washings indicate that it is not merely absorbed.
2. The triazine ring system is no longer dichlorinated, suggesting that a reaction has taken place via a reactive chlorine.

As a final point, it should be pointed out that the spectrum of the derivitized surface does not show any bands associated with cyanuric acid, indicating that hydrolysis has not taken place.

On the basis of the above information, the following reaction sequence is tentatively suggested.

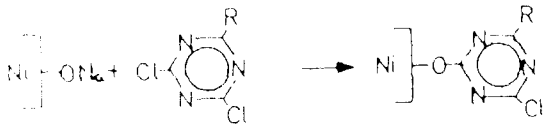

The experimental techniques discussed above were used whenever the derivitization step was carried out.

ENZYME IMMOBILISATION

From a synthetic point of view, the derivitized surface of the porous nickel can now be viewed as a triazine surface.

The reaction of triazines with amino groups, the chemical basis of the immobilisation, has already been discussed.

The immobilisation reaction was standardized as follows.

1) Concentration of enzyme was 1mg/ml in 0.1M carbonate buffer pH 12. The high pH was chosen to ensure that the surface amino groups would be present in their active form, i.e. $-NH_2$ and not $-NH_3^+$. Carbonate buffer was chosen since this represented a non nucleophilic buffer and would therefore not compete with the reaction. The high concentration of enzyme was chosen to maximize the immobilisation reaction.

2) The derivitized porous nickel was left in contact with the enzyme solution for 12 hours at 4°C.

After this time, the square was removed from the reaction vessel and washed with copious amounts of cold high purity water to remove all traces of adsorbed enzyme. The squares were finally washed in 0.1M phosphate buffer pH 7, until no enzyme activity was detected in the washings.

In order to unequivocally ascertain immobilized activity, the following criteria had to be fulfilled:

1. The response should be dependent on the concentration of substrate in that the larger the amount of substrate present in this solution, the faster the reaction rate. (This is of course assuming that the concentration of substrate is below the K_M value for the enzyme.)

2. If the nickel square is removed from the solution, then

the reaction should cease. (In effect this is the same as removing the enzyme from the reaction mixture). The reaction should commence once the porous nickel is reimmersed into the solution. Note that if the reaction is seen to proceed after the square has been removed, it would imply that enzyme has desorbed from the support.

3. If the immobilized enzyme is denatured, e.g. by heat treatment, then no activity should be recorded from the porous nickel.

Figure 5.7 shows such results for Ribitol dehydrogenase immobilized onto the surface of the porous nickel. Note that each of the three criteria described above is satisfied. Similar results were obtained for immobilized glucose oxidase and alcohol dehydrogenase.

Immobilized Enzymes

The general techniques currently in use for insolubilizing enzymes have already been reviewed in Chapter 1. It is now pertinent to discuss the effects that immobilization can have on the enzyme, both in terms of its physical and kinetic parameters. The types of changes which can result following immobilization can be considered as follows.

i) Change in the K_m of the enzyme and in the reaction rate.

ii) Change in the pH optimum of the enzyme.

iii) Altered thermal and storage properties of the enzyme.

In terms of an altered reaction rate, the diffusion of substrate from the bulk to the immediate environment (micro-environment) of the immobilized enzyme can be an important

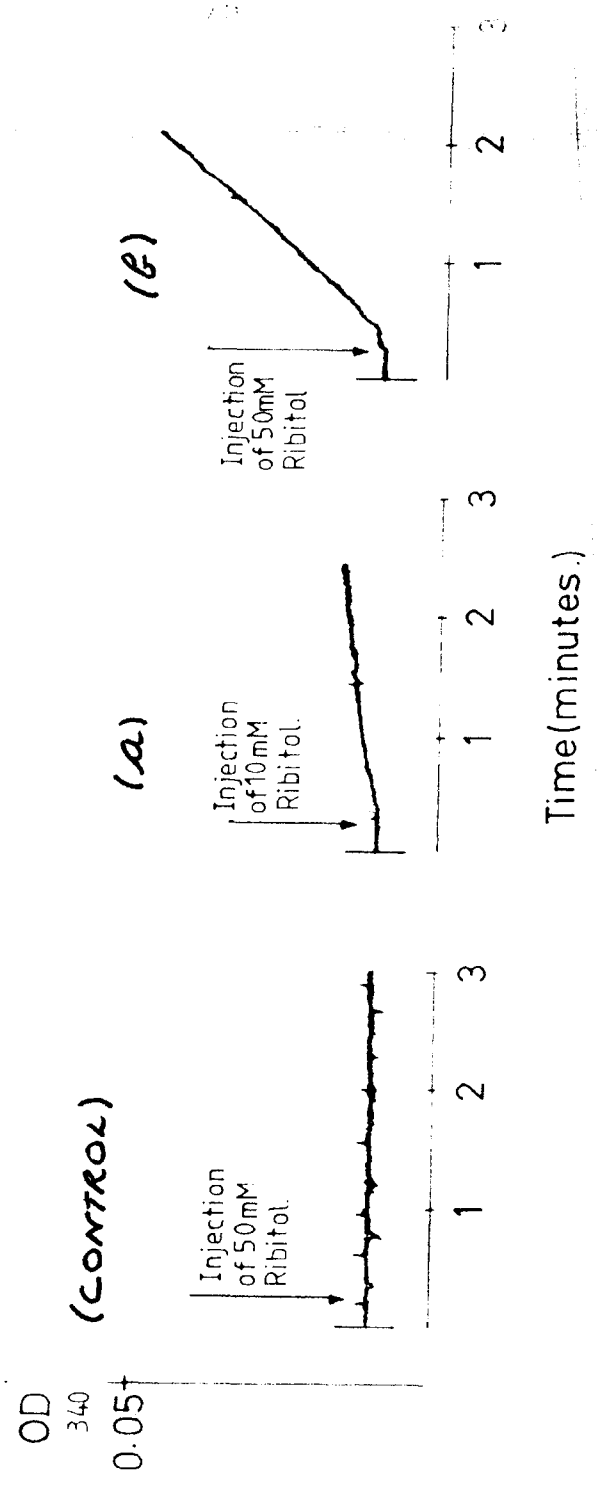

Fig 5.7 (1). Effect of varying the concentration of substrate on the rate of the reaction catalysed by the immobilized enzyme.

Trace (a) shows the response when 10mM ribitol is injected into the reaction vessel. The rate of the reaction (ΔOD_{340} /hour is 0.15).

Trace (b) shows the response when 50mM ribitol is injected into the reaction vessel. In this instance, the rate of the reaction (ΔOD_{340} /hour is 0.99).

This type of observation is consistent with the idea of enzyme catalyzed reactions, i.e. the greater the amount of substrate present the greater the rate of the enzyme catalysed reaction

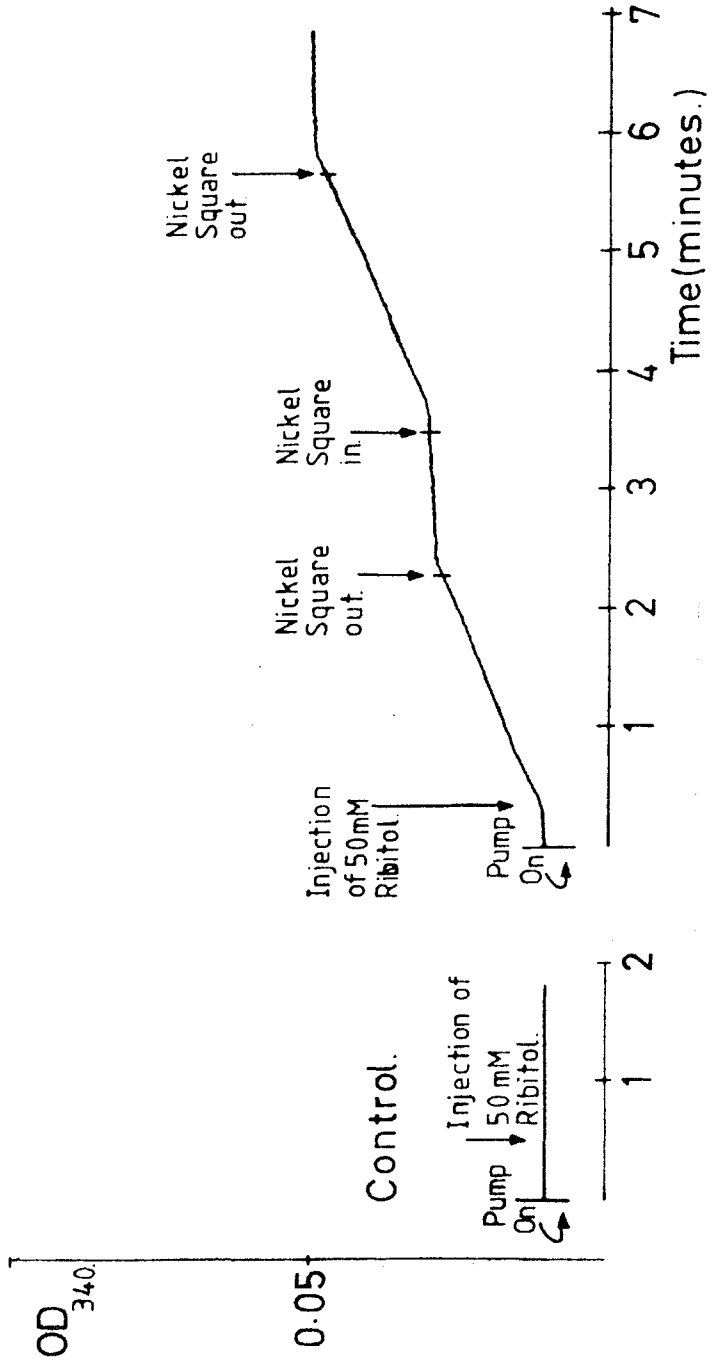

Fig 5.7 (2). Effect of removing the nickel support from the reaction vessel at the times indicated above.
As can be seen, when the porous nickel support is removed from the reaction vessel the reaction ceases, i.e. ΔOD_{340} becomes zero.

This finding is consistent with the idea of a reaction catalysed by an immobilized enzyme since removing the support is equivalent to removing the enzyme from the reaction which would result in the reaction ceasing. Note, had the reaction continued after the porous nickel had been removed, this would have been indicative of the enzyme having become unstuck from the support.

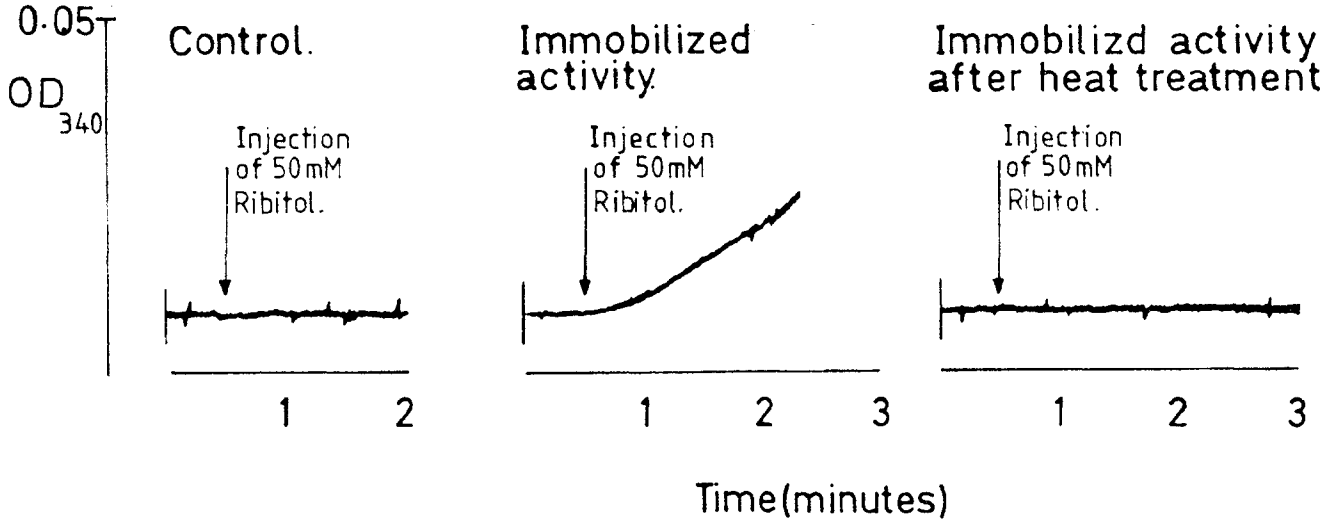

Fig 5.7 (3). Effect on the reaction after having subjected the nickel support to a temperature of 100° C for 3 minutes. As can be seen, after this treatment no reaction is detected, i.e. OD_{340} is zero over the time scale of the experiment. Again, this finding is consistent with the idea of an enzyme catalysed reaction since the heat treatment would inactivate the enzyme and thus it would no longer be able to catalyse the reaction.

Notes:

In all these examples, the control was immobilized BSA. Before any experiments were attempted it was important to establish a steady base-line. Only then was the experiment started.

factor. (This factor becomes particularly relevant when the enzyme is encapsulated within a gel matrix such as polyacrylamide where large diffusional resistances can be encountered).

In the microenvironment of the immobilized enzyme the substrate concentration is generally lower than in the overall bulk (Katchalski, E. et al (1971)). This concentration is dependent, to some extent, upon the rate of flow of substrate to the immobilised enzyme, which in turn also influences the concentration of product and its rate of removal. Consequently, within limits a faster flow of substrate over a packed bed or faster stirring of suspended enzyme, will increase the rate of the reaction.

Another important parameter which affects the concentration of substrate in the microenvironment is the molecular weight of both the substrate and product, which will influence their diffusional resistances and hence the overall role of the reaction. These diffusional resistances are of two kinds:

i) The diffusional resistance for the external transport of substrate and products between the bulk solution and the external surface of the enzyme containing matrix. This is influenced by the hydrodynamics of the system and can be improved, for example, by increasing the flow rate or stirring speed in the reactor vessel.

ii) The diffusional resistance for the internal transport of these species within the internal matrix of the support, e.g. within the pores of porous nickel or the pores within a polyacrylamide gel matrix.

Theoretical models have been reported in the literature

dealing with the effects of both external and internal diffusion on the rate of an enzyme catalyzed reaction (RUCKENSTEIN, E. et al (1982)). As a general rule, it is true to say that the larger the molecular weight of the substrate, the lower the overall reaction rate. This point is reflected in the current industrial processes based on immobilized enzymes which are all dominated by small molecular weight substrates such as fructose or glucose.

Finally, it is also important to consider the nature of the support, especially in terms of its surface electrical charge. This is important particularly if either the substrate or product are charged species since ultimately the transport of these species and the equilibrium concentration, due to partitioning, will be influenced by the resulting electric field in the microenvironment. The electrical charge on the surface of the support is assumed to arise from the dissociation of acidic and basic groups present on both the enzyme and the support (RUCKENSTEIN ,E. et al (1982)).

Observed changes in the apparent K_m of the immobilized enzyme can be explained in terms of the parameters discussed above but can also be explained in changes occurring in the enzyme itself. This is particularly the case if the method of immobilisation involves chemical modification of the enzyme, which is likely to result in conformation changes in the protein. Consequently, these conformation changes can be manifest in changes in the kinetic parameters of the enzyme such as an improved K_m.

Another important parameter which is affected by the electrical charge on the surface of an insoluble enzyme support is the apparent pH optimum of the immobilized enzyme.

For example, pH gradients may develop from the bulk to the surface of the support and that the pH of the microenvironment is considerably different from that of the bulk solution. It is evident from this that if the pH of the enzyme microenvironment is closer to the stability optimum than that of the solution, then an apparent "stabilization" of the immobilized enzyme against pH inactivation will be seen. In the opposite situation an apparent "destabilization" will be seen.

An interesting case of altered pH optimum can arise when the microenvironment of the immobilized enzyme possesses buffer properties. This can be due to either the nature of the support surface or an effect produced by neighbouring protein molecules. If so, even considerable changes in the bulk solution will produce only small pH shifts in the microenvironment. This mechanism may be responsible for an observed stabilization of lactate dehydrogenase against acid inactivation. While the free enzyme is completely inactivated on incubation at pH 3.2 for one hour, lactate dehydrogenase covalently attached to porous glass beads, under the same conditions, retains 100% of its catalytic activity, even after 35 days (Klibanov, A.M. (1978)). As a final point, it is necessary to establish that the carrier is itself stable under the pH conditions of the reaction and will not steadily dissolve. Glass, for example, will dissolve at alkaline pH, lowering the retention of the bound enzyme.

The inactivation of water soluble enzymes by heat involves considerable conformational changes in the protein molecules such as unfolding. On the basis of this, it can be appreciated that if the protein molecule is fixed firmly

to a support, it will be more difficult to unfold. This is shown below in diagrammatic form. As a consequence, it is more difficult to inactivate.

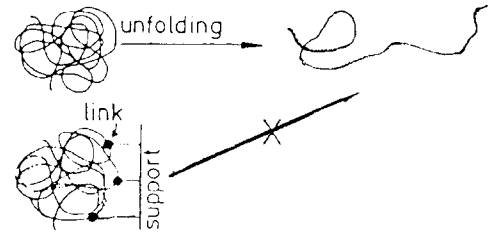

If the enzyme is linked to the support by several strong chemical bonds, case (b) above, the structure of the protein molecule as a whole will be much more rigid and therefore unfolding, as well as heat inactivation, will be much more difficult to accomplish than in the case of the free enzyme, example (a) above. Experimental proof for such a model has come from the work of Delaage and co-workers (Delaage, M. and Lazdunski, M. (1968)), who showed that the more linkages that existed between trypsin and Sephadex, the more stable the protein appeared against inactivation, e.g. by urea.

It must be pointed out, however, that some enzymes are very sensitive to chemical modification and hence inactivate upon covalent immobilization, even though many stable links may have been formed between the enzyme and the support. Under these conditions, physical methods, e.g. adsorption or gel entrapment, must be used for their immobilization. Thus, the means of immobilization can be a very important parameter in determining the apparent stability of the immobilized enzyme.

Finally, the main principles concerned, all or in part, with enzyme stabilization, may be summarized as follows.

i) Localization of enzyme molecules in the parts of the supports where they are sterically inaccessible from the

action of microorganisms and proteases.

ii) Mutual spatial fixation of enzyme molecules to prevent intermolecular inactivation processes, such as autolysis and aggregation.

iii) Multipoint attachment of enzymes to prevent unfolding of the protein molecules.

iv) The attachment of oligomeric enzymes to the supports via all their subunits and therefore preventing dissociation.

v) The attachment to enzymes to surfaces possessing buffering groups.

vi) Reactivation of inactivated enzymes through the use of unfolding-refolding procedures.

Experimental

The activities of the three immobilized enzymes were assayed as outlined in Materials and Methods.

Having successfully developed a protocol for the covalent immobilisation of enzymes to the surface of the porous nickel, the first parameter to be investigated was the apparent kinetics of the immobilized enzyme preparations.

Results showed, fig. 5.8, that under the experimental conditions reported above the apparent K_m values of immobilized ribitol dehydrogenase for both ribitol and NAD^+ were identical to those of the soluble enzyme.

In terms of the above discussion, this can be explained by suggesting that the diffusion of these species is in no way limited by the insoluble matrix. Thus, the concentration of both NAD^+ and ribitol in the microenvironment of the enzyme are sufficiently close to those in the bulk solution so as not to alter the kinetics of the reaction. This also implies

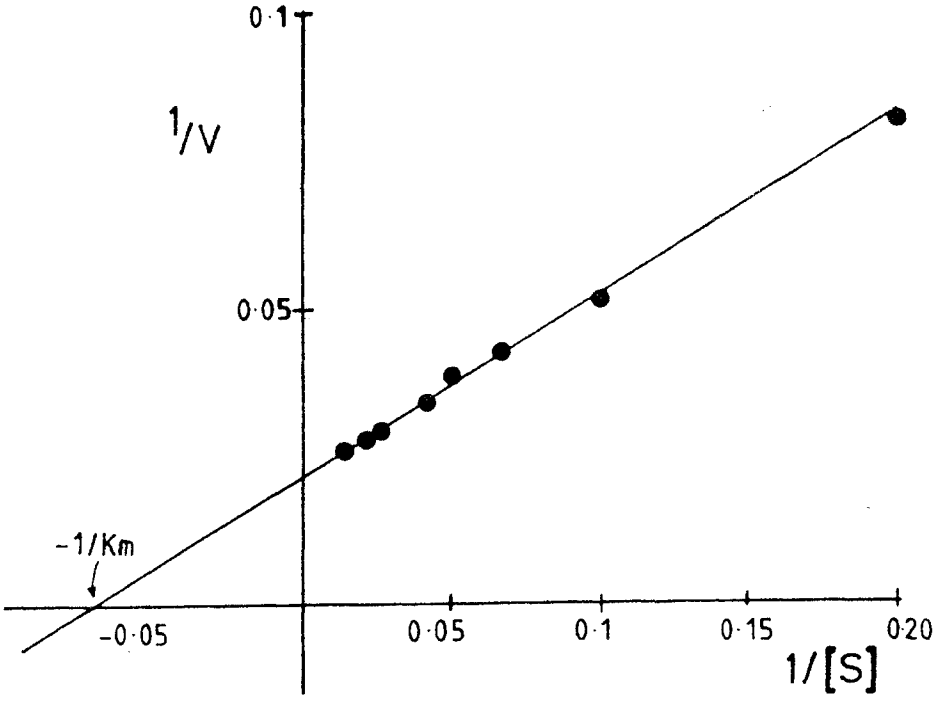

Fig 5.8. Lineweaver-Burke plot of kinetic data for porous nickel immobilized ribitol dehydrogenase.

An apparent K_m value for ribitol of 14.9mM is obtained for immobilized RDH.

It must be appreciated that this approach neccesitates the lumping together of the combined effects of internal diffusion rates and reaction rates into an apparent K_m. This of course makes any interpretation of the results in terms of Michaelis - Menten kinetics extremely difficult.

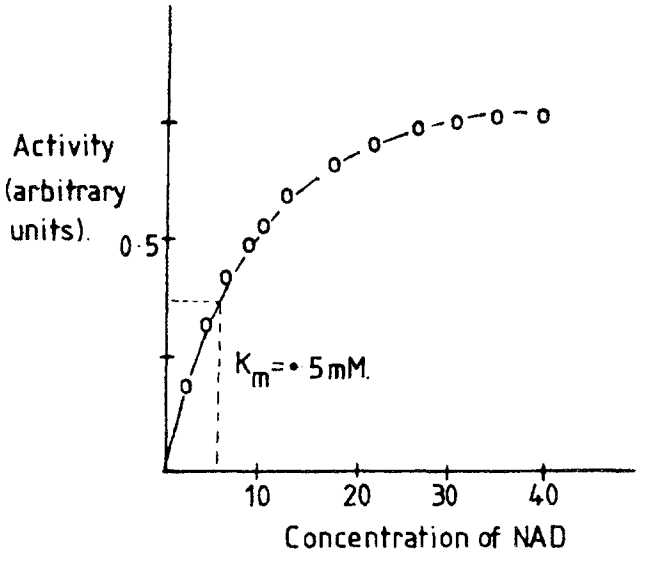

The activity of the immobilized enzyme was measured

in the presence of saturating amounts of ribitol.

The assay buffer was as described in materials and methods.

that the basic properties of the enzyme, e.g. conformation, have not been altered during the immobilisation. Alternatively, it could be argued that some structural change in the enzyme has resulted, following the immobilization and this is some way cancels out any concentration effects in the microenvironment of the enzyme. It is of course extremely difficult to differentiate either of these possibilities.

Similar results were obtained with immobilized alcohol dehydrogenase. With this enzyme, identical kinetics to those of the soluble enzyme were observed.

More interesting results were obtained with immobilized glucose oxidase (fig. 5.9 . As can be seen from the data, the apparent sensitivity of glucose oxidase for its substrate increases following immobilisation onto porous nickel. This is manifest in two ways:

1. The decreased K_m observed with the immobilized enzyme.
2. The steepness of the curve in the linear portion of the curve.

The explanation for this result is complex. It may be that the observed kinetics can be accounted for by conformational changes occurring in the enzyme following the immobilization onto the porous support.

Alternatively, it may be argued that the concentration of glucose in the microenvironment of the immobilized enzyme is greater than in the bulk solution and that this accounts for the lowering of the apparent K_m. However, it is difficult to accept this, particularly in the light of the results obtained with ribitol dehydrogenase. As a final point it is worth noting that for its catalytic activity, glucose oxidase

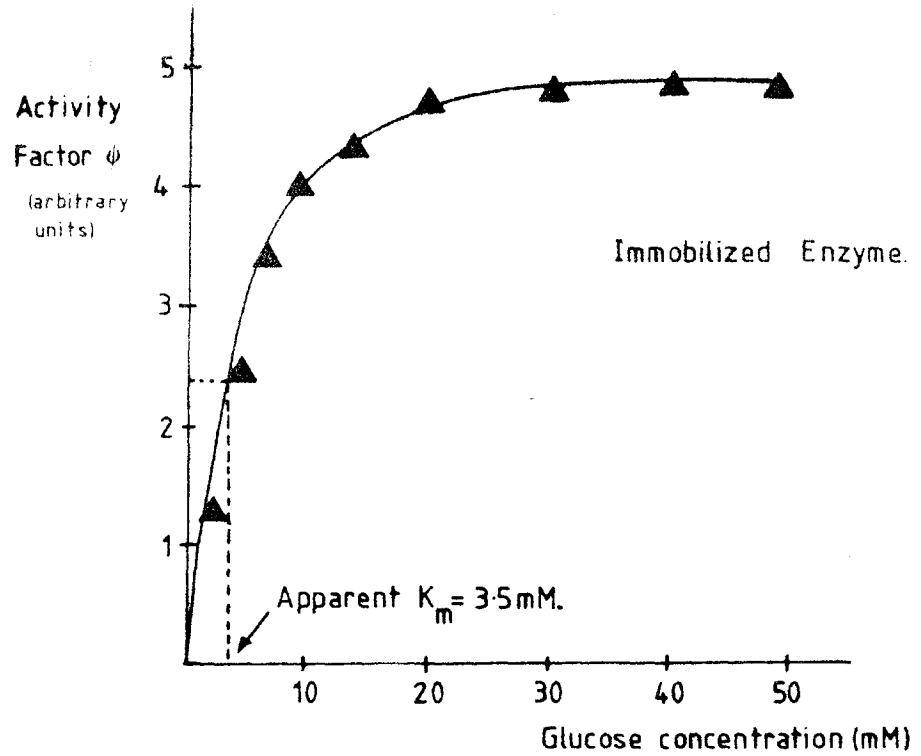
Activity
Factor ψ
(arbitrary
units)
5
4
3
2
1
Immobilized Enzyme.
Apparent K_m = 3·5mM.
10
20
30
40
50
Glucose concentration (mM)

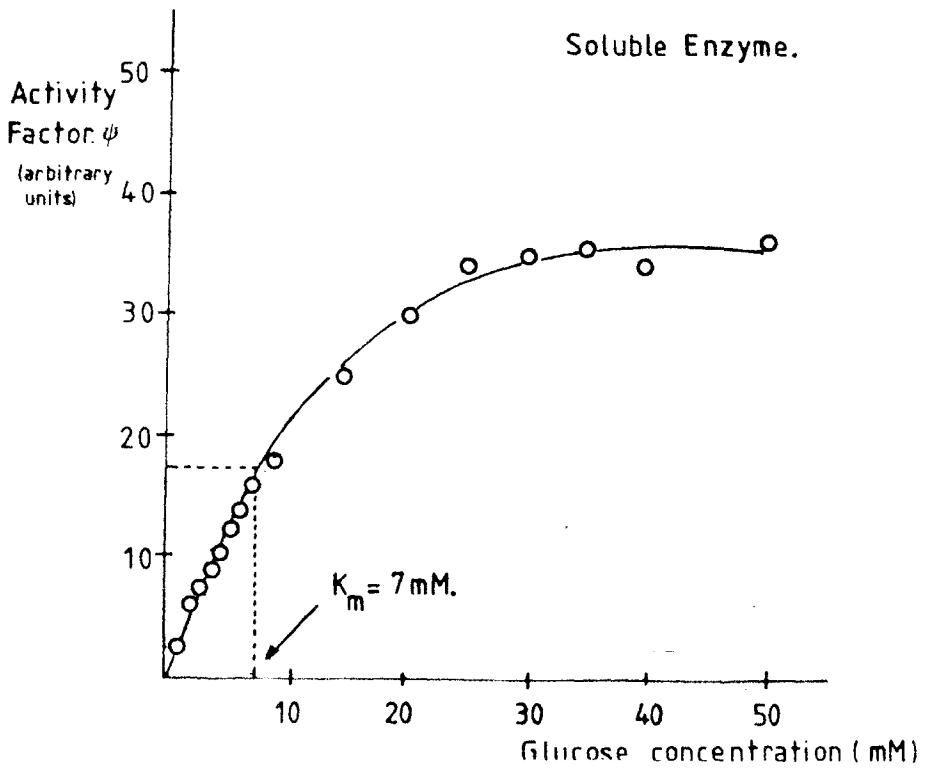
Soluble Enzyme.
Activity
Factor ψ
(arbitrary
units)
50
40
30
20
10
K_m = 7mM.
10
20
30
40
50
Glucose concentration (mM)

Fig 5.9.

is dependent on oxygen and so it may be argued that under these conditions there may be partitioning effects between the dissolved oxygen in the bulk solution and that seen by the enzyme in the internal matrix of the porous support. Such an effect, i.e. an apparent decrease in the dissolved oxygen tension, would result in the concentration of oxygen being rate limiting and hence explain the decreased apparent K_m.

For the sake of comparison, the apparent Michaelis-Menten kinetics for immobilized glucose oxidase from other workers is shown below:-

Support	K_m
Activated carbon (30°C pH5)	3.40 mM
Collagen (30°C pH5.9)	7.1 mM
Polystyrene tube (35°C pH5.6)	15 mM
Non porous glass bead (25°C pH5.5)	0.07 mM

(Data adapted from Cho, Y.K. and Bailey, J.E. (1978))

As can be seen, the range of reported values is large, presumably indicative of differences in mass-transfer intrusions among these various forms of immobilized glucose oxidase and differences due to immobilisation chemistry.

The next parameter to be investigated was the effect that the immobilization had on the thermal stability of the three test enzymes. The results obtained in this investigation, fig. 5.10, indicated that in all cases the observed thermal stability was greater for the immobilized enzymes than for the corresponding solution enzymes. This result can be explained in terms of the model presented above, i.e. immobilization of the enzyme to the support increases the rigidity of the enzyme and is therefore less easy to denature, at the elevated temperatures.

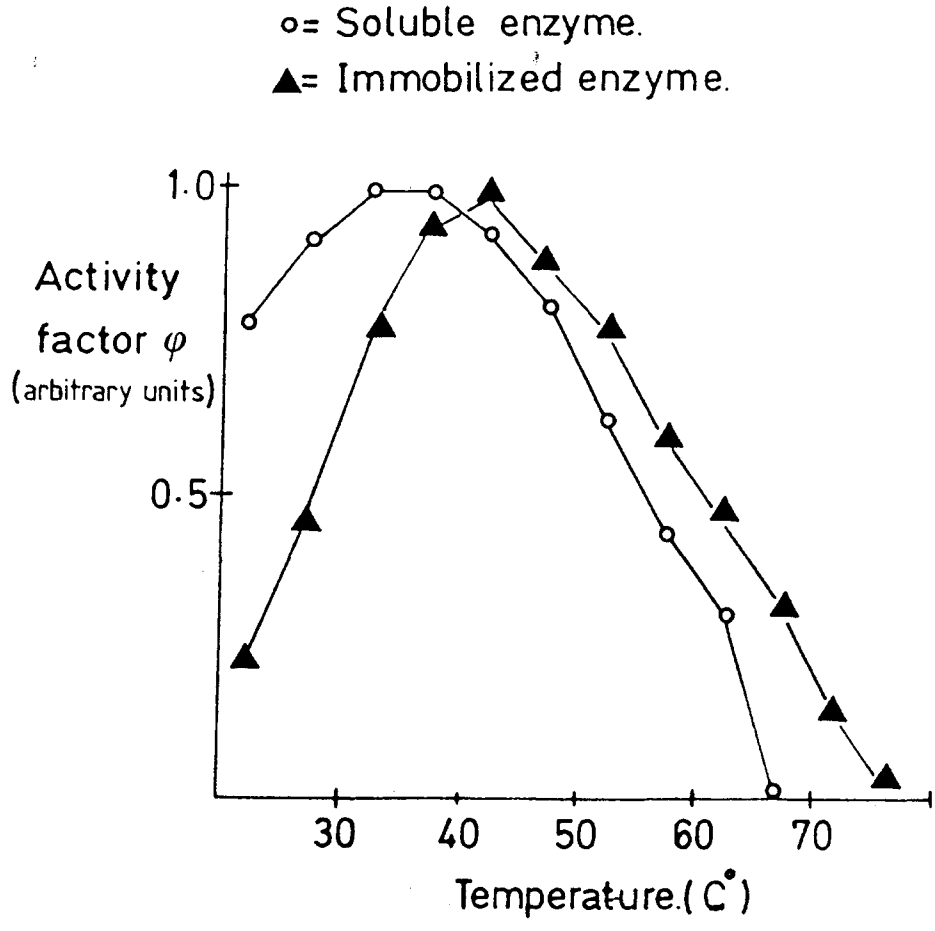

Fig 5.10.

Apparent thermal stabilization of ribitol dehydrogenase following its immobilization to the porous nickel support with cyanuric chloride.

T_{max} soluble enzyme.	T_{max} insoluble enzyme.
36°C	42.5°C

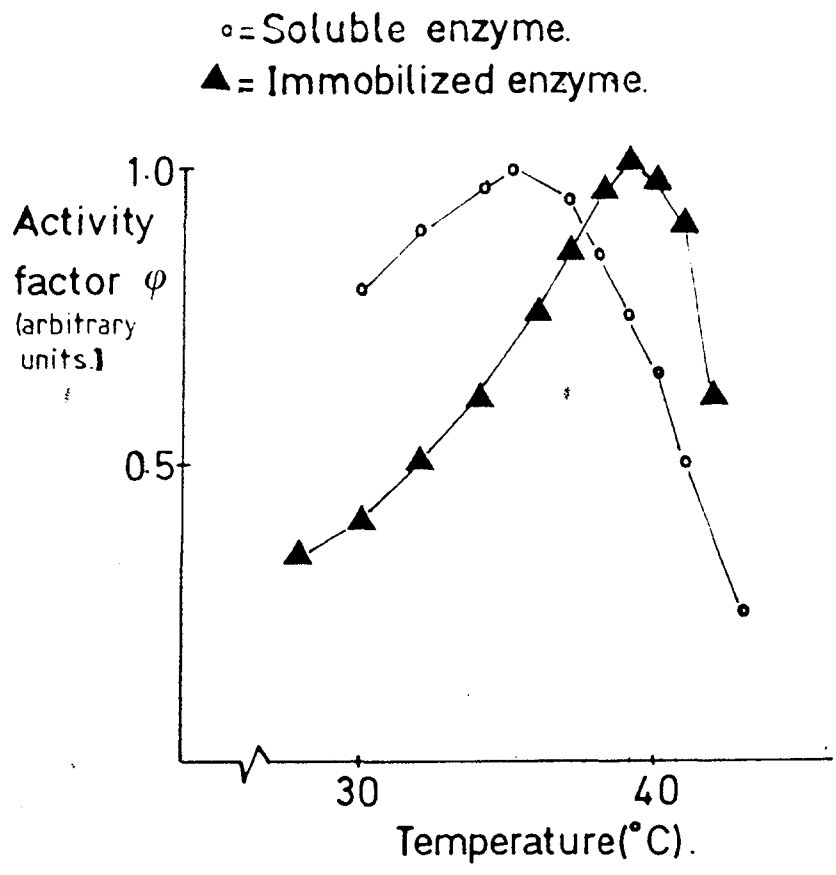

Fig 5.10. cont'd.

Apparent thermal stabilization of alcohol dehydrogenase following its immobilization to the porous nickel support with cyanuric chloride.

T_{max} soluble enzyme. 35.5°C.

T_{max} insoluble enzyme. 39°C.

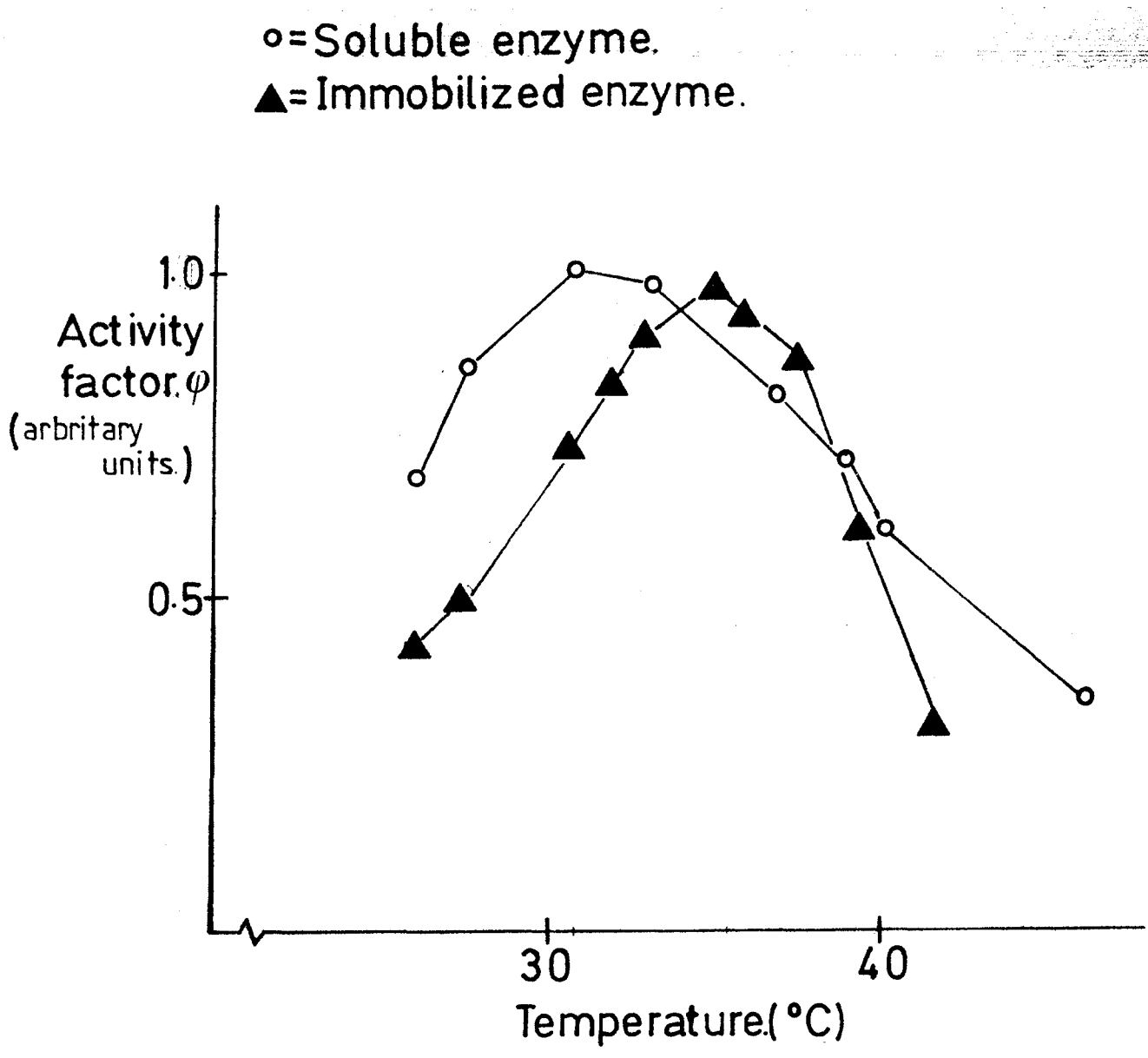

Fig 5.10. cont'd.
Apparent thermal stabilization of glucose oxidase following its immobilization to the porous nickel support with cyanuric chloride.

T_{max} soluble enzyme. 30.8°C

T_{max} insoluble enzyme. 35.5°C

Another important finding which came out of this work was the stability of the bond formed between the enzyme and the support using cyanuric chloride as the linking agent. In this context it was found that the immobilized enzyme preparations could be used continuously (up to three hours) without any apparent loss of immobilized enzyme. In this respect the immobilization reported in this work appears more stable than that reported by Halling and Dunnill (Halling, P.J. and Dunnill, P. (1979)). It is difficult to explain this finding by suggesting that a Ni-O-C linkage is more stable than a Ni-O-Si bond. Rather, the reason for this apparent linkage stability may lie in the fact that the oxide layer prepared on the surface of the nickel is a more stable coating than that reported by Dunnill. (The importance of a stable surface oxide film in terms of manufacturing stable modified electrodes has been alluded to by Murray and others (Murray, R.W. (1980)) and (Bocarsly, A. and Sinha, S. (1982)). Clearly, an unstable oxide film would lead to desorption of the immobilized enzyme under operational conditions.

Finally, the effect of pH on the activity of immobilized glucose oxidase was investigated. The results of this investigation are shown in fig.5.11.The shift in pH optimum reported here is approximately 1 unit towards the alkaline and furthermore the pH curve appears broader.

Storage stability of the immobilized enzyme preparations

The stability of the immobilized enzyme preparations was tested every day for a period of 10 days. The results, fig. 5.12 show the following. (Common decay patterns of enzyme activity of immobilized systems are shown in fig. 5.13).

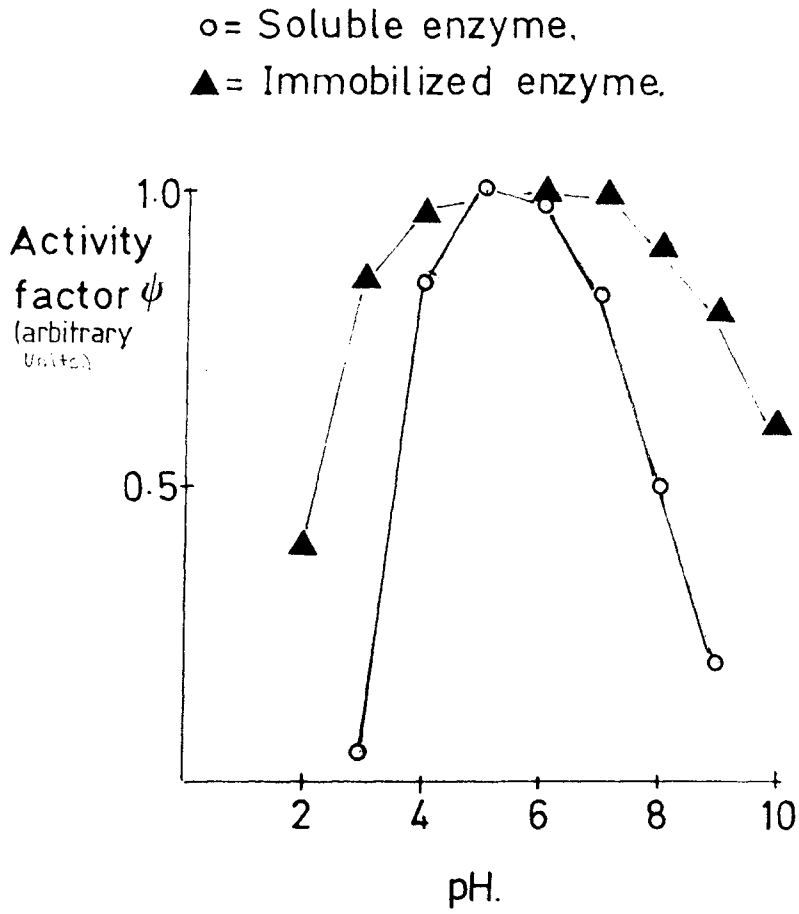

Fig 5.11.

Comparison of the pH dependence of glucose oxidase activity in solution and of apparent activity of glucose oxidase immobilized onto porous nickel.

The shift in the pH optimum in this example is approximately 1 unit toward the alkaline. Note also a broadening of the pH activity profile resulting from immobilization. This apparent decrease in parametric sensitivity of the immobilized enzyme may be a result of diffusion reaction interactions within the porous matrix.

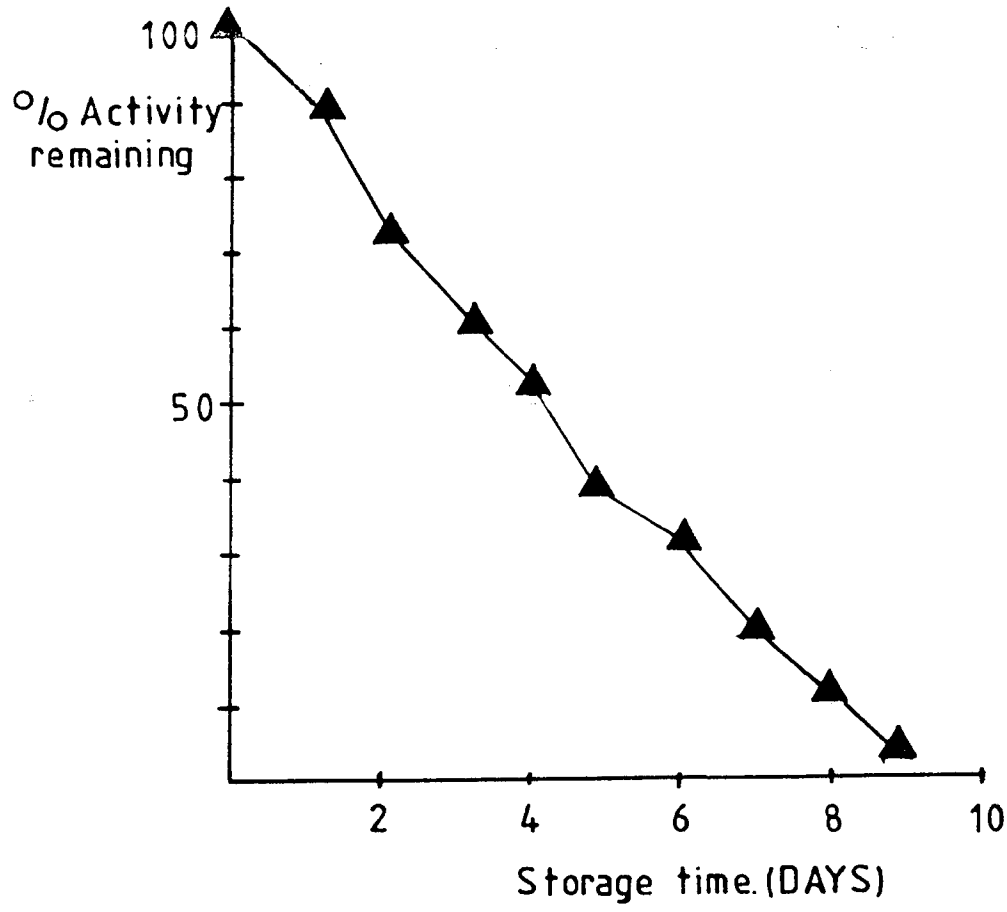

Fig 5.12. Decay pattern for immobilized RDH on porous nickel. (Each point represents the average of three separate determinations).

Storage conditions.

Buffer: 10mM potassium phosphate pH 7.0.
25mM EDTA.
1mM NAD.
5mM 2-mercapto ethanol.
(Final volume 5mls.)

Temperature: 4° C.

As can be seen, the decay proceeds at a constant rate with all enzyme activity being lost after 10 days.

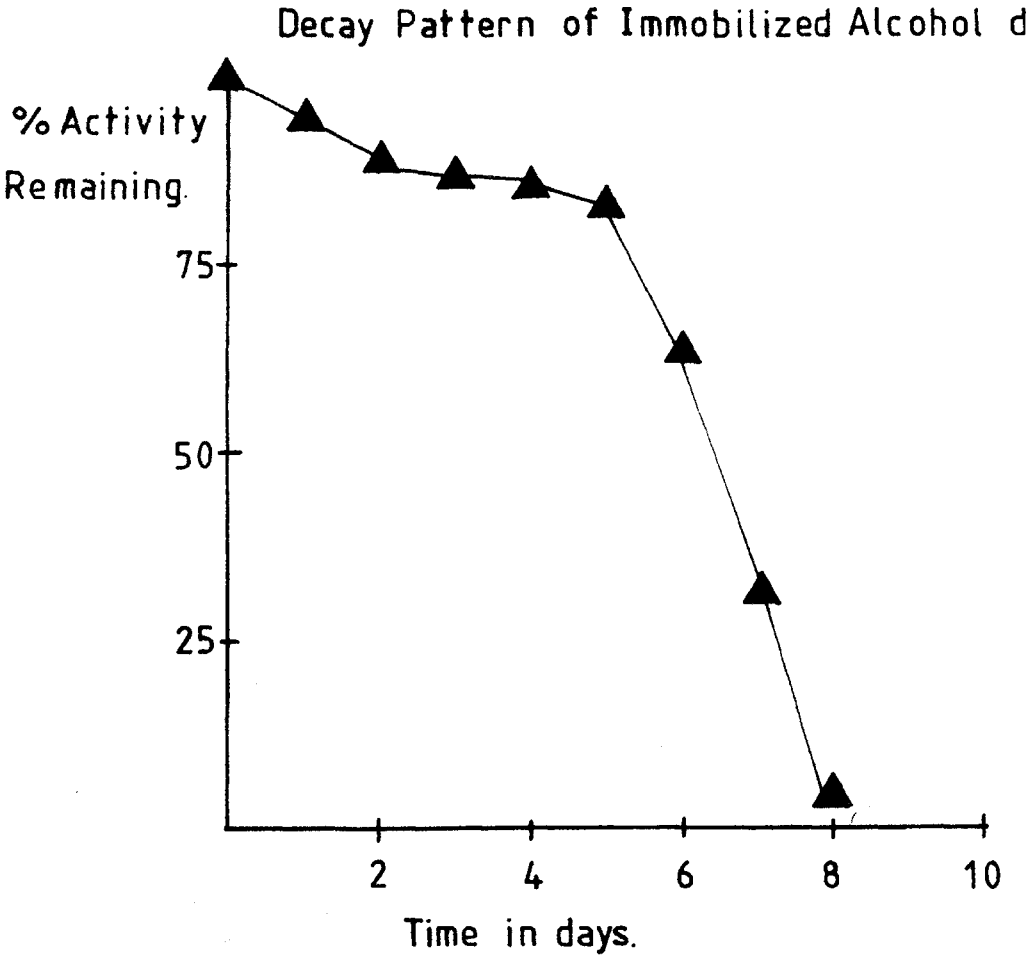

Fig 5.12. Decay pattern for alcohol dehydrogenase immobilized onto porous nickel. (Each point represents the average of three separate determinations).

Storage conditions.

Buffer: 10mM potassium phosphate pH 7.0.
25mM EDTA.
1mM NAD.

Temperature: 4° C.

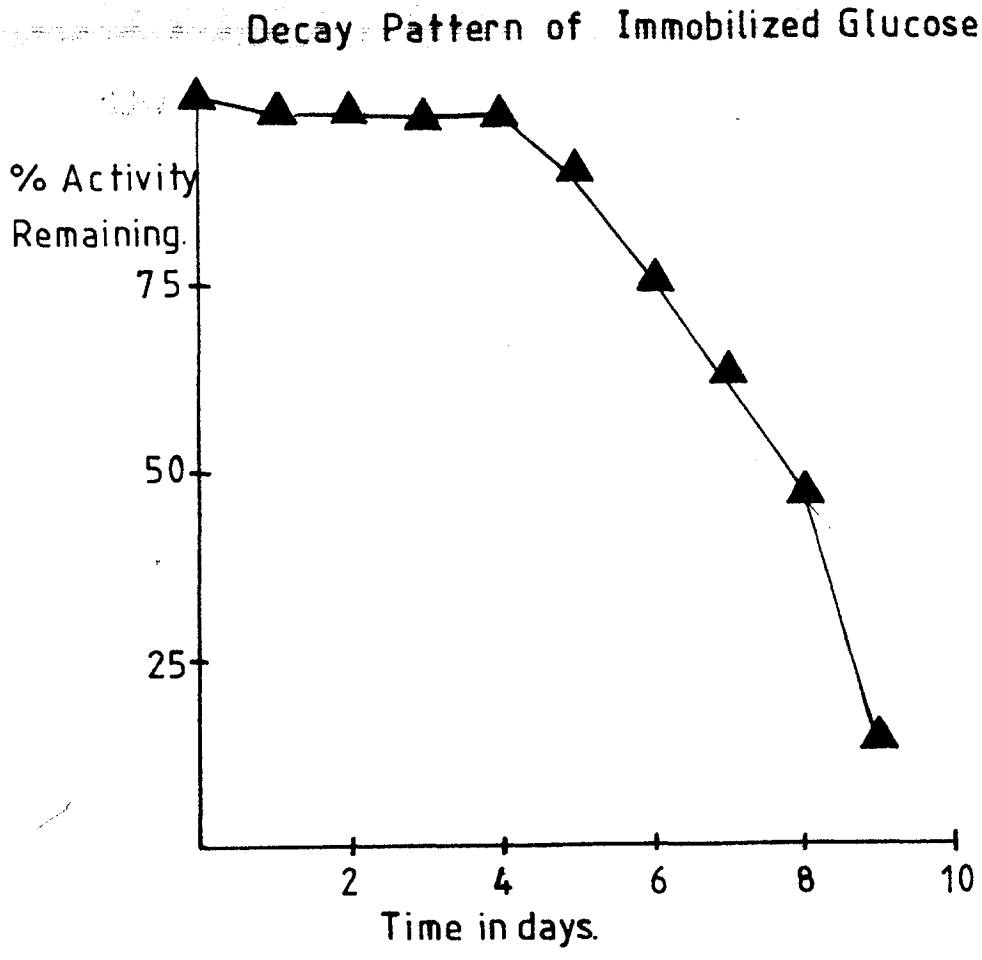

Fig 5.12. Decay pattern for glucose oxidase immobilized onto porous nickel. (Each point represents the average of three separate determinations).

Storage conditions.

Buffer:	10mM potassium phosphate pH 7.0.
	25mM EDTA.
	1mM FAD.
	2mM Glucose.
Temperature:	4° C.

Fig 5.13.

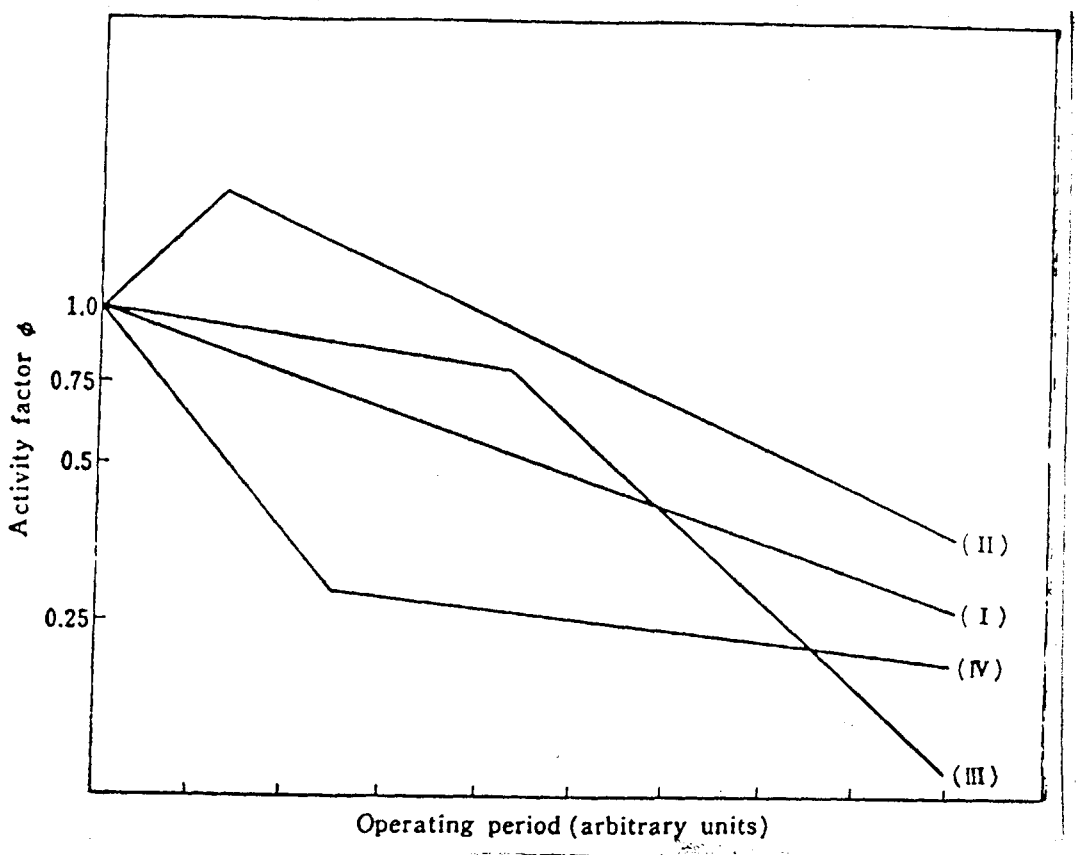

Decay patterns of enzyme activity of immobilized systems.

I Typical and normal decay pattern.

II Preliminary activation pattern.

III Two phase pattern. The enzyme activity is very stable for some time but then decreases for some reason. The following factors may be involved: i) Incorrect operation or storage conditions, ii) bacterial contamination, iii) decrease in the concentration of some essential factor, iv) accumulation of some inhibitory factor.

IV Two phase pattern. In this instance the decrease in enzyme activity is rapid from the initial state but then becomes very slow. In this case the immobilization of the enzyme is incomplete and leakage of the enzyme from the matrix occurs.

(Data adapted from Chibata, I. (1978)).

for comparison).

i) The least stable immobilized enzyme preparation appears to be immobilized ribitol dehydrogenase. The decay pattern is constant with all activity being lost after 6 days. During the decay in immobilized activity no enzyme activity was detected by the Coomassie Blue protein assay. Taken together, these observations suggest that the loss of enzyme activity is not due to desorption of the ribitol dehydrogenase from the support. Rather, the loss in activity appears to be due to irreversible denaturation of the enzyme while attached to the porous nickel support.

The stability curves obtained with immobilized alcohol dehydrogenase are much more interesting. These curves are biphasic. The enzyme activity in both cases is stable (almost 100% activity is detected for immobilized glucose oxidase) for some time, but then decreases and eventually reaches zero. Using the same arguments as above, it was shown that the loss of activity was probably not due to desorption of enzyme from the surface of the porous matrix. Rather, it appears that a "poison" is accumulating in the storage buffer, or more probably, in the microenvironment surrounding the immobilized enzyme, which eventually leads to its inactivation. Bacteria, or protease enzymes, were eliminated as possible poisons by the addition of azide and PMSF to the storage buffers. A possible explanation for this particular pattern will be given later.

Various attempts were tried to increase the storage stability of immobilized ribitol dehydrogenase. These included:-

i) Storing the immobilized enzyme in a dry state at -20°C.

ii) Storing the immobilized preparation in glycerol at -20°C.

iii) Varying the pH of the storage buffers.

In all these attempts, however, no increased stability was detected. This was particularly true in cases i) and ii), where it was noted that after a period of overnight storage no enzyme activity could be detected. Taken together, these results seem to suggest that in this particular immobilization an unstable preparation is obtained.

Returning to the question of the decay pattern observed with immobilized alcohol dehydrogenase and glucose oxidase, it was decided to assay the storage solution after the period in which all enzyme activity had been lost. Of particular interest was the possibility of finding free Ni^{++} ions.

Analysis by X-ray absorption gave rather surprising results in so far that the results obtained indicated the presence of Fe^{++}/Fe^{+++} ions in the solution. The presence of Fe^{+++} ions was further shown by the formation of a blue colour, resulting from the addition of ferrocyanide to a small portion of the solution.

Taken together, these results suggest that the observed decay pattern results because of the corrosion of the matrix, more specifically the nickel plated iron support grid, yielding Fe^{++} which with time accumulate and eventually reach such a level that the immobilized enzyme becomes poisoned. (A possible mechanism for the corrosion of the support grid will be given in the discussion). Addition of EDTA to the storage buffer did not give any increased stability, suggesting that other factors may be involved in the observed loss of enzyme activity.

The porous nature of the nickel matrix lends itself to another type of immobilization, namely that of encapsulation either by gel entrapment or by cross-linking in the presence of a reagent like polygluteraldehyde. Physical immobilisation experiments were carried out exclusively with glucose oxidase, particularly because of its potential use in enzyme electrode work.

Preliminary immobilisation experiments were carried out by gel entrapment techniques using polyacrylamide. Various gelling recipes were investigated, but the results obtained were unfavourable in all cases, indicating that the immobilized enzyme preparations were unstable and total enzyme activity was lost very quickly, usually after about 2 hours. Assaying these preparations proved difficult, especially since there appeared to be mass transport limitations.

A more suitable preparation was made by forming a glucose oxidase/BSA membrane on the surface of the porous nickel, as described overleaf. The apparent kinetics and thermal stability of this preparation are summarized in fig. 5.14. The results show that under these conditions the apparent K_m of the immobilized glucose oxidase is similar to that of the soluble enzyme. The thermal stability of the enzyme has increased.

The BSA-glucose oxidase membranes were prepared as follows. BSA and glucose oxidase, dissolved in high purity water, were mixed in equimolar volumes (10 moles of each) giving a final volume of 1 ml. Glutaraldehyde was then added in a dropwise manner to a final concentration of 1 mM. The solution was mixed and then poured onto a nickel square. The square was then placed at 4°C overnight to allow the gelling reaction to take place. In the morning it was noted that the porous support was covered with an extremely thin yellowy membrane. The support was then washed until no U.V. absorbing material was detected in the washing. The immobilized enzyme was assayed by the usual techniques.

The results show that (1) the kinetics of the glucose oxidase immobilized in this manner are the same as that of the soluble enzyme, that is, the K_m values are the same.

(2) the enzyme appears to have gained a degree of thermal stabilization. This result can again be explained in terms of the rigidity model presented earlier. It is interesting to note that the enzyme activity decays more gradually at the higher temperatures for either the cyanuric chloride immobilized glucose oxidase or the soluble glucose oxidase. This finding may be attributable to the immobilization procedure, that is, it is reasonable to assume that one glucose oxidase molecule is linked by many other protein molecules and therefore resulting in a much more rigid molecule, and therefore, are that less easily denatured at high temperatures.

Fig 5·14.

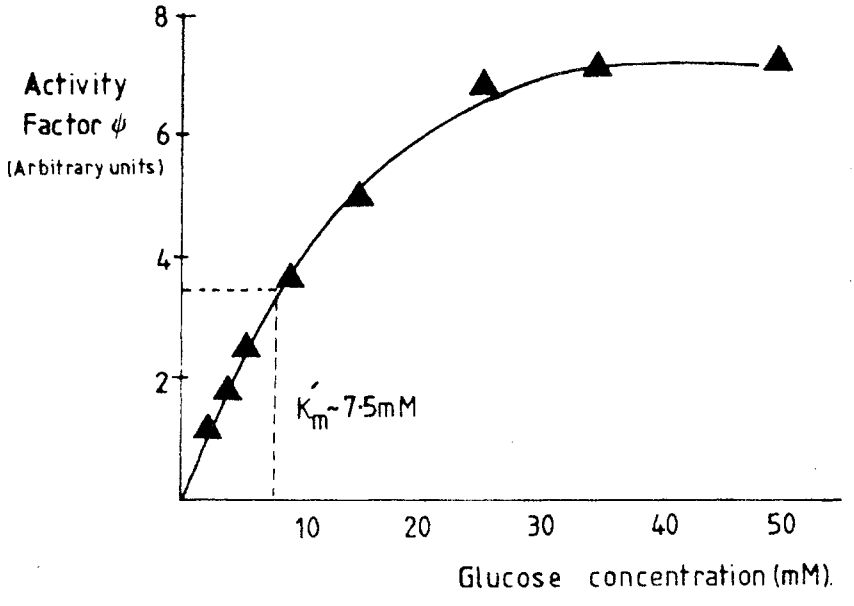

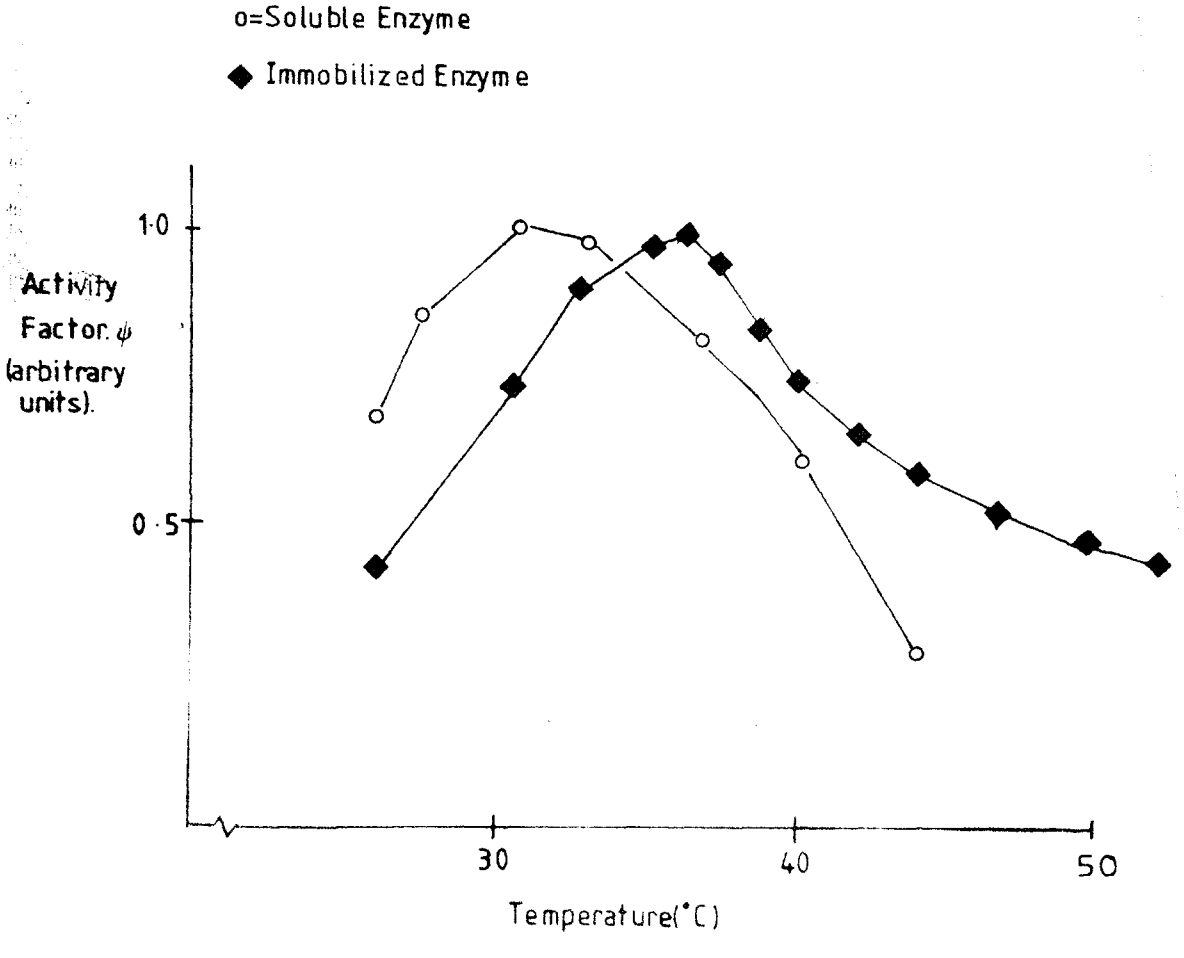

Fig 5.14.

CHAPTER 6

DISCUSSION ON SECTION I

The aim of the investigation reported in section I was to determine if porous nickel, a sintered nickel preparation made by INCO, would be useful as a support for enzyme immobilisation. The attractive features offered by porous nickel are:

1) High surface area. The manufacturers report an effective surface area of 0.15m^2/g of nickel. This is an important parameter since for an enzyme support the specific surface area is a most important variable in determining the amount of enzyme that may be immobilized and hence the final specific activity of the immobilized enzyme preparation.

2) High porosity of the sintered material. The manufacturers report a porosity of 70-90%. Scanning electron microscopy (plate 2.1) reveals a mean pore diameter of$\sim$10μm. It is important to determine this parameter since a large pore size would ensure access of an enzyme directly to the internal matrix of the support and hence ensure a high enzyme loading. Furthermore, large pores would be essential to ensure rapid mass transport of subtrate from the bulk solution to enzyme buried deep in the matrix. This would be facilitated by efficient stirring of the reaction solution or even by pumping the solution through the matrix. In this respect, the disadvantages of pressure drop would be less pronounced in a support with large pore sizes.

3) The porous matrix would provide a mechanically stable support for the purposes of immobilisation.

From a theoretical standpoint it is reasonable to suppose

that if an enzyme is covalently bound to the surface of the porous nickel, the enzyme would be present as a single monolayer and would therefore not cause any clogging of the pores and so would not limit mass transport of substrate from the bulk solution. For this reason, greater emphasis was given to successfully achieving a covalent link between the enzyme and the support rather than employing encapsulation within the pores.

One of the main problems associated with using metals as supports is their tendency to corrode when placed in contact with aqueous electrolyte solutions. The susceptibility of a metal towards corrosion, $M \longrightarrow M^{n+} + ne^-$, will be dependent on its standard redox potential in the sense that the higher the potential, the lower will be the tendency for the metal to dissolve. Corrosion of the support can be disadvantageous for two important reasons. The first of these is that the corrosion reaction will undermine the mechanical strength of the support, eventually resulting in its disintegration. This effect would be especially pronounced if the support was subjected to extreme hydrodynamic forces, for example as a result of agitating the solution. The other problem associated with corrosion is the possibility of the hydrated metal ions formed by the dissolution of the metal inactivating the immobilized enzymes. This occurs because the metal ions bind to accessible amino and/or sulfhydryl groups present on the enzyme. Such interactions could result in inactivation via two possible mechanisms.

i) By causing local changes in the surface electrical charge of the protein, thereby resulting in local conformational changes which may be transmitted to the active site of the enzyme.

ii) By forming complexes with essential active site residues and thereby preventing the enzyme from carrying out its normal function.

The particular advantages offered by nickel in terms of passivating the metal against corrosion by surface oxide formation have already been discussed. Furthermore, surface oxide films can be reacted with suitable solution reagents, thereby allowing the parent metal to become functionalized.

Formation of a surface oxide on the porous nickel was carried out as previously described. The resultant film was characterized by powder X-ray diffraction which unequivocally showed the presence of the Ni-O phase. Analysis by scanning electron microscopy revealed that the oxidation process had not altered the porous nature of the matrix. In fact, a mean pore diameter of $\sim$ 10μm could still be detected. The implications of large pores has already been discussed. Furthermore, the micrographs did not reveal any evidence of the sintered nickel having fused together, which would have resulted in a lowering of the specific surface area. It was noted, however, that the oxidation process had produced a smoother, more rounded surface. Presumably this is simply due to the presence of the surface oxide film, suggesting that it had been produced in a homogeneous manner. It was also observed that, following the oxidation, the porous nickel had become brittle and could easily be damaged by mechanical shock. The implication of this finding is that the forces holding the sintered material together have been weakened. This may be due to the fact that the cellulosic material present in the sintered matrix has been burned away due to the extreme oxidizing conditions found in the furnace.

The reasons for having selected cyanuric chloride as

the linking agent have already been discussed. From the results presented by Kuruwana et al (Kuwana, T. et al (1979)) the following mechanism was suggested.

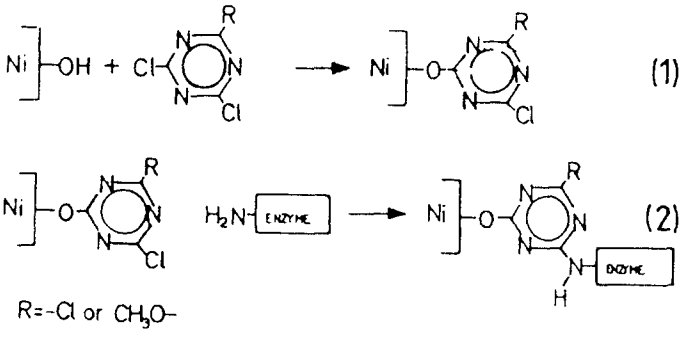

As can be seen, this is a two stage reaction. Stage 1 represents the derivitization of the porous nickel, giving a triazine surface. This can then be reacted with enzyme, under suitable conditions to give the immobilized enzyme preparation. The chemical basis of this reaction is the nucleophilic attack on the reactive carbon of the triazine. In the first instance the surface hydroxy group of the porous nickel acts as the nucleophilic agent and in the second instance a surface amino group on the enzyme acts as the nucleophile. In this respect it was important to carry out the reaction at an elevated pH so that the equilibrium $-NH_3^+ \rightleftharpoons -NH_2 + H^+$ lies towards the r.h.s.

It was important to have a technique to monitor both the derivitization reaction and the functionalization reaction. In terms of the derivitization reaction (reaction with cyanuric chloride) the choice of technique was largely governed by the availability of instrumentation. Consequently Infra Red spectroscopy was chosen.

The first problem to be overcome was the preparation of a suitable sample. The sample had to fulfil two important criteria:

i) It had to contain sufficient material (derivitized nickel oxide) so as to produce a reasonable signal which could

be both detected and interpreted.

ii) The sample had to be sufficiently transparent so as to allow sufficient radiation to reach the infra red detector.

Because of these criteria, the potassium bromide disc technique was the most applicable. The exact ratio of nickel oxide to potassium bromide was ultimately determined empirically.

Another problem which had to be overcome in this work resulted from the fact that the I.R. spectrum of any surface bound species would be superimposed on that of nickel oxide and would therefore be seen only after computer subtraction. Unfortunately it was found that nickel oxide absorbs I.R. radiation strongly over a wide range and therefore only a small window existed through which bands attributable to cyanuric chloride would be visible. Simple calculations predicting the expected spectrum following derivitization, and assuming the chemistry described above, revealed that only one band would be seen in the window. The only way to remedy the situation was to introduce further chromophores into the triazine structure. Such a rationale, however, must be approached with caution since it is important that the resultant molecule should fulfil the following criteria:

i) The new chromophore should be I.R. active within the region of interest.

ii) The resultant molecule should possess identical chemistry to the parent molecule so that the new molecule will behave in exactly the same way as the parent molecule.

In this respect, 2,4,dichloro-6-methoxy-5-triazine is extremely useful, particularly since both of the above criteria

are satisfied. Furthermore, the methoxy group is stable and would therefore not be lost, e.g. through hydrolysis. Typical spectra obtained from this work have been presented in Chapter 5.

On the basis of available information, the reaction between the derivitized nickel oxide and the enzyme has been presumed to proceed via the reaction of surface amino groups. In this respect, the immobilization procedure reported in this work should be general and applicable to a large range of enzymes. It is important to note, however, that an immobilization proceeding via a surface amino group presupposes that the amino groups in question are not essential to the activity of the parent enzyme. It is important to appreciate this point since immobilization via such an essential residue would result in the enzyme becoming inactivated.

Having successfully immobilized three enzymes onto porous nickel, it was then pertinent to monitor the kinetic behaviour of the immobilized enzymes. The results presented in Chapter 5 showed that for two of these enzymes, ribitol dehydrogenase and alcohol dehydrogenase, the kinetics of the immobilized enzymes appeared identical to those of the solution species. This was manifest by identical K_m values for both substrates. The implication of this finding is twofold.

1. The inherent properties of these enzymes have not been altered as a result of the immobilization.

2. The mass transfer effects do not alter the observed kinetics of the reaction in the sense that the concentration of the various reactants in the microenvironment surrounding the enzymes is similar to that of the bulk solution.

It should be noted, however, that the observed kinetics may be an artifact in the sense that mass transport effects together with altered properties in the enzymes resulted in

the observed kinetics. Unfortunately, this point highlights one of the main problems concerned with enzyme immobilization, namely that it is often extremely difficult to have a total understanding of exactly what is going on. This point is also manifest in the fact that it is extremely difficult to predict exactly the outcome of any immobilization technique both in terms of the observed kinetics and the observed stability of the resultant preparation.

Different results were obtained with immobilized glucose oxidase. In this instance, it was noted that the enzyme had an increased sensitivity towards glucose, which was manifest by a decrease in the K_m value of the immobilized enzyme towards the substrate. Once again it was difficult to rationalize this observation. For example, these observed kinetics may be due to one of (or possibly all) the following:

i) Altered properties of the enzyme following the immobilization.

ii) Mass transport effects, e.g. increased glucose concentration in the microenvironment or a decreased oxygen tension in the microenvironment, thus making this the rate limiting factor.

In terms of thermal stability, it was found that all the enzymes showed improved characteristics. This was explained in terms of a stabilization towards unfolding at the elevated temperatures. The basis of this model is that if the enzyme is attached by many links to a support, then the unfolding of the protein becomes considerably hindered. As a consequence, it will be harder to inactivate its catalytic centre by conformational changes. It is important to note that this model suggests that multipoint binding of the enzyme molecule to the

support makes the molecule more rigid without necessarily altering its fundamental properties. The fact that only a light enhancement of thermal stability is observed can be explained by suggesting that even when multipoint binding is realized, it is only a small portion of the enzyme that is bound to the support; this is because the protein and the support have their own configurations which are unlikely to be congruent, and so one should not expect rigidity over the whole molecule. It is for this reason that, in general, enzymes cross-linked within a gel matrix show better thermal stability, in which case the enzyme is attached to the three-dimensional lattice of the polymeric gel.

Results showed that the pH optimum of immobilized glucose oxidase was shifted by ~ 1pH unit towards the alkaline end of the pH range. A shifting of the pH optimum of glucose oxidase in this way is commonly found for immobilized glucose oxidase (Ianniello, R.M. and Yacynych, A.M. (1981)) and (Cho, Y.K. and Bailey, J.E. (1978)). The basis of this shifting can be explained by two possible mechanisms. The first of these may be related to a pH shift in the microenvironment of the immobilized enzyme relative to that in the bulk solution. Remember that in this context, when an enzyme is immobilized to a solid support the protein is in effect removed from its native aqueous milieu and exposed to a different local microenvironment, the characteristics of which are determined by the nature and structure of the support and the electrical charge on the surface of the immobilized enzyme. It is evident from this that if the pH of the enzyme microenvironment is closer to the stability optimum than that of the solution then the apparent stabilization

of the immobilization against pH inactivation will be seen. This model could explain the results observed in this work by suggesting that any unreacted sites on the surface of the oxide film, $Ni\text{-}O^-$ would attract hydrogen ions from the solution. Alternatively, it can be suggested that the pH inactivation of the soluble enzyme occurs due to factors such as dissociation of oligomeric subunits or even gross conformational changes due to protein unfolding. In this respect stabilization may be achieved by a tightening of the enzyme as a result of multipoint binding. Note that this model is analogous to that suggested for the thermal stabilization reported above.

In terms of storage stability, rather poor results were obtained for the various immobilized enzyme preparations. The most unstable immobilized enzyme, in terms of storage stability, was ribitol dehydrogenase. The results presented in Chapter 5 represent a typical decay curve obtained under the most optimal storage conditions which were determined. The results obtained with immobilized glucose oxidase and alcohol dehydrogenase were different. These showed biphasic decay in both cases in the sense that the enzyme activity was found to be very stable for some time, but then decreased. Three possibilities may account for this behaviour:

i) Bacterial contamination.

ii) Decrease in the concentration of some essential factor.

iii) Accumulation of some inhibitory factor.

The first two factors were eliminated by the addition of reagents to the storage buffers such as PMSF, azide, FAD and 2-mercaptoethanol. Bearing in mind the third possibility,

it was decided to analyze the components present in the storage buffers, after a period of two weeks, after which time all activity had usually been lost. The analysis revealed quantities of iron present in the storage buffers. This was an unexpected result, but the source of the iron was readily appreciated as coming from the support grid of the porous nickel matrix. Fig. 6.1 represents a plausible model which would account for the production of iron ions in the solution. The ions are produced as a result of the electrical interface formed by overlaying iron with nickel. A break in the nickel coating would expose the iron to the solution, which would then corrode in preference to the nickel. In this respect it is unfortunate that any oxide coating formed on the iron would passivate it from further corrosion. The effects that metal ions can have on immobilized enzymes have already been discussed, and therefore it is suggested that the activation of the immobilized enzymes is due, albeit maybe in part, to the corrosion of the iron support grid. The addition of exogeneous EDTA did not restore enzyme activity, an observation also reported by Munro et al (Munro, P.A. et al (1977)).

Particular difficulty was encountered in this investigation in obtaining an accurate measure of the amount of protein that had been immobilized onto the support. Traditional techniques are based on measuring the concentration of a particular amino acid, such as tryptophan or methionine after it has been released from the immobilized protein as a result of acid or alkali hydrolysis. Application of this technique to this work, however, resulted in extensive corrosion of the matrix, yielding solutions which were not amenable to amino acid analysis. It was also found that utilizing a difference assay of the stock protein solution before and after the

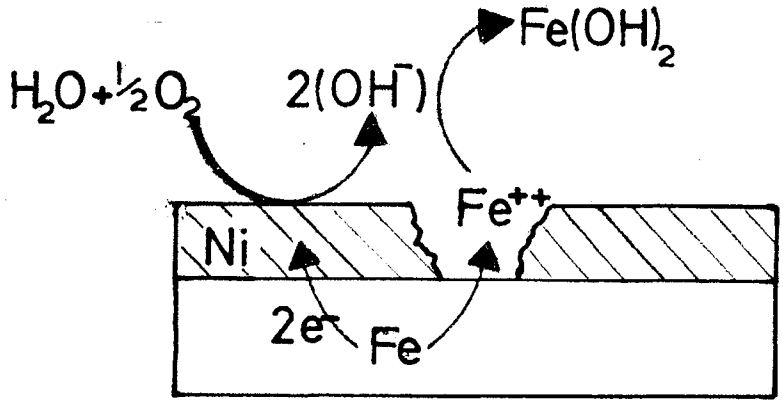

anodic reaction. $Fe \longrightarrow Fe^{++} + 2e^-$

cathodic reaction. $\frac{1}{2}O_2 + H_2O + 2e \longrightarrow 2(OH)^-$

E° $Fe \longrightarrow Fe^{++} + 2e^-$ = +0.44 volt.

E° $Ni \longrightarrow Ni^{++} + 2e^-$ = +0.25 volt.

Model accounting for the occurance of iron ions in the storage solutions.

A break in the nickel coat would expose the underlying iron to the solution and corrosion would result. Note, that because of its E° value the iron rusts in preference to the nickel.

Unfortunately, the only way to overcome this problem is to either ensure a defect free nickel coating or to replace the iron with an unreactive metal such as platinum. A further alternative would be to store the support under strict anaerobic conditions. This could be achieved by adding compounds to the storage buffer such as Na_2SO_3 to mop up any dissolved oxygen.

immobilization was also not applicable. This was because the concentration of the solution was so large compared to the amount of enzyme immobilized that the difference in concentration could not be measured accurately. Lowering the enzyme concentration did not help matters since it was observed that in the low enzyme solutions extremely low enzyme loadings were obtained, presumably because under these conditions hydrolysis of the surface triazine is the predominant reaction. The low enzyme loadings meant that measurement of the immobilized activity was not readily detected. Unfortunately, therefore, the activities of the immobilized enzymes were not expressed in terms of specific activities. Similar difficulties were reported by Halling and Dunnill (Halling, P.J. and Dunnill, P. (1979)).

Concluding remarks

Although the work presented in section I indicated the formation of a stable linkage between Ni/NiO and an enzyme by utilizing cyanuric chloride chemistry, it was unfortunate that the resulting immobilized enzyme preparations exhibited poor storage properties. Metal ion inactivation was implicated as a possible mechanism by which the enzymes were becoming inactivated. Addition of EDTA to the storage buffer did not increase the stabilities of the immobilized enzymes, which may imply that the effective concentration of EDTA in the microenvironment is sufficiently low, perhaps due to partitioning, so as to be ineffective as a chelating agent, or alternatively it may be possible that the metal-chelate complex is still able to inactivate the enzyme. Certainly no nickel ions were detected in the solution, suggesting that complete protection had been achieved by surface oxide

formation. Munro (Munro, P.A. et al (1977)) suggested that BSA, because of its ability to bind metal ions by attachment to its sulfhydryl groups, could be used to protect immobilized enzymes from the effects of metal ion inactivation. In view of this, it is possible to explain the greater stability of glucose oxidase immobilized by crosslinking with gluteraldehyde in the presence of BSA. In this instance it is suggested that any metal ions produced from the surface of the supporting grid are immediately chelated by the BSA which is held in close proximity to the support. Munro has also presented a similar model to explain the effects of BSA on stabilizing chymotrypsin immobilized onto nickel powder. It has also been suggested that haemoglobin is another protein which can protect a protein against inactivation by metal ions. The basis of this protection is identical to that offered by BSA. The achievement of very high concentrations of proteins in large volumes of chemical reactors is impractical, whereas it can be done in small volumes containing immobilized enzyme. Such an approach has been exploited in the encapsulation of asparaginase and catalase in microcapsules containing a 10% concentration of haemoglobin with consequent considerable stabilization of the enzymes (Klibanov, A.M. (1978)). In view of this it may be argued that the storage stability of the immobilized enzymes on porous nickel could be increased by immobilizing the enzymes in the presence of BSA. In order to preserve the porous structure of the matrix it may be necessary to immobilize a monolayer of BSA onto the surface of the porous nickel using cyanuric chloride and then further immobilizing a layer of active enzyme onto the BSA by using gluteraldehyde. In this way, the nickel would be covered by a protective layer of BSA which would be able to chelate any

metal ions formed from the corrosion of the matrix.

In terms of future work it is now important to maximize the storage stability of the immobilized enzymes. From the data presented in this work it seems that techniques based on stabilizing the enzyme against inactivation against metal ions should be pursued. Techniques by which this can be achieved have been mentioned above.

The ultimate aim of this work should be to use immobilization technology and the properties of porous nickel in the design of novel reactors. To this end, the large surface areas and porous structure of the support could be put to the best advantage by adopting a tube design. In order to increase the surface area available to the solution the porous nickel could be wound in a spiral. Because of the effects that the oxidation reaction has on the flexibility of the support, the nickel would have to be cast as a tube prior to oxidation.

CHAPTER 7

INTRODUCTION TO SECTION II

The Enzyme Electrode

An enzyme electrode is a chemical device which functions by combining an electrochemical process with immobilized enzyme activity. The basic operational features of an enzyme electrode are simple. All that is required is an enzyme, a transducer, a suitable reference electrode and a circuit for measuring either the potential difference between two electrodes or the current that flows between them. The transducer in this context is either a potentiometric or an amperometric indicator electrode. When an amperometric electrode is used as the base sensor the circuit contains some source of potential to drive the current.

The enzyme in the probe plays a dual role. First, it confers selectivity upon the device and, secondly, it catalyses a reaction which produces a species that can be detected by the transducer. Because enzymes are sensitive to pH the sample is usually immersed in the solution and the steady state current or potential recorded. Wherever possible, the solution is stirred so as to speed up mass transfer and so provide fast response times.

Tremendous interest in enzyme electrodes has existed since they were first described by Updike and Hicks (Updike, S.J. and Hicks, G.P. (1967)). There are a number of reasons why these devices have such an appeal.

i) Enzyme electrodes can provide convenient and straightforward measurement methods for species of biological and clinical interest.

ii) Pretreatment of samples is at a minimum. Prior removal of cells, proteins and other materials is often

unnecessary.

iii) The devices are both easy to use and to calibrate.

iv) Enzyme electrodes are very sensitive. Detection limits of 10^{-5}- 10^{-4}M are often quoted in the literature.

v) The devices are fast and suitable for use with automatic analysers.

vi) The technique is virtually non-destructive. The sample can be retested for other constituents after the initial measurement has been made.

vii) Only small sample volumes are required.

viii) Individual probes can be inexpensive.

ix) The scope of application is in principle very broad.

x) Microprobes could be developed to be placed in a catheter and be used for continuous in vivo monitoring of the critically ill.

Design and operation of an amperometric enzyme electrode

It is possible to use an indicator electrode with a soluble enzyme and implement either a bulk kinetic or equilibrium assay but if the enzyme can be immobilized in a stable fashion a number of major advantages result. First, the enzyme can be reused. Sometimes as many as 1,000 determinations can be made with the same probe (Guilbault, G.G. and Montalvo, J.G. (1970)). Because of the proximal arrangement of the enzyme to the transducer a rapid response and high sensitivity can be achieved. The latter is due to the fact that the concentration of product becomes diluted only to a slight degree because of the short distance it has to diffuse to reach the transducer. Finally, when the enzyme loading is sufficiently high the electrode response becomes independent of the amount of enzyme. This has been shown to be the case for both potentio-

metric (Guilbault, G.G. and Montalvo, J.G. (1970)) and amperometric (Mell, L.D. and Maloy, J.G. (1975)) electrodes. Excess enzyme will also decrease the sensitivity of the assay to all those variables which influence the rate of an enzyme catalysed reaction, e.g. pH, inhibitor and activator concentration, temperature and most significantly loss of enzyme activity.

Immobilization is normally achieved by either trapping a thin layer of enzyme behind a semi-permeable membrane or by occluding the enzyme in a gel matrix. More recently covalent attachments of enzymes directly to the surface of the transducer have been reported (Bourdillon, C. et al (1979) and Cass, A.G. et al (1984)).

A schematic drawing of an immobilized enzyme probe and the sequence of events leading to a response is shown in fig. 7.1. As indicated, the enzyme is held in close proximity to the active surface of the transducer. The outer edge of the enzyme layer is exposed to the solution, and a membrane is placed over the probe assembly. The membrane should be sufficiently thin such that the response time is not unduly affected. The first step in the sequence of events leading to a response is transport of substrate from bulk solution to the outer surface of the membrane at point L'. The substrate then diffuses through the outer membrane toward the enzyme layer at point L. Here the substrate will undergo an enzyme catalysed conversion. The sensor which detects this reaction is at point O. The rate of the chemical reaction in the enzyme layer is usually governed by Michaelis-Menten kinetics. Ideally the only slow steps in such an immobilized enzyme probe will be diffusion through the trapped layer and

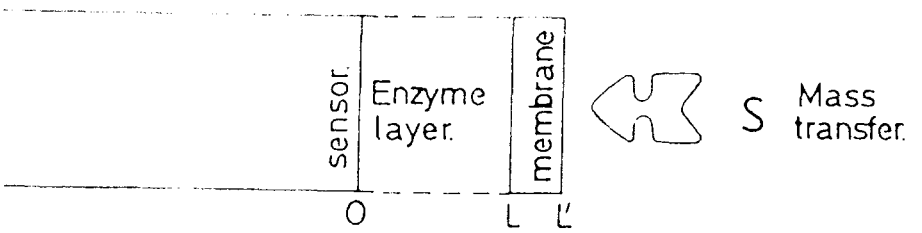

Fig 7.1.

Schematic drawing of the sequence of steps which take place at an enzyme probe. The substrate is transported from the bulk to the outer membrane surface located at L' diffuses through the membrane to point L and undergoes simultaneous reaction and diffusion in the enzyme layer.

For ideal operation the bulk solution should be stirred so as to speed up mass transfer and furthermore the membrane should be as thin as possible and not present any permeability restrictions to the substrate.

the enzymatic reaction. Clearly the primary sensor should be rapidly responding, the membranes thin, the enzyme activity high and the bulk solution well stirred.

If an amperometric electrode is employed as the base sensor one of the species involved in the overall enzyme catalysed reaction will be electrochemically consumed. This can be illustrated with the glucose oxidase electrode used to measure the concentration of glucose (Updike, S.J. and Hicks, G.P. (1967)). Glucose oxidase catalyses the reaction;

$$\beta\text{-D-glucose} + O_2 \longrightarrow \text{gluconolactone} + H_2O_2$$

The concentration of glucose in the sample is measured by monitoring the decrease in the dissolved oxygen tension by its reduction at a base platinum electrode. When oxygen is in non rate limiting excess and the glucose concentration well below the apparent K_m for the immobilized glucose oxidase, there is a linear relationship between glucose concentration and the decrease in oxygen tension. It is also possible to monitor the hydrogen peroxide produced during the reaction by oxidation at a base platinum electrode. Whichever technique is used, it is clear that the electrode must interact directly with the reaction products.

With an amperometric sensor the measured variable is current. Maximal sensitivity will be obtained when the electrode potential is set to oxidize or reduce the electroactive species at a diffusion controlled rate. Furthermore, the current that is measured will be related to the flux of analyte at the surface of the transducer by the equation;

$$i = nFAD \left.\frac{\delta[P]}{\delta X}\right|_{X=O}$$

The flux of product to the electrode might be limited by either external mass transfer diffusion or by diffusion in the enzyme layer. Theoretical models for amperometric enzyme electrodes have been presented by Racine and Mindt (Racine, P. and Mindt, W. (1971)) and Mell and Maloy (Mell, L.D. and Maloy, J.T. (1976)).

In the simplest model, mass transfer is rate limiting. It is assumed that the enzyme layer is so thin that all the reaction product reaches the electrode surface and is measured. Under these conditions the current will be limited by the rate of product formation. In the steady state, the rate of the enzyme reaction will be equal to the rate of supply by mass transfer through the outer membrane. When the enzyme layer is thick and diffusion through it is slow compared to the rate of mass transport from the bulk solution, the situation becomes more complex. Under these conditions one must consider the simultaneous occurrence of an enzyme catalysed reaction and diffusion. Mell and Maloy have studied this particular case by the use of digital simulation. Analytically the major results of their calculations are;

i) The prediction that at high enzyme loadings the current will be a linear function of substrate concentrations at concentrations greater than K_m.

ii) The prediction that the current at low substrate concentrations increases as the thickness of the layer decreases.

iii) An equation which gives the maximum time needed to obtain a steady state response.

Practical Aspects in the Use of Amperometric Enzyme Electrodes

By and large all electroanalytical techniques based on current measurement are affected by;

i) The magnitude of the background current.

ii) Noise.

Taken together, these factors tend to fix the lower limits of detection. Practical limits can vary quite considerably, but typical values of 10^{-5}-10^{-4}M are often quoted in the literature. It is clear that the best limit of detection will be obtained by minimizing the background current and maximizing the slope of the calibration curve. Mell and Maloy (Mell, L.D. and Maloy, J.T. (1976)) have indicated that the two major factors which influence the slope are the amount of enzyme present and the thickness of the layer. In other words, the slope of the calibration curve will increase as the enzyme concentration increases until it is equal to the value dictated by mass transfer. Techniques for reducing the level of the background current and noise have been reviewed in the literature (Hubaux, A. and Vos, G. (1970)). It should also be noted that the limit of detection can be no better than the limit of the base sensor for the analyte in question.

In general terms, the upper limits of detection are set by:

i) The Michaelis-Menten kinetics of the enzyme.

ii) The enzyme loading in the sense that if there is a high enzyme activity on the electrode, the response will be linear above the K_m value. A very high enzyme loading is required, however, if the K_m value is of the order of a few mM.

A problem commonly associated with the use of enzyme electrodes is that of interference. Interference is caused

by any chemical species which alters, either by increasing or decreasing, the response of the sensor to the sample. One can generalize and divide interference into three main categories.

(1) Interference caused by ions or molecules which affect the base sensor.

(2) Interference by ions or molecules which affect the enzyme.

(3) Interference by ions or molecules which react with the measured species.

Direct electrochemical interference with amperometric probes results if there are ions or molecules in the sample which can be reduced or oxidised at or below the potential of the species of interest. In general terms, this problem has been overcome by the use of semi-permeable membranes, e.g. the teflon membrane in the Clark O_2 electrode only allows oxygen to pass through it, or alternatively by implementing a dual electrode system so that a reading corresponding to the difference between two electrodes, one in the presence of the species of interest and the other a control, is obtained. Another approach to this problem will be discussed later.

The enzyme is probably the major source of problems in terms of chemical interference. This is because, in the most fundamental terms, an analysis with an enzyme electrode is a kinetic analysis. Thus an enzyme probe may be quite sensitive to the presence of inhibitors and activators in the sample and may give inaccurate results. Once again, this problem is overcome through the use of semi-permeable membranes, which will allow the substrate to diffuse freely into the enzyme

layer but will prevent entry of known inhibitors. As can be appreciated, the success of this technique can be largely a matter of luck in so far as the substrate and the inhibitors must be of opposite charges. This technique has been used successfully in the glucose electrode described by Cass et al (Cass, A.G. (1984)) in which a cation exchange membrane was used to prevent ascorbate, a compound known to cause interference at the monitoring potential, from entering the reaction layer. As has already been mentioned, high enzyme loadings can also reduce this problem.

Another related problem which can occur is when an ion or molecule is present in the sample which can react with the product of the enzyme catalysed reaction. Whether or not this will cause an error in the measurement depends upon what is analysed. For example, ascorbate consumes oxygen and an amperometric probe which detects glucose by monitoring the decrease in oxygen tension will show an error. In this instance a hydrogen peroxide sensor would give a better result. Alternatively, a dual electrode system could be used.

One of the most critical factors affecting the usefulness of an immobilized enzyme electrode is its long term stability. For an amperometric enzyme probe this can be defined as the resistance to change in the calibration curve as a function of time. The factors which can influence the stability of the enzyme probe are listed in table 7.1.

It is generally very difficult to predict the useful lifetime of a particular electrode. Some reported probes can only be used a few times (Aizawa, M. et al (1974)), whereas others can be used for several months (Guilbault, G.G. and Lubrano, G.J. (1972)). It is also important to appreciate

Table 7.1

Factors which determine enzyme electrode stability

I. Physical factors

i The thickness of the enzyme layer.

ii The mechanical stability of the trapped layer.

II. Chemical factors

i Immobilization method

- a. Soluble trapped layer.
- b. Physically occluded.
- c. Covalent attachment.

ii Total enzyme activity in the trapped layer.

iii The stability of the enzyme.

iv Chemical conditions of use.

- a. pH.
- b. Temperature.
- c. Accumulation of inhibitors, etc.

v Storage conditions.

that the apparent stability of a probe will depend on whether the electrode is tested at high or low substrate concentrations. Guilbault has shown that this is best when the concentration is low (Guilbault, G.G. and Montalvo, J.G. (1970)).

Finally, it is important to consider the sensor itself. Clearly, if this changes the response will also change. To date this has not been a limiting factor due to the stability of the electrode materials in current usage.

As will be seen later, this is not necessarily the case if a chemically modified electrode is used as the base sensor.

Modern Concepts in Amperometric Enzyme Electrodes

(1) The mediated glucose sensor

A major drawback of classical glucose sensors is their dependence on oxygen. For successful operation, therefore, it is necessary to provide a steady supply of oxygen. Correct responses will be obtained only when the oxygen tension in the sample is not limiting - a condition that can only be realistically met in the laboratory. This seriously limits their scope of application, e.g. they can not be used under anaerobic conditions.

The sensor can be made independent of oxygen by providing an alternative electron acceptor. If the acceptor can accept electrons from the enzyme and pass them to the electrode, it is called a mediator. Although the enzyme no longer interacts with oxygen the same must also be true of the mediator. Studies have shown that ferrocene and its derivatives will accept electrons from reduced glucose oxidase, but at the same time will not react with oxygen (Cass, A.G. et al (1984)). It follows, therefore, if ferrocene is used in conjunction with glucose oxidase, a sensor can be made which is totally

independent of oxygen. In the mediated sensor the enzyme links the oxidation of glucose with the reduction of the mediator, which in turn is oxidized at the electrode. Another advantage is that the sensor operates at the potential of the mediator. This is considerably less than the potential for the oxidation of hydrogen peroxide with the result that the possibility of electrochemical interference is reduced. Fig. 7.2 illustrates the basic operational differences between a classical glucose sensor and a mediated one.

(2) Direct Electron Transfer from a Protein to the Electrode

Although sensors which incorporate mediators are an improvement on the classical sensors in terms of sensitivity to oxygen, it is likely that their properties will still reflect not only the behaviour of the enzyme, but also that of the mediator, e.g. the ferricinium ion is an unstable species. Further improvements would result if direct electron transfer between the enzyme and the electrode could be achieved.

The most significant steps toward this goal have been made by Hill's group in Oxford. They showed that direct electron transfer from cytochrome c to a base metal electrode proceeded very slowly. With suitable modification, however, the process could be accelerated dramatically. Rapid electron transfer was observed between cytochrome c and a gold electrode coated with a layer of 4,4'-bipyridyl or 1,2-bis(4-bipyridyl) ethylene (Eddowes, M.J. and Hill, H.A.O. (1979)). These compounds were termed promoters of electron transfer. Later experiments showed that a number of compounds which were known to inhibit the binding of cytochrome c to its natural redox partner, cytochrome

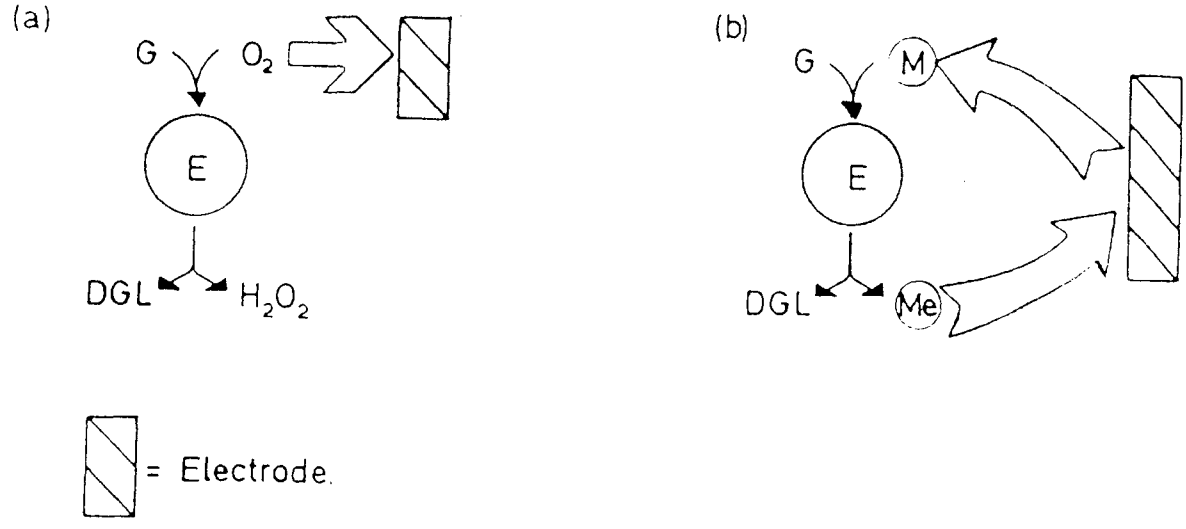

Fig 7.2.

(a) Classical design for a glucose sensor. The enzyme links the oxidation of glucose to the reduction of molecular oxygen. The fall in the concentration of oxygen is registered by the base sensor.

(b) The mediated sensor. The enzyme links the oxidation of glucose to the reduction of the mediator which in turn is reoxidized at the base sensor. In this way the sensor can be made independent of oxygen.

G = glucose, DGL = gluconolactone, M = mediator,
e = electron, E = enzyme.

oxidase, also prevented the transfer of electrons from cytochrome c to the modified gold electrode (Eddowes, M.J. et al (1979) and Albery, J. et al (1981)). These experiments supported the view that the 4,4'-bipyridyl imitated the behaviour of cytochrome oxidase in presenting a surface to cytochrome c to which it could bind productively prior to electron transfer. It was suggested that the lysine residues which surround the electro-active haem edge of cytochrome c interact electrostatically with the 4,4'-bipyridyl, thereby allowing transfer to take place efficiently. The hypothesis that rapid electron transfer can take place if the electrode mimics the protein's own natural partner gained further encouragement from the observation that magnesium ions promoted electron transfer from reduced ferrodoxin to a graphite electrode (Armstrong, F.A. et al (1982)).

Porous Nickel as the Amperometric Sensor in Enzyme Electrodes

Porous nickel is a potentially attractive material for two important reasons.

i) Because of its porous nature it is possible to obtain a high enzyme loading. In the simplest case this can be achieved by dipping the electrode into a concentrated solution of the enzyme and allowing the pores of the matrix to become flooded. A suitable membrane placed over the probe assembly would serve to keep the enzyme in place.

ii) An electrode made out of porous nickel would have a large surface area. Large currents would therefore be expected for a given concentration of analyte. Furthermore, a large surface area nickel electrode would be cheaper than the corresponding gold or platinum electrode. These advantages however must be offset by the possibility of large background currents.

In general terms there are two important criteria which determine the suitability of a metal as an electrode material. The first of these is its useful potential range. The upper limit is usually set by the potential at which the metal begins to oxidize. The second criterion is the magnitude and reproducibility of the peak currents obtained with the electrode. Surface film formation, adsorption of reactants, intermediates or products are known to influence the reproducibility of the peak current measurements. Traditional electrode materials are gold, platinum and mercury, which are all extremely stable under the conditions in which they are normally used. Below are listed the standard redox potentials of these metals and nickel for comparison.

Electrode reaction	
$Au = Au^{3+} + 3e^- \longrightarrow$	+ 1.50
$Hg = Hg^{2+} + 2e^- \longrightarrow$	+ 0.85
$Ni = Ni^{2+} + 2e^- \longrightarrow$	+ 0.25

Current electrochemical uses of nickel

The current uses of nickel as an electrode material are unusual in as far as the electrochemical reactions rely on the formation of a strong surface oxidant. The surface active species is Ni^{3+} which is thought to occur as NiO(OH). Fig. 7.3 shows a cyclic voltammogram corresponding to the formation of the higher valence species. Ni^{3+} compounds can be prepared in the laboratory by the action of Br_2 on alkaline solutions of Ni^{2+}. This gives rise to a black hydrous oxide with the average composition NiO(OH). This species is an extremely powerful oxidizing agent. As a result of this property, nickel has found two important applications.

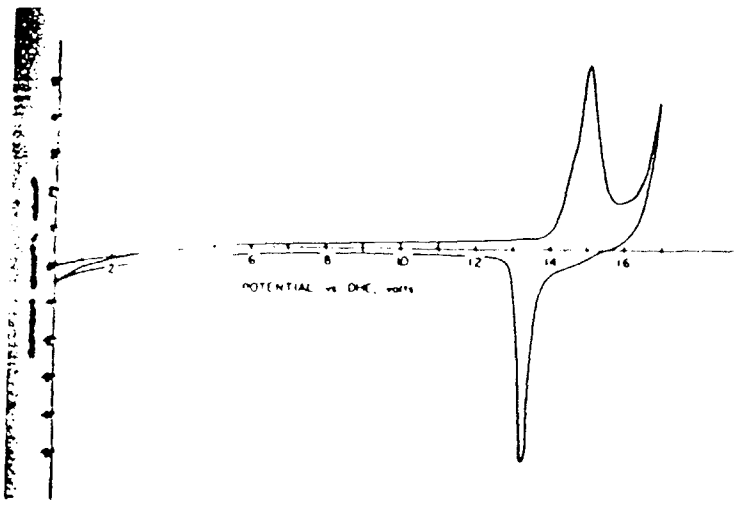

Fig 7.3. Cyclic voltammogram for nickel in 50 weight percent (w/o) potassium hydroxide at 47°C. The scan rate was 50mV sec^{-1}.

The peak before oxygen evolution is believed to correspond to Ni^{2+}/Ni^{3+} oxidation.

(1) As the anode in water electrolysers.

Oxygen evolution occurs at an oxide surface where the average oxidation state of the Ni is +3. At potentials higher than 1.5 volts vs rhe the Ni^{3+} is converted to Ni^{4+} which is inactive for oxygen evolution. Furthermore, nickel is stable under the conditions of anodic polarization in the alkaline solution.

(2) In the electrochemical oxidation of organic compounds.

Oxidations of simple functionalities such as -OH and $-NH_2$ have been carried out by anodically formed oxide films on nickel electrodes. Thus, 1° alcohols have been oxidized to carboxylic acids (Fleischmann, M. et al (1972)), 2° alcohols to ketones (Amjad, M. et al (1977)) and 1° amines to nitriles (Fleischmann et al (1972)). It should be noted that in these examples the electrochemical system serves only to provide a way of continuously regenerating the higher valence state of the reactive oxidant.

Concluding Remarks

Although the nickel oxide system is potentially very attractive, it is of course not suitable for use with enzyme electrodes. This is because of two important reasons. The first of these is due to the fact that, although the anodically produced oxide could, in principle, be used, e.g. in the oxidation of H_2O_2 produced by glucose oxidase, it would oxidize any susceptible species present in the solution. This would lead to erroneous results, although theoretically one could get around the problem by utilizing a dual electrode set-up. The second problem is much more serious and arises from the fact that the electrode would probably oxidize surface groups on the enzyme such as $-NH_2$, -OH, -SH. This would cause the properties of the enzyme to alter, at worst

the enzyme would denature, and incorrect and irreproducible results would be obtained from such a probe. Different avenues must therefore be explored.

CHAPTER 8

MATERIALS AND METHODS FOR SECTION II

Reagents

Unless otherwise stated, all solutions were prepared from Aristar grade (BDH) chemicals in high purity water (Millipore). Stock solutions of D-glucose (1.0M) were stored overnight at room temperature to allow equilibration of the α and β-anomers. Phosphate buffers were adjusted to the correct pH by the dropwise addition of 1.0M NaOH. Tris buffer was adjusted to the correct pH with 0.1M HCl.

Glucose oxidase (EC 1.1.3.4 type 2) from Aspergillus niger, mol wt 186,000, was supplied from Boehringer Mannheim and had an activity of 247 I.U. mg^{-1}. In this report the concentration of glucose oxidase is expressed in terms of the molarity of catalytically active FAD. This was determined spectrophotometrically using a lambda 3 Perkin Elmer and a molar extinction coefficient of 1.31×10^4 l mol^{-1} cm^{-1} at 450 nm (Duke, R.F. et al (1969)). Fresh solutions of enzyme were prepared on a daily basis.

Ferrocene carboxylic acid and dimethyl-amino-ethyl ferrocene were purchased from Aldrich Chemical Co. The other ferrocene derivatives mentioned in this work were synthesized by methods described later. Prior to use, the concentrations of stock ferrocene solutions were determined by Atomic Absorption Spectroscopy; the iron was released by adding 2 mls of aqua regia to the sample and incubating the solution at 40°C for 30 minutes.

Apparatus

D.C. cyclic voltammetry experiments and steady state measurements were performed, using a two component cell that

had a working volume of 1 ml (Plate 8.1). The glass cell was manufactured by the departmental glass blower. In addition to the nickel disc working electrode, the cell contained a 1 cm^2 platinum gauze counter electrode (Plate 8.1) and a saturated calomel electrode (SCE), purchased from Radiometer, as reference. In this work all potentials are referred to the saturated calomel electrode. The working compartment of the cell could be stirred during operation with a magnetic stirrer bar. Additions could be made directly to the cell via an injection port on the side of the working electrode.

Electrode construction

The main body of the working electrode was machined out of PTFE plastic by the departmental workshop. 0.25" diameter discs were cut from sheets of nickel with a steel punch.

Bulk nickel discs were spot welded to the brass rod, thus making an electrical connection to the external circuit, and then potted into the main electrode assembly with epoxy resin.

Porous nickel discs were potted into the electrode with nickel Araldite, a preparation made out of resin and finely ground nickel powder. Not only did the nickel Araldite seal the disc in place, but it also provided electrical contact and prevented the electrolyte solution from reaching the brass rod. A schematic drawing of the working electrode is shown in fig. 8.1.

Electrode pretreatment

i) Bulk nickel electrodes.

After manufacture, initial polishing was carried out by hand using wet Silicon Carbide paper. The polishing was started with coarse grade paper and finished with fine grade

Plate 8.1.

A shows a photograph of the electrochemical cell. The working compartment,1, had a volume of 1ml. 2, is the reference compartment.

B shows a photograph of both the platinum counter electrode and the finished nickel disc working electrode.

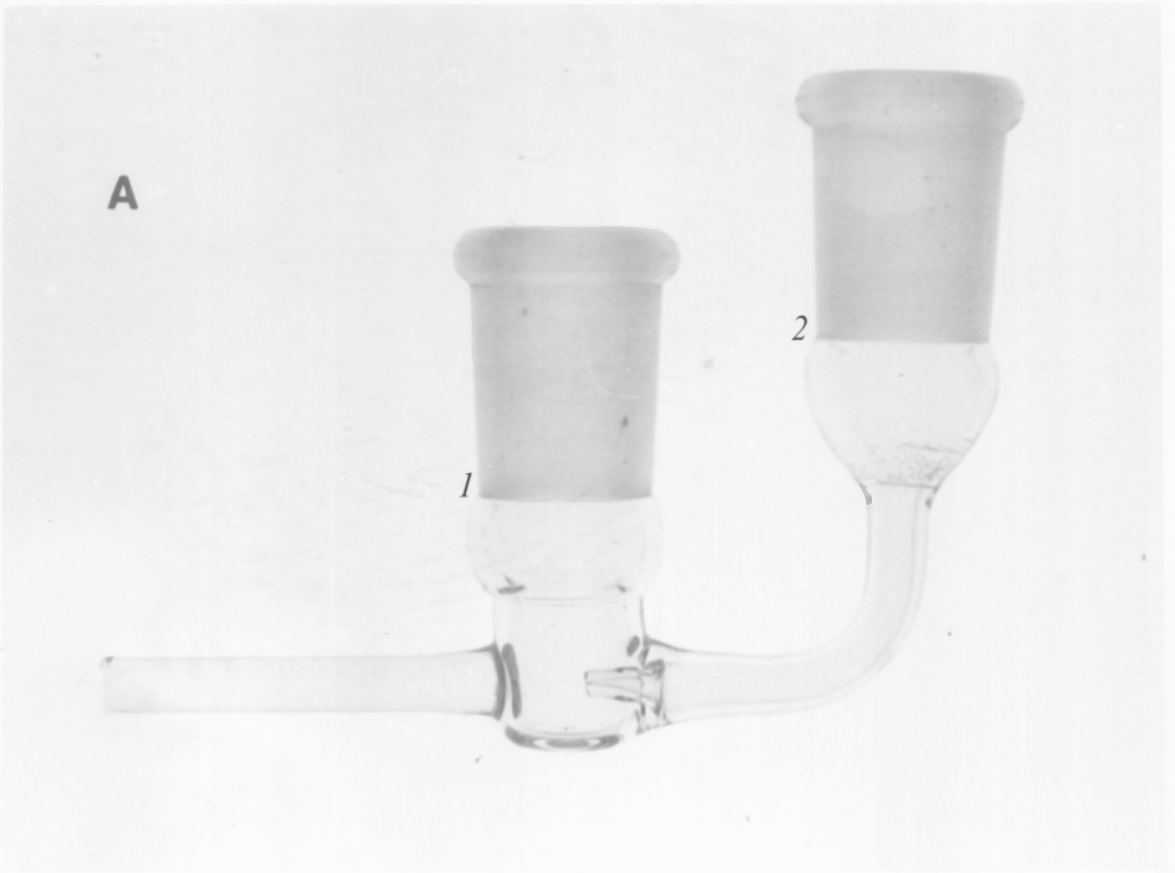
A
1
2

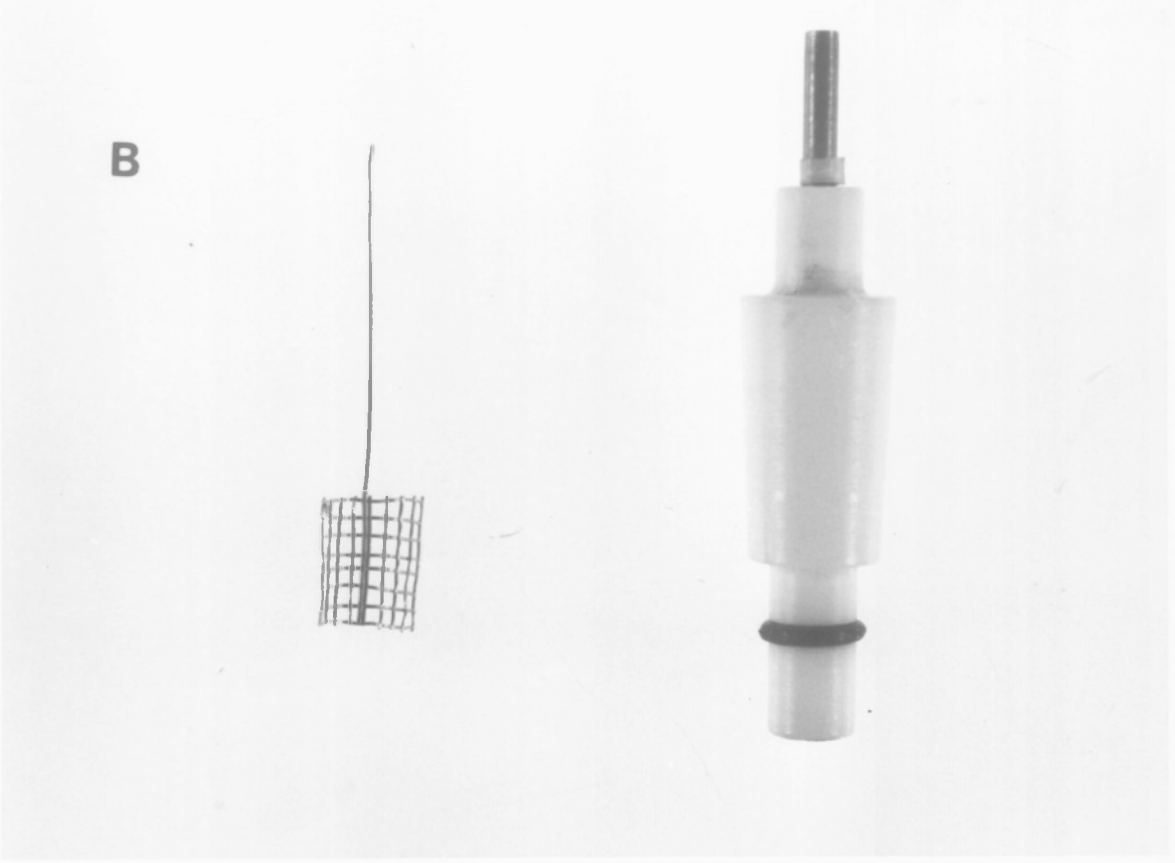
B

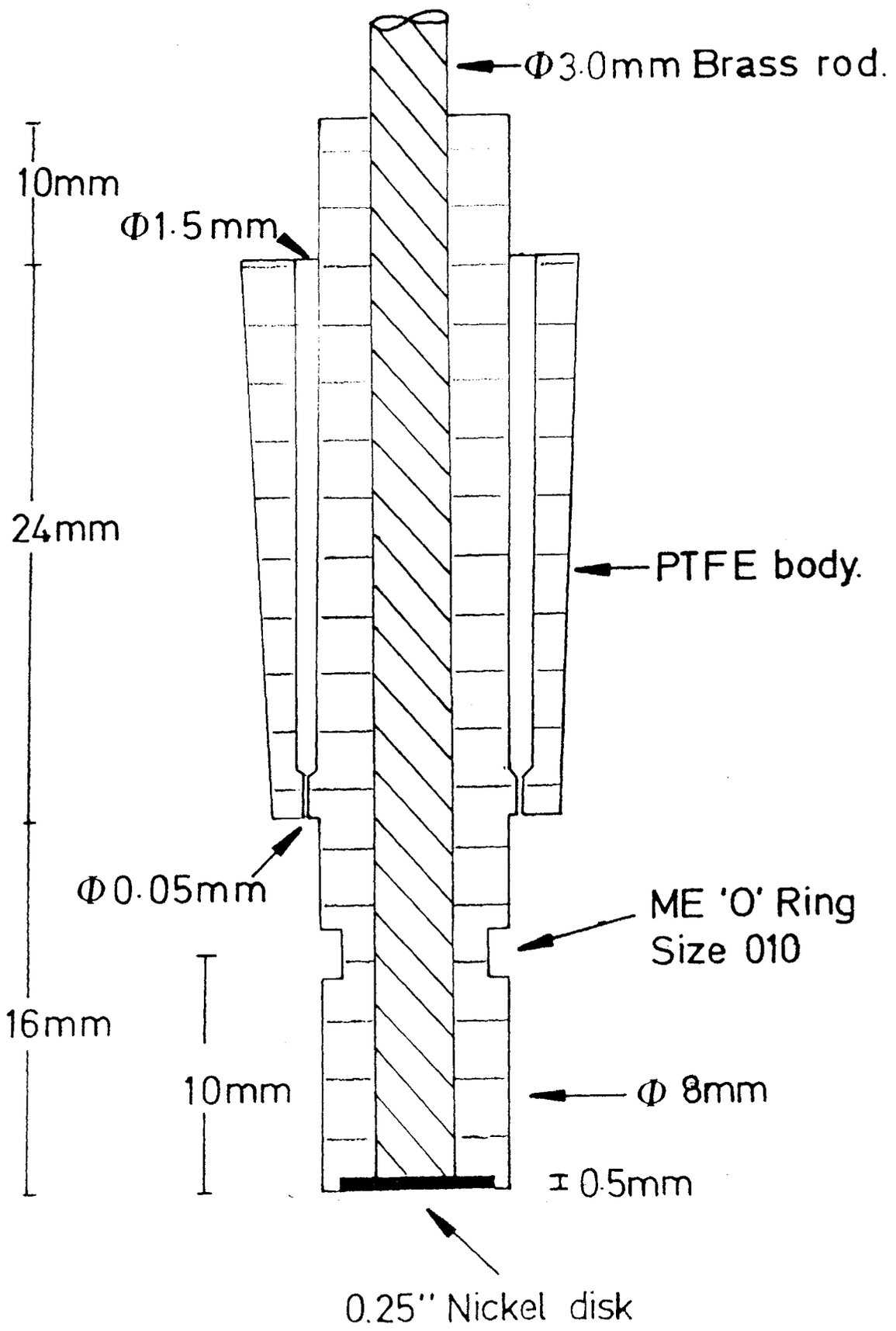

Fig 8.1.
Schematic drawing of the nickel disk working electrode.

6000 paper. When the surface of the electrode appeared smooth to the naked eye it was transferred to a cloth polishing wheel impregnated with diamond paste. Acetone was used as the lubricant. The appearance of the nickel surface was checked periodically using a low power metallurgical optical microscope. When the surface was judged to be free of gross imperfections the electrode was washed thoroughly in acetone, using an ultrasonic cleaning bath. The electrode was then stored in a dry cabinet until needed.

Immediately before use, the electrode was given a quick polish using high grade purity alumina powder (BDH) and then electrochemically cleaned by placing it in a solution of 0.1M H_2SO_4 and cycling the potential from 0 to -1V vs SCE for 15 minutes.

ii) Porous nickel electrodes.

Techniques involving abrasion were not applicable in this case. Furthermore, it was found that the porous electrodes could not be cleaned electrochemically as described above, since it was observed that under these conditions the iron in the supporting grid corroded. Consequently the following regime was adopted.

1) Surface grease was removed by washing the electrode with acetone using a sonicating water bath.

2) Immediately before use, any surface oxide was stripped by placing the electrode in dilute ammonia for a period of 2 hours. (The chemical basis of this treatment is that the surface layer is dissolved due to the formation of the soluble $[Ni(NH_3)_6]^{++}$ complex ion.

3) Finally, the electrode was washed with plenty of distilled water.

Instrumentation

D.C. cyclic voltammetry and steady state current measurements were made using a triangular wave generator and a potentiostat designed and built in the Chemistry Department. The applied potential was monitored using a Fluke digital multimeter. Current-time and current-potential curves were recorded using a Servogor x-y-t flat bed recorder.

Organic syntheses

i) Synthesis of trimethyl-amino-ethyl ferrocene $[Fe(Cp)_2(CH_2)_2N(CH_3)_3]^+I^-$.

The basis of this synthesis is the methylation of a 3° amine to give the corresponding quaternary ammonium salt. The reaction is summarized below.

$$R_3N: + R\text{-}X \longrightarrow R_4N^+ X^-. \quad (X = Cl^-, Br^-, I^-.)$$

In this reaction the alklyl halide undergoes nucleophilic substitution with the basic amine acting as the nucleophile.

Procedure

1g of dimethyl-amino-ethyl ferrocene (6.5 mmoles) was dissolved in 10 mls of toluene. To this was added 1 ml of methyl iodide (20 mmoles). Almost immediately a yellow precipitate was formed. The reaction mixture was left for 30 minutes in a well ventilated fume cupboard. After this time the reaction was considered complete. The precipitate was filtered, washed with dry ether (50 mls) and dried under vacuum so as to remove all traces of toluene and methyl iodide. T.L.C. analysis of the precipitate showed that the reaction had gone to completion.

Because it was known that Iodide (I^-) would be electroactive in the potential window of interest it was necessary to exchange it for an electroinactive anion. To this end, 5g of Dowex-1 (Cl^-) form was converted to the $H_2PO_4^-$ form by

repetitive washing with 1.0M NaH_2PO_4. The resin was then filtered and washed exhaustively with distilled water until the conductivity was zero. The resin was then removed and added to 10 mls of Millipore water. The precipitate was dissolved in 5 mls of the same and then added to the resin. The ion exchange reaction was allowed to proceed for 60 minutes. After this time, the resin was removed and the filtrate reduced by rotary evaporation. The resultant solution was then freeze dried overnight, giving a yellow amorphous residue. Finally, the product was characterized by D.C. cyclic voltammetry on a gold electrode (Fig. 8.2).

The steps involved in this synthesis are outlined below.

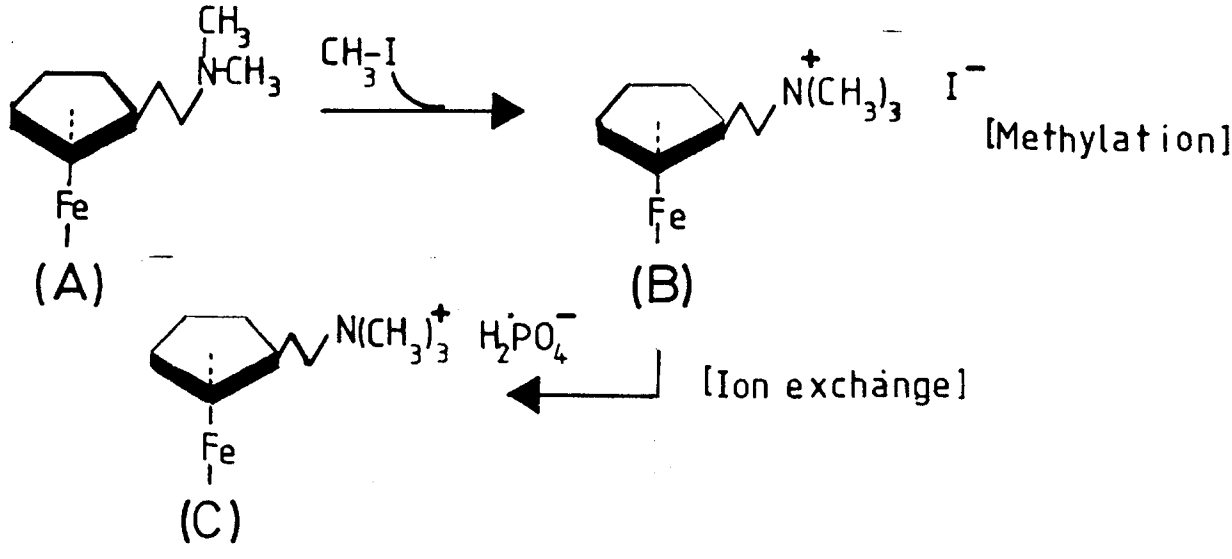

ii) Synthesis of Ferrocene-1-aminohexyl-carboxamide

$(Fe(Cp)_2 \cdot CONH \cdot (CH_2)_6 \cdot NH_2)$

The chemical basis of this synthesis was to make a stable peptide bond between the carboxyl group of ferrocene carboxylic acid and one of the free amino groups present on the diamino hexane moiety. To this end the synthesis was carried out in two steps.

Step (1) Activating the carboxyl group of the ferrocene

Fig 8.2.

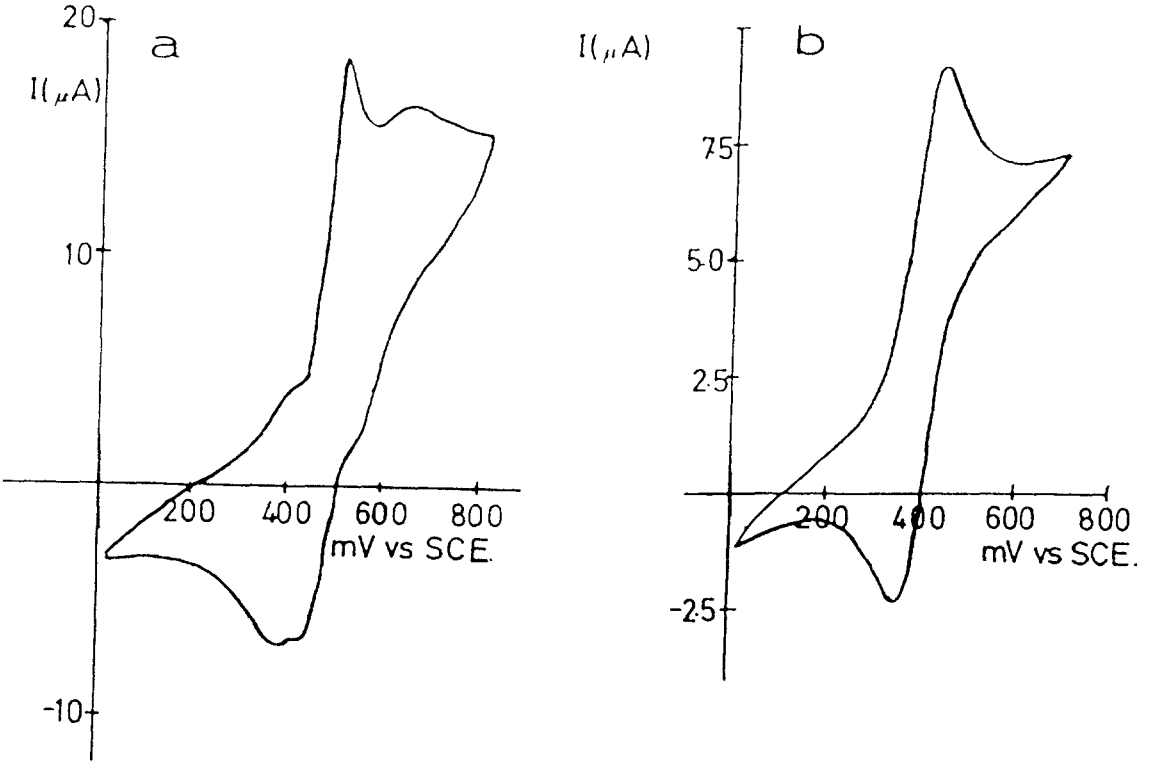

(a) D.C. cyclic voltammogram of B in $NaClO_4$ (0.1M) obtained at a gold electrode. The scan rate was $5mVs^{-1}$.
(b) D.C. cyclic voltammogram of C in $NaClO_4$ (0.1M) obtained at a gold electrode. The scan rate was $5mVs^{-1}$.

carboxylic acid.

Step (2) Form the peptide linkage.

Step (1):

There are many techniques reported in the literature for making a peptide bond between a terminal carboxylic acid group and a free amino group. Various techniques were tried in this work but for brevity only the successful protocol will be described.

The chemical basis of the activation step was to form a mixed anhydride between ferrocene carboxylic acid and iso-butyl-chloroformate. The reaction is summarized below.

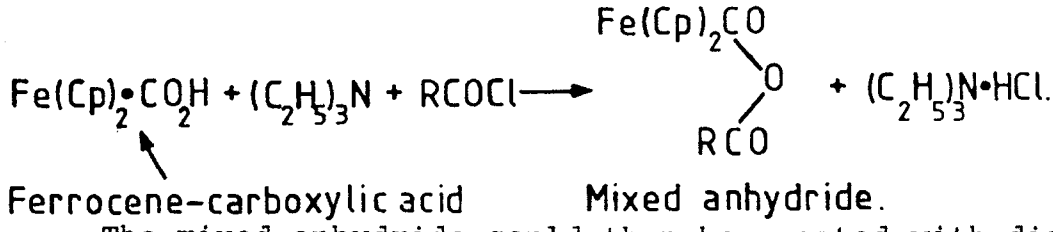

The mixed anhydride could then be reacted with diamino hexane to produce the desired compound. (Wieland, T. et al, (1950)).

Protocol:

0.5g of ferrocene carboxylic acid (2.17 mmoles) was dissolved in 50 mls of distilled toluene. This required vigorous stirring for one hour. The resultant yellow solution was filtered. To this was added 2.2 m moles of triethylamine. The solution was transferred to a 250 mls round bottom flask and cooled by placing it on ice.

Next, 2.2 mmoles (270 µl) of iso-butyl-chloro-formate was added with stirring. On addition of the above compound white fumes were seen at the surface of the liquid and the reaction solution turned a deep red colour. The reaction mixture was left for two hours and then filtered to remove any insoluble triethylamine hydrochloride. T.L.C. analysis

analysis showed that the reaction had gone to almost total completion (Fig. 8.3).

Step (2):

2.3g (20 mmoles) of 1,6-diaminohexane were crushed in a pestle and mortar to give a white amorphous powder. The powder was dried under vacuum in the presence of phosphorous pentoxide.

The dried powder was then dissolved in the minimum amount of distilled dimethyl formamide (~ 50 mls). The solution was filtered and made up to 100 mls with chloroform. (This step was necessary to ensure the solubility of the mixed anhydride prepared in step 1). The resultant solution was then cooled.

The filtered solution from step 1 was then added in a dropwise fashion. Almost immediately a fine precipitate formed. When the addition was complete the resultant mixture was covered with silver foil and stored overnight at 4°C. The next day, the solution was filtered, yielding a yellow filtrate and an orange precipitate.

T.L.C. and spectrophotometric analysis revealed that the precipitate was ferrocene carboxylic acid. The T.L.C. results are summarized in fig. 8.3.

Proof that the filtrate contained the desired product was obtained as follows:

(1) On T.L.C. a single yellow spot was detected. The yellow colour was indicative of the ferrocene chromophore. (This was also shown spectrophotometrically). If the plate was then sprayed with ninhydrin, the yellow spot turned a deep purple colour. This reaction is indicative of the presence of a free amino group. Note also that diamino hexane and the unknown

Fig 8.3.

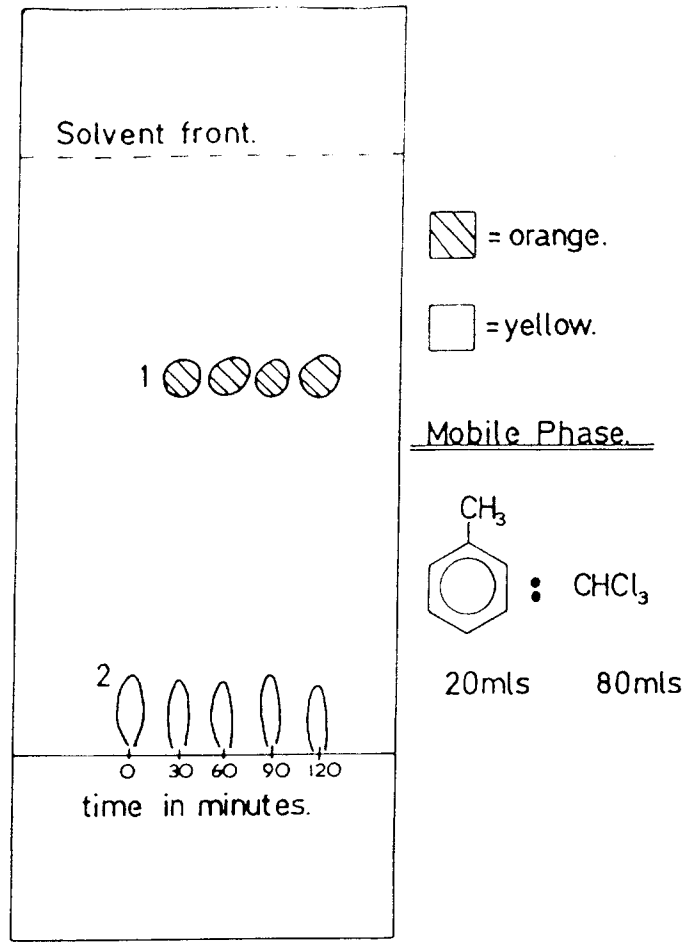

Plate: DC-Alufolien Kieselgel 60.

TLC analysis of Step (1).

2 represents the starting material, ferrocene carboxylic acid.

1 represents the product, the mixed anhydride.

Because both compounds were coloured, no stain was used.

Rf values of the compounds.

Spot No	:	Rf value
1		0.063
2		0.620

Fig 8.3 cont'd.

1 = 1,6-diaminohexane.
2 = Ferrocene Carboxylic acid.
3 = Supernatant.
4 = Precipitate.

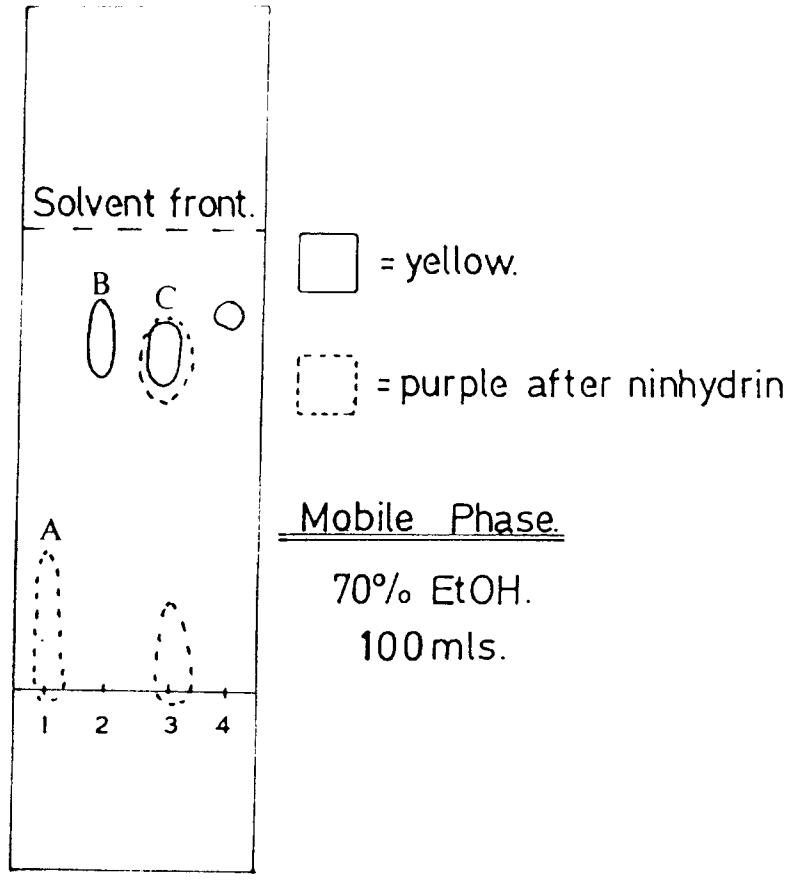

Plate: DC-Alufolien Kieselgel 60.

TLC analysis of Step (2).

A represents 1,6,diaminohexane.

B represents ferrocene carboxylic acid.

C represents the product.

Rf values of the compounds.

Spot No	:	Rf value.
A		0.17
B		0.78
C		0.73

are sufficiently separated so as not to make contamination a problem.

(2) If the compound was purified from a preparative plate and re-run on another system, again only one spot was detected. This also turned purple, following the ninhydrin treatment.

The presence of the ferrocene group plus the reactions indicative of a free amino group were taken as evidence for the structure;

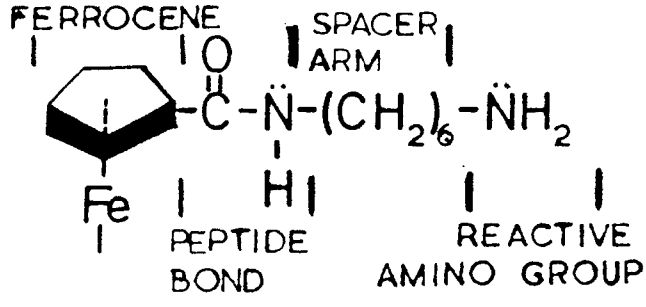

CHAPTER 9

RESULTS

In the following investigation I decided to use the glucose-glucose oxidase system as a paradigm enzyme electrode. The reasons for this choice were as follows.

i) It is a well characterized and well understood system.

ii) There is tremendous interest in developing a glucose sensor for use in the general management of diabetes. Any results obtained in this work might prove useful.

iii) Because of the fact that a variety of compounds can accept electrons from reduced glucose oxidase. This is important in the sense that if monitoring the reaction by the usual electrochemical means proves unsuccessful, e.g. the anodic oxidation of hydrogen peroxide, there is an alternative approach available.

Oxidation of hydrogen peroxide on base nickel

First, I investigated the possibility of using a nickel electrode to carry out the anodic oxidation of hydrogen peroxide present in the electrochemical cell. Steady state current-potential curves were obtained in the presence and absence of hydrogen peroxide.

The data indicated that in the presence of 20mM hydrogen peroxide a current flowed at potentials greater than 800mV vs SCE. This was attributed to the oxidation of the hydrogen peroxide at the electrode surface. When the experiment was repeated in the absence of hydrogen peroxide it was seen that a current also flowed at similar potentials. This was attributed to the onset of nickel oxidation, i.e. $Ni \longrightarrow Ni^{2+} + 2e^{-}$. Because the two events are superimposed it does mean that nickel cannot be used to carry out the oxidation of the

peroxide. Eventually, the surface of the nickel electrode would become covered with an inert oxide film. Recalling the standard redox potential for the oxidation of nickel this result should not be too surprising.

Oxidation of ferrocene carboxylic acid

Next, the electrochemical behaviour of ferrocene-carboxylic acid was investigated on base nickel by cyclic voltammetry. (A discussion of this technique is given in the appendix). A typical cyclic voltammogram obtained in this work is shown in fig. 9.1.

This represents an extremely irreversible voltammogram indicating that under these experimental conditions the electron transfer reaction of the ferrocene to the electrode is very slow.

Because of the poor results obtained with ferrocene carboxylic acid, I investigated the electrochemistry of other compounds, which were known to accept electrons from reduced glucose oxidase, on base nickel. Promising results were with potassium ferricyanide, where reversible one electron cyclic voltammetric waves were observed. Furthermore, if the potential was repetitively cycled between 0 and 800mV vs SCE waves were observed, which were indicative of a surface deposition phenomenon. Following such treatment, when the electrode was removed, washed thoroughly with distilled water and placed in a solution of background electrolyte (0.1M $NaClO_4$) the cyclic voltammogram shown in fig. 9.2(b) was observed. Fig. 9.2(a) represents the cyclic voltammogram obtained from an unreacted nickel electrode under identical conditions.

The observation of a persistent voltammogram, together with the fact that it was not affected by stirring the electro-

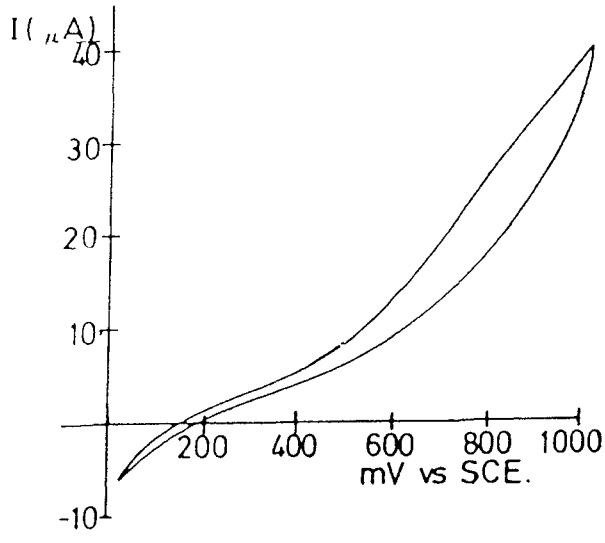

Fig 9.1.

D.C. cyclic voltammogram of 20mM carboxy ferrocene on a bare nickel electrode at a scan rate of $5mVs^{-1}$. This represents an extremely irreversible cyclic voltammogram.

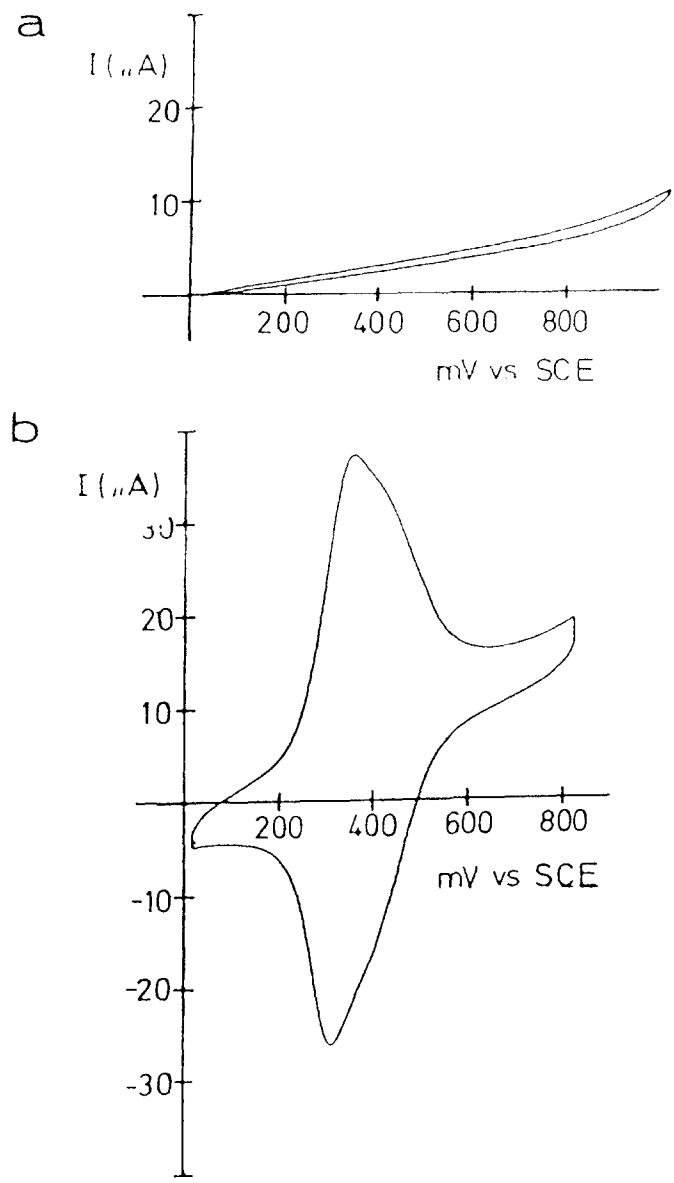

Fig 9.2.

(a) D.C cyclic voltammogram of an unreacted nickel electrode in $NaClO_4$ (0.1M) at $2mVs^{-1}$.

(b) D.C. cyclic voltammogram of a derivitized nickel electrode in $NaClO_4$ (0.1M) at $2mVs^{-1}$.

By measuring the area under both peaks it is possible to show that the same quantity of material is oxidized and reduced in each cycle. In this respect, the reaction is reversible.

lyte, was taken as evidence of prolonged surface attachment.

Similar findings have since been reported in the literature by Bocarsly et al (Bocarsly, A.B. and Sinha, S. (1982)), who modified a nickel wire by anodic potentiostating in an electrolyte solution containing potassium ferrocyanide.

Description of the modified nickel electrode

From the results presented by Bocarsly et al (Bocarsly, A.B. and Sinha, S. (1982)), as well as those described here, it can be concluded that the basis of this particular modification is the formation of an insoluble precipitate on the surface of the nickel with a complex anion, in this instance $Fe(CN)_6^{3-}$, which has the ability to both oxidise Ni^0 and precipitate Ni^{2+} from solution. The net result is a chemi-sorbed salt with the following general composition.

$$Ni_x^{II}[Fe(CN)_6]_y^{n-}$$

Bocarsly's hypothesis is supported by the following lines of evidence.

i) If nickel powder is reacted with $Fe(CN)_6^{3-}$, washed with distilled water and then stripped by washing with 1.0M NaOH, it can be shown by optical spectroscopy that the only material present in the basic stripping solution is $Fe(CN)_6^{4-}$. This shows that the surface species is intact $Fe(CN)_6^{4-}$ and implies that the electroactive material is the $Fe(CN)_6^{4-/3-}$ redox couple. The fact that only $Fe(CN)_6^{4-}$ is observed, although the initial reactant was $Fe(CN)_6^{3-}$, establishes the surface oxidation of $Ni^0 \longrightarrow Ni^{2+}$.

ii) Surface derivitisation of the nickel powder is not

observed when it is reacted with material which either cannot oxidize Ni^0 or form a precipitate with Ni^{2+} ions in solution. Such material includes $Fe(CN)_6^{4-}$, $Fe(CN)_5H_2O^{2-}$ and $Fe(CN)_5NO^{2-}$.

A final line of evidence to support the proposed nature of the surface species comes from considering the $E_{\frac{1}{2}}$ value for the immobilized salt. (In this context the $E_{\frac{1}{2}}$ value is taken as the average potential for the cathodic and anodic peaks). From fig. 9.2(b) an $E_{\frac{1}{2}}$ value of +340mV vs SCE is obtained. (Bocarsly et al present a similar value). This is fairly close to the value reported in the literature for the solution $Fe(CN)_6^{4-/3-}$ redox couple (+210mV vs SCE) (Gutmann, G. et al (1976)).

The synthesis of the modified electrode proved exciting for a number of reasons. First, the presence of the surface film meant that the nickel was now protected and as a result would be stable under anodic potentiostating. Secondly, it was now possible, at least in theory, to carry out reversible electrochemistry with ions since the redox reaction would be mediated by the surface film. Finally, because $Fe(CN)_6^{3-}$ was a known electron acceptor of reduced glucose oxidase, it seemed reasonable to suppose that direct electron transfer from reduced enzyme to the modified electrode might take place.

Preparation of derivitized nickel electrodes

For routine applications it was found that a convenient way of derivitizing the nickel surface was to place the electrode in a solution containing 50mM potassium ferrocyanide, $Fe^{II}(CN)_6^{4-}$ and then apply an anodic potential of +450mV vs SCE for one hour. A bright yellow band, indicating the formation of $Fe^{III}(CN)_6^{3-}$, was seen to form at the surface of

the electrode. This diffused into the bulk electrolyte during the course of the experiment. It was observed that the best surface coverages were obtained when the experiment was carried out in a quiescent solution. Note that this finding is consistent with the idea of a surface precipitation reaction.

Although identical experimental conditions were always employed it was difficult to obtain exactly reproducible surface films. The reason for this is unclear at the moment but may have something to do with the fact that identical electrode surfaces may not always have been presented to the derivitizing solution.

Finally, it was found that some electroactive material could be deposited onto the surface of the electrode simply by dipping it into a strong solution (0.1M) of potassium ferricyanide. This procedure, however, was not very satisfactory and gave even more irreproducible coatings.

The sequence of reactions giving rise to the surface material can be summarized as:

i) $Fe^{II}(CN)^{4-} \longrightarrow Fe^{III}(CN)_6^{3-}$ (Electrochemical oxidation)

ii) $2Fe^{III}(CN)_6^{3-} + Ni^0 \longrightarrow Ni^{2+} + 2Fe^{II}(CN)_6^{4-}$ (Surface oxidation)

iii) $Ni^{2+} + 2Fe^{II}(CN)_6^{4-} \longrightarrow Ni_x^{II}[Fe(CN)_6]_y^{n-}$ (Precipitation)

Modified Electrodes

Before presenting further experimental data it is pertinent to give a general discussion on modified electrodes. This will serve two purposes in that it will (a) acquaint the reader with the subject, and (b) help to explain the rationale behind subsequent experiments.

Modified electrodes differ from ordinary base electrodes in that the electrochemical reactions of species in solution take place through a thin surface film. As a result, instead of a direct electron transfer between the Fermi layer of the metal and an ion in solution, the electron transfer is mediated by the redox groups present in the layer. A schematic drawing of this is shown in fig. 9.3. It follows from this that the generation of a chemically derivitized surface can significantly alter the charge transfer properties of the native electrode.

The movement of charge through a surface attached electroactive film proceeds in an outward direction from the electrode surface towards the film solution interface. Direct electron transfer between the electrode and the layer involves only those redox centres immediately adjacent to the electrode surface. Subsequent charge transfer to the sites in the layer furthest from the electrode surface is driven by the difference in the ratio of the reduced and oxidized centres in the film and that dictated by the Nernst equation at the applied potential. It has been shown that the movement of charge through the layer obeys Fick's laws of diffusion (Daum, P. and Murray, R.W. (1974)).

Conceptually it seems likely that electron hopping between adjacent localised oxidation states is the mechanism for the migration of charge through the fixed surface film. The rate at which the charge migrates through the film can be dependent upon:

1) The rate of charge transfer between the electroactive centres.

2) The rate at which counterions move through the surface matrix (Murray, R.W. (1980)). In this context

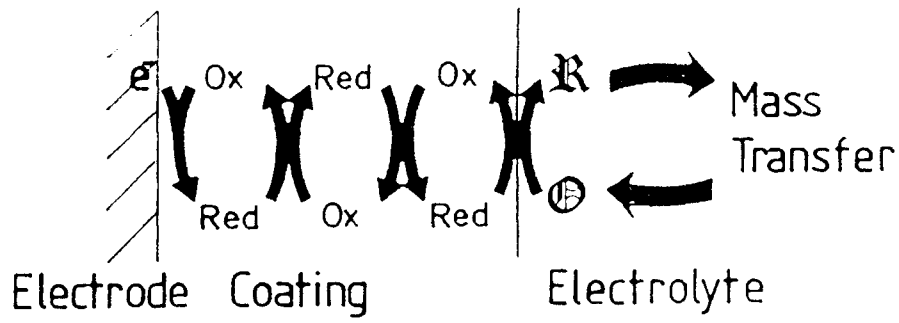

O & R = Solution redox couple.

Fig 9.3.
Diagrammatic representation of mediated electron transfer in a modified electrode. Electrochemical reactions of the solution species is mediated by the redox groups present in the surface film. The movement of charge through the film is driven by the difference in the ratio of the reduced and oxidized centres in the film and that predicted by the Nernst equation.

$$E_{eq} = E^{\circ} + \frac{RT}{nF} \ln \frac{[Ox]}{[Red]}$$

Nernst equation

counterions move into and out of surface films in order to maintain charge neutrality in the bulk matrix in response to changes in the applied potentials. The significance of this will become apparent later.

Ferricyanide as a Surface Mediator to Glucose Oxidase

Having prepared the modified nickel electrode, I investigated the possibility of obtaining direct electron transfer between it and reduced glucose oxidase. As it is known that the kinetics of charge transfer through a surface layer can be influenced by the transport of counterions (Murray, R.W. (1980), Kaufmann, F.B. et al (1979)), it was first necessary to investigate the properties of the modified electrode in different buffer systems which would also be suitable for the enzyme reaction.

The buffers used in this investigation were;

1) 0.1M Sodium Phosphate pH 7.0
2) 0.1M Potassium Phosphate pH 7.0
3) 0.1M Tris/Cl pH 7.0

The relevant data obtained in this investigation are presented in fig. 9.4.

The results show that the midpoint potential of the surface attached species, $E_{\frac{1}{2}}$, is dependent upon the nature of the supporting counterion. This is most clearly shown when Tris/Cl is used as the supporting electrolyte, fig. 9.4(b). In this case only an oxidation wave is seen when the potential is scanned. Furthermore, if the potential is repetitively swept the anodic peak current, ip_a, decreases and eventually becomes zero. The reason for this behaviour will be discussed later. The results obtained with the two phosphate buffers are summarized below;

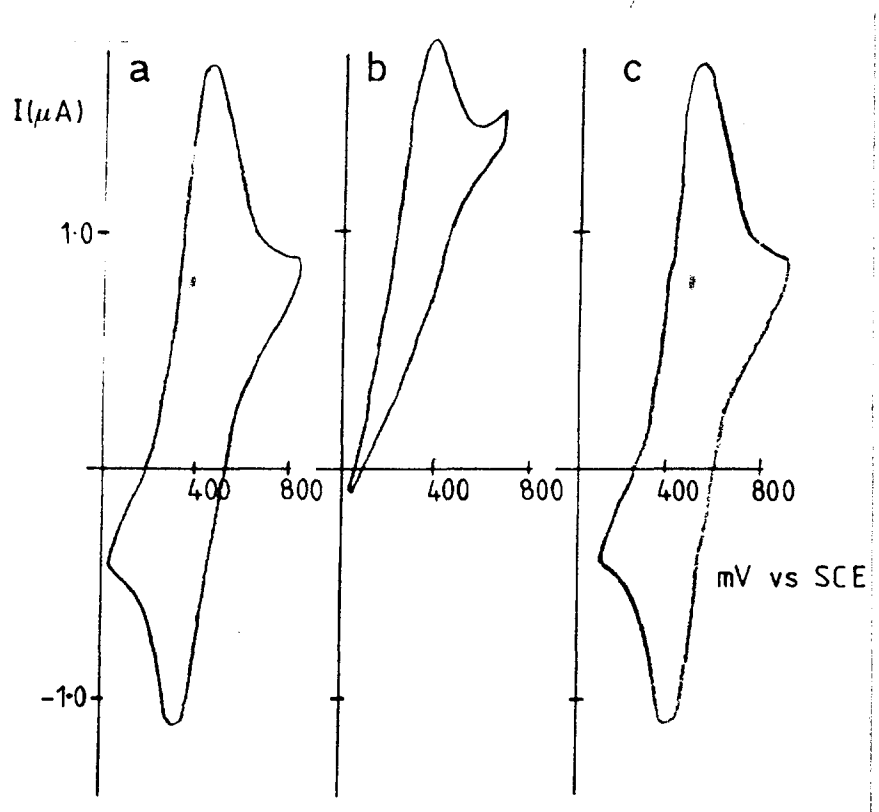

Fig 9.4. Cyclic voltammograms of the Ni/$Fe(CN)_6^{4-/3-}$ modified electrode obtained in different electrolyte systems.

a Sodium phosphate pH 7.0.

b Tris/HCl pH 7.0.

c Potassium phosphate pH 7.0.

Cation	:	$E_{\frac{1}{2}}$
Na^+		365mV vs SCE
K^+		490mV vs SCE

As a final point, it was observed that, irrespective of the buffer used, the process was completely reversible in that changing the cation from one to the other and then back again always reproduced the original voltammogram.

In their most recent report, Bocarsly *et al* have communicated their findings of a similar investigation (Bocarsly, A.B. and Sinha, S. (1982)). I have summarized their results below;

Cation	:	$E_{\frac{1}{2}}$
Cs^+		700mV vs SCE
Li^+		110mV vs SCE
Na^+		355mV vs SCE
K^+		470mV vs SCE

From this data it is also evident that the kinetics of charge transfer through the surface films is influenced by the nature of the counterion.

If the above observations, and those reported here, are compared to those seen with the solution $Fe(CN)_6^{4-/3-}$ redox couple a discrepancy is seen to arise. The literature indicates at most a 10-30mV shift in the midpoint potential as a function of the supporting electrolyte (Eaton, W.A. *et al* (1967)). The anomalous behaviour of the modified electrode can be explained as being due to differential counterion transport through the surface matrix. Recalling that counterions function to preserve charge neutrality, it follows that ideal behaviour will only be observed when the transport of counterions through the matrix is not limiting. In this respect size

is often an important parameter in determining the rate of migration of counterions through surface films since it follows that counterions have to permeate through the crystal lattice of the surface bound material. Consequently, the effects of counterion transport will be least pronounced in those films whose crystal lattice is open in structure. It must also be pointed out that sometimes small counterions, rather than being beneficial, can cause defects to occur in the structural matrix of the surface bound material. Bocarsly has shown this to be the case for the Cs^+ ion. The effects of Cs^+ ion transport were manifest as a broadening of the cathodic and anodic peaks in the voltammogram and a shifting of the $E_{\frac{1}{2}}$ value to very positive potentials.

Taken together, the results presented above show that the surface bound material cannot be thought of as simply a tethered solution redox couple which keeps its solvation sphere and has a chemical reactivity similar to the solution $Fe(CN)_6^{4-/3-}$ redox couple. Rather, one must invoke a model which presents the chemically synthesized interface as a solid phase with a definite geometrical structure and possessing minimum solvent interactions, yet being capable of sustaining ionic transport. A similar model has been proposed for Prussian Blue modified electrode surfaces (Itaya, K. et al, (1982)).

In the light of such a model it is now possible to explain the result obtained when Tris/Cl was used as the supporting electrolyte. In simplistic terms, this is due to the fact that the counterion, fig. 9.5, is too massive to pass through the surface film. Consequently, it can not support appreciable charge transfer with the result that the voltammogram eventually collapses.

Fig 9.5.

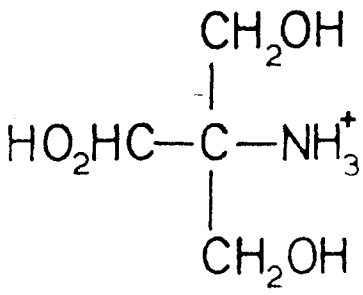

Returning to the question of electron transfer from reduced glucose oxidase to the modified electrode, it is clear from the results presented above that Tris/Cl is unsuitable as a buffer-electrolyte system. As the redox potential was seen to be sensitive to both Na^+ and K^+ preference was given to using sodium phosphate as the buffer system for the following reasons.

i) The redox waves observed with the sodium buffer occur at lower potentials than those seen with potassium phosphate. The implication of this is that the kinetics of charge transfer in the film are more rapid when Na^+ is the counterion.

ii) The $E_{\frac{1}{2}}$ value more closely resembles that of the solution redox couple when Na^+ is the counterion. Again, this implies that the charge transfer kinetics and hence counterion transport are more favourable in the sodium salt buffer.

Having established sodium phosphate as the ideal buffer-electrolyte system, it was then important to determine the stability of the surface under these conditions since this would ultimately determine the usefulness of the modified electrode. In this particular case instability would be manifest as the decay in the electrochemical response as a function of time. In turn, this could be due to factors such as the reaction of the electroactive film with impurities in the base electrolyte or desorption of electroactive material from the surface of the electrode.

Under conditions in which the potential was swept from 0 to +800 mV vs SCE in a repetitive manner, the film showed remarkable stability. For instance, it was noted that if the potential was cycled one hundred times there was no decrease in the amount of current that was passed. The electrode could be removed from the solution, stored in a dry place overnight and used the next day without any apparent deterioration. It was noticed, however, that several cyclic potential sweeps (usually between five and ten) were required for the film to become fully electroactive and reach a state which yielded reproducible current-voltage curves. The reason for this behaviour is probably due to solvent swelling effects.

Finally, the modified electrode was characterized by cyclic voltammetry. The results obtained, presented in fig. 9.6, were interpreted as follows:-

According to current electrochemical theory, the peak to peak separation for non diffusive reversible charge transfer is zero, while a one electron reversible solution process should yield a peak to peak separation of 59mV. In both cases, the peak to peak separation remains unchanged irrespective of the sweep rate, v (Laviron, E. (1979), Nicholson, R.S. and Shain, I. (1964)).

A peak width at half height, $\Delta E_{\frac{1}{2}}$, of 90mV is predicted, assuming a one electron reversible process (Laviron, E. (1979)).

Finally, for non diffusive charge transfer the peak current (ip_a and ip_c) should be directly proportional to the scan rate. For a solution species the peak current is predicted to be proportional to the square root of the scan rate, $(v)^{\frac{1}{2}}$.

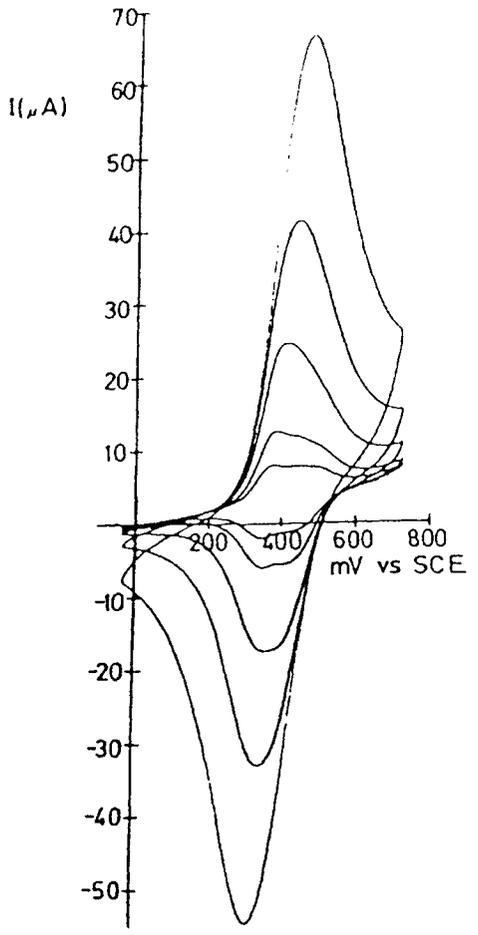

Fig 9.6.

D.C. cyclic voltammogram of the Ni/$Fe(CN)_6^{4-/3-}$ electrode in NaH_2PO_4 (0.1M) pH 7 showing scan rate dependence of peak current and peak to peak separation.

Analysis of the results presented in fig. 9.6 reveals that the kinetic behaviour displayed by the modified nickel electrode is not totally consistent with the idea of non diffusive reversible charge transfer. The observed behaviour is summarized below.

i) The peak to peak separation is greater than zero, particularly at the fast scan rates, and increases with increasing sweep rates. This is indicative that at the faster sweep rates the movement of charge through the surface film is limited by diffusion.

ii) The peak currents are linearly proportional to v only up to 20mV sec^{-1} (fig. 9.7). Again, this suggests the diffuse nature of the waves.

iii) The observed $\Delta E_{\frac{1}{2}}$ is greater than 90mV. This particular instance of non ideality may be due to

(a) Repulsive interactions in the film (Murray, R.W. and Mosed, M. (1977)).

(b) Differences in the spatial distribution of the redox centres present in the surface film (Itaya, K. and Bard, A.J. (1978)).

(c) Distribution within the surface film of redox centres with slightly different E^{o} values (Wrighton, J. et al (1978)).

The reason for the large $\Delta E_{\frac{1}{2}}$ can be elucidated by analyzing the shapes of the cyclic waves and in particular those obtained at slow scan speeds. As can be seen, these represent complex cyclic voltammetric waves which consist of a wave and a corresponding shoulder. This type of complex wave form is indicative of example c. The presence of non equivalent sites suggests that the film has been deposited on the surface of the nickel in a non homogeneous manner.

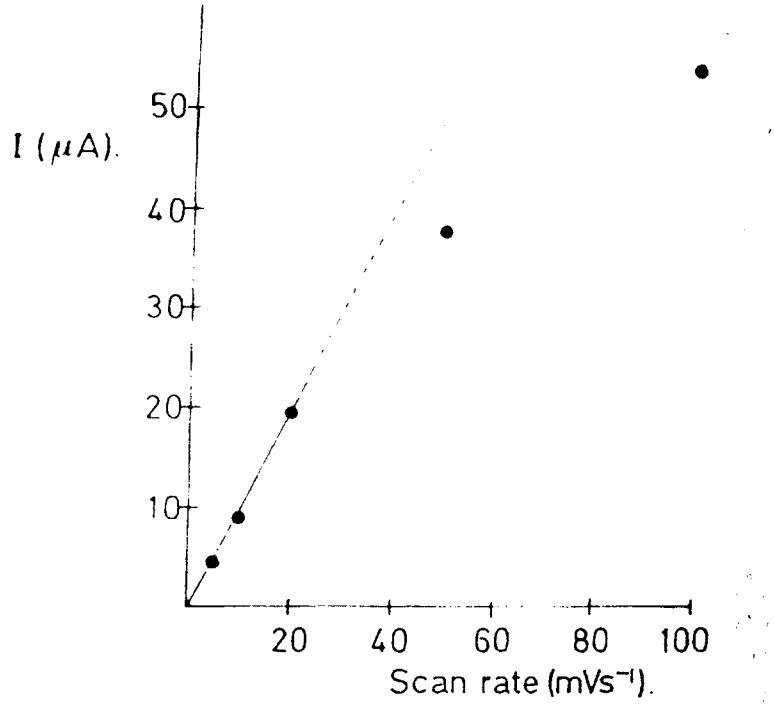

Fig 9.7.

Plot of i_{peak} vs scan rate for the Ni/$Fe(CN)_6^{4-/3-}$ modified electrode. The loss of linearity suggests that at scan rates greater than 20mVs^{-1} the flux of charge through the surface film becomes diffusion limited.

(Note, the data presented above has been corrected for any charging contributions.)

In such a film the chemical environments of the individual redox centres may be sufficiently different to alter their E^{o} values. (Note that this situation is analagous to the effect that different chemical environments can have on the pk values of acid or basic moieties).

The diffusion limited kinetics observed for the flux of charge through the film could be due to either slow counterion movement or sluggish charge transfer between non equivalent redox centres.

Having characterized the modified electrode, the stage was now set to see if electron transfer would take place rapidly from reduced glucose oxidase to the surface groups of the modified electrode.

It soon became evident that, irrespective of the experimental strategy employed, direct electron transfer from the reduced enzyme to the modified electrode was not observed. A possible explanation for this disappointing result may be that the electroactive moiety of glucose oxidase, the FAD cofactor, is buried deep within the structure of the enzyme and is therefore not accessible to the surface of the electrode. Unfortunately there is no X-ray data available at present to support this hypothesis.

A new approach was therefore needed, and the obvious line of investigation to follow was to see if the electrochemistry of ferrocene, or its derivatives, could be mediated by the redox groups present on the modified electrode.

Electrochemistry of ferrocene derivatives at the modified nickel electrode

Ferrocene is a transition metal π-arene complex which consists of an iron atom sandwiched between two cyclopentadienyl rings (fig. 9.8).

Fig 9.8.

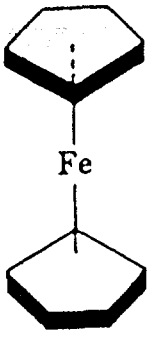

The sandwich structure has been verified by x-ray studies. Only one type of C-H bond is found in I.R. and n.m.r. The ferrocene rings are electron rich, each carbon atom having 1.2x greater electron density than the carbons in benzene. As a result, amino ferrocene is much more basic than aniline and ferrocene carboxylic acid is more acidic than benzoic acid.

Oxidation of ferrocene can be effected by a wide variety of organic and inorganic agents. Furthermore, ferrocene can also be oxidized electrochemically (Cass, A.G. et al (1984)).

Preliminary experiments were carried out to see if dimethylaminoethyl ferrocene would undergo reversible electrochemistry at the derivitized nickel electrode. Fig. 9.9(b) shows the oxidation voltammogram for a stirred solution (a polarogram) of this compound at the modified electrode. Fig. 9.9(a) shows the cyclic voltammogram corresponding to the surface film of the modified nickel electrode. The results show that the oxidation wave of the ferrocene is superimposed onto the cyclic voltammetric waves of the surface film in so far as:

(1) The oxidation of the ferrocene commences at the onset potential for the surface bound material.

(2) The half wave potential for the oxidation of the ferrocene is very close to the peak oxidation potential (ip_a) of the surface immobilized redox couple. Together, these

Fig 9.9.

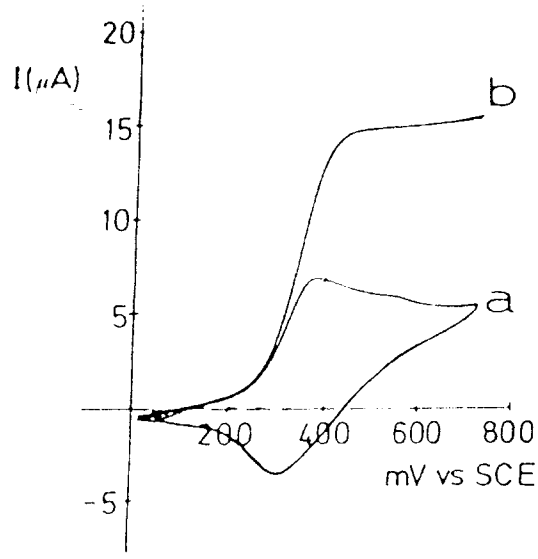

(a) D.C. cyclic voltammogram of the Ni/$Fe(CN)_6^{4-/3-}$ electrode in $NaClO_4$ (0.1M). The scan rate was $1mVs^{-1}$.

(b) Current potential curve for the oxidation of 20mM dimethyl amino ethyl ferrocene at the modified electrode. The electrolyte was $NaClO_4$ (0.1M) and the scan rate was $1mVs^{-1}$. This experiment was carried out in a stirred solution.

Note that the steady-state voltammogram for the oxidation of the ferrocene (b) is superimposed on the cyclic voltammogram of the modified electrode and commences at the onset potential for $Fe(CN)_6^{4-}$ oxidation. Furthermore, the half-wave potential for the oxidation reaction is very close to the peak oxidation potential of the surface layer. This suggests that the oxidation of dimethyl amino ethyl ferrocene is mediated by the redox groups present in the layer.

Under these conditions the sequence of redox reactions occurring at the modified electrode can be represented as;

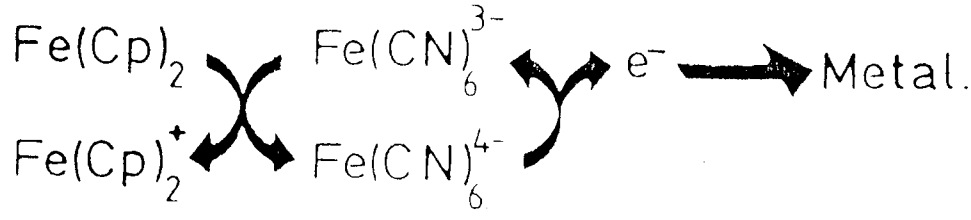

Fig 9.9. cont'd

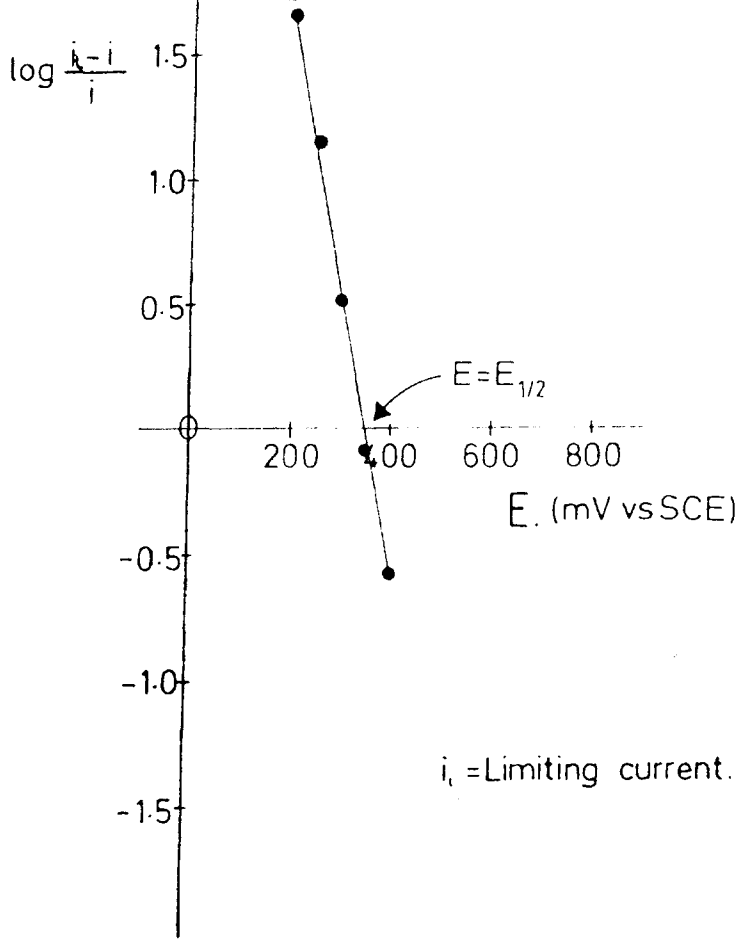

Logarithmic analysis of the oxidation wave (b) corresponding to the reaction of dimethyl amino ethyl ferrocene at the Ni/$Fe(CN)_6^{4-/3-}$ electrode.

The intercept on the x-axis gives the half wave potential, $E_{1/2}$, of the polarographic wave. The value obtained is 360mV vs SCE. This value is very close to the peak oxidation potential of the modified nickel electrode which is 380mV vs SCE.

(Note, the data presented above has been corrected for any charging contribution.)

two observations are suggestive of the fact that the oxidation of the solution ferrocene is mediated by the surface groups of the Ni/$Fe(CN)_6^{4-/3-}$ electrode. Under these conditions the electron transfer mechanism taking place at the modified electrode can be represented as;

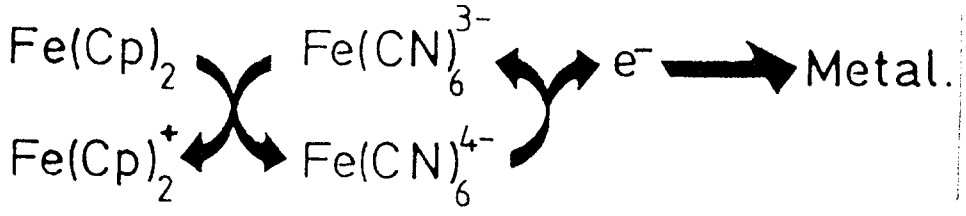

In order to further investigate the oxidation reaction I measured the steady state current at the modified electrode. Because of the above observations the potential was set at +380mV vs SCE, the value corresponding to the peak oxidation potential of the surface immobilized film of the modified nickel electrode.

Fig. 9.10 shows the variation in the current as a function of the amount of dimethyl amino ethyl ferrocene. The results show that the current is linearly proportional to the amount of the ferrocene only at low concentrations. At the higher concentrations the current becomes independent of the amount of dimethyl amino ethyl ferrocene and eventually reaches a plateau.

The hyperbolic nature of the curve can be explained by a model involving saturation of the surface, in fact, a model analagous to the Michaelis-Menten treatment of enzyme catalysed reactions. In the electro chemical model it is assumed that, prior to electron transfer, the solution species must bind to the surface redox couples of the modified electrode. It follows that it is only this complex which undergoes the electrochemical reaction, releasing the oxidized species into the solution and regenerating the vacant

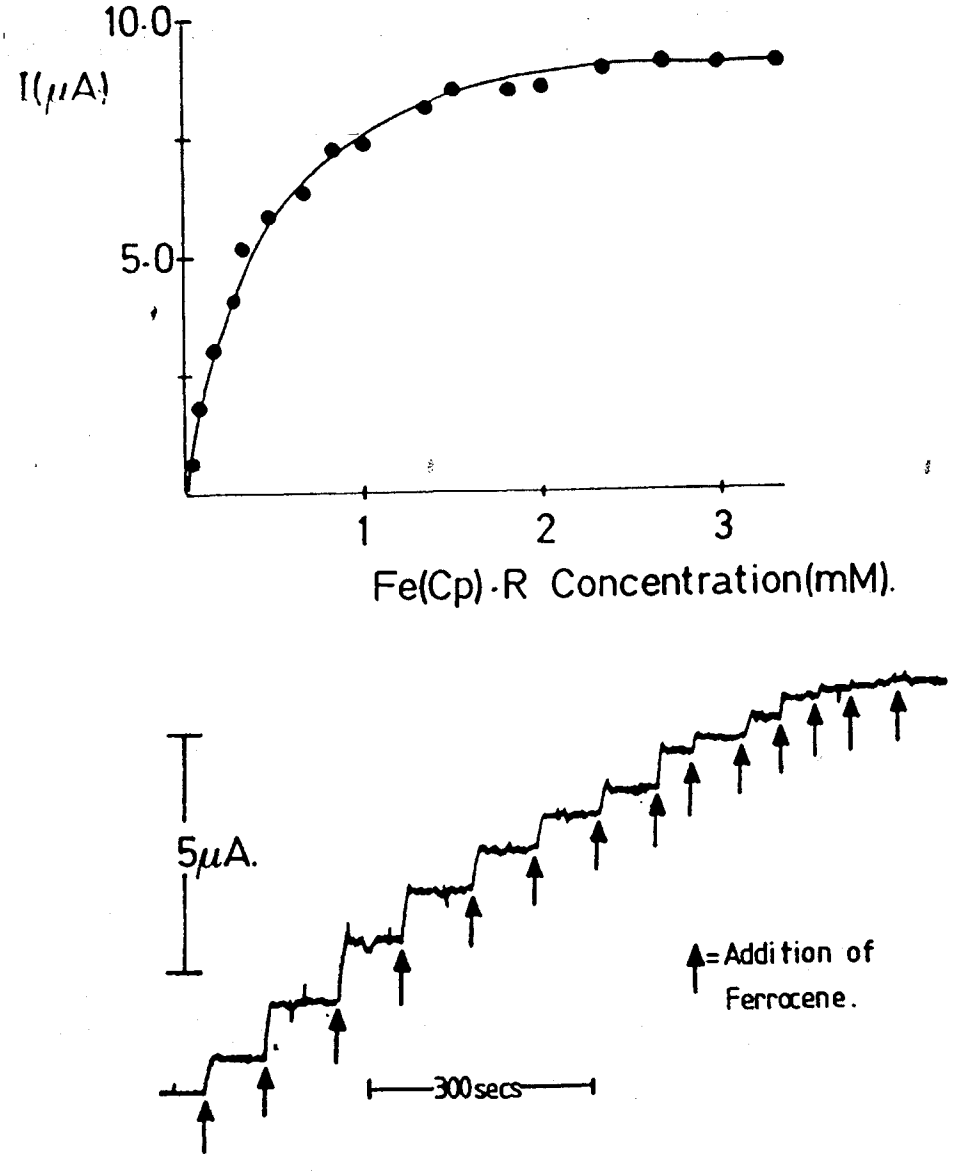

Fig 9.10. Variation in current as a function of the amount of dimethyl-amino-ethyl-ferrocene present in the electrochemical cell.

The electrolyte was 0.1M sodium phosphate pH 7.0. The modified nickel electrode was potentiostatted at +380mV vs SCE.

binding site. The oxidized binding site is then regenerated as the electron is passed to the underlying metal electrode. A schematic diagram showing this sequence of reactions is presented in fig. 9.11.

Proposed model for the oxidation of $Fe(Cp)_2 \cdot R$ at the $Ni/Fe(CN)_6^{4-/3-}$ modified electrode.

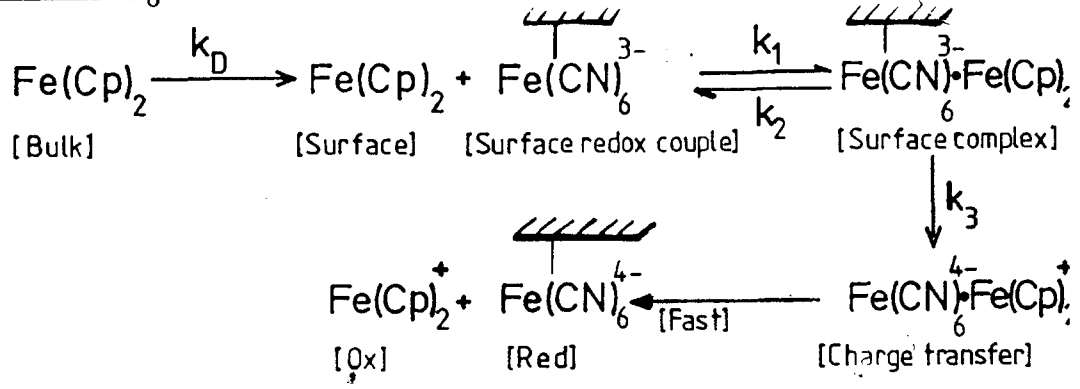

Under these conditions, the flux of current, j, is given by

$$j = k_3[Fe(CN)_6^{3-} \cdot Fe(Cp)_2] = k_3(1-\theta)N. \quad \text{(equn 1)}$$

where $N = \left[[Fe(CN)_6^{3-}]_{Surface} + [Fe(CN)_6^{3-} \cdot Fe(Cp)_2]\right]$

$$\Rightarrow [Fe(CN)_6^{3-}]_{Surface} = N\theta. \qquad (0 \leqslant \theta \leqslant 1)$$

$$\Rightarrow [Fe(CN)_6^{3-} \cdot Fe(Cp)_2] = (1-\theta)N.$$

$$\Rightarrow \frac{d[(1-\theta)N]}{dt} = k_1[Fe(Cp)_2]_{[Surface]}N\theta - (k_2 + k_3)(1-\theta)N$$

continued overleaf.

applying the steady state approximation,

$$\frac{d[(1-\theta)N]}{dt} = 0$$

Solving for θ,

$$\theta = \frac{k_2 + k_3}{k_1[Fe(Cp)_2]_o + k_2 + k_3}$$

$$\Rightarrow 1-\theta = \frac{k_1[Fe(Cp)_2]_o}{k_1[Fe(Cp)_2]_o + k_2 + k_3}$$

but $j = k_3(1-\theta)N$

i.e. $$j = \frac{k_1 k_3 N[Fe(Cp)_2]_o}{k_1[Fe(Cp)_2]_o + k_2 + k_3} \quad \text{(equn 2)}$$

deviding equation 2 by k_1

$$= \frac{k_3 N[Fe(Cp)_2]_o}{[Fe(Cp)_2]_o + \left(\frac{k_2 + k_3}{k_1}\right)} \quad \text{(equn 3)}$$

The analogies between this model and that proposed for enzyme catalysed reactions can be further highlighted as follws.

k_3 in equation three is analogous to k_{cat}.

N, the total number of binding sites is equivalent to [E] the total enzyme concentration.

$\frac{k_2 + k_3}{k_1}$ is analogous to the Michaelis constant K_m.

Fig 9.11.

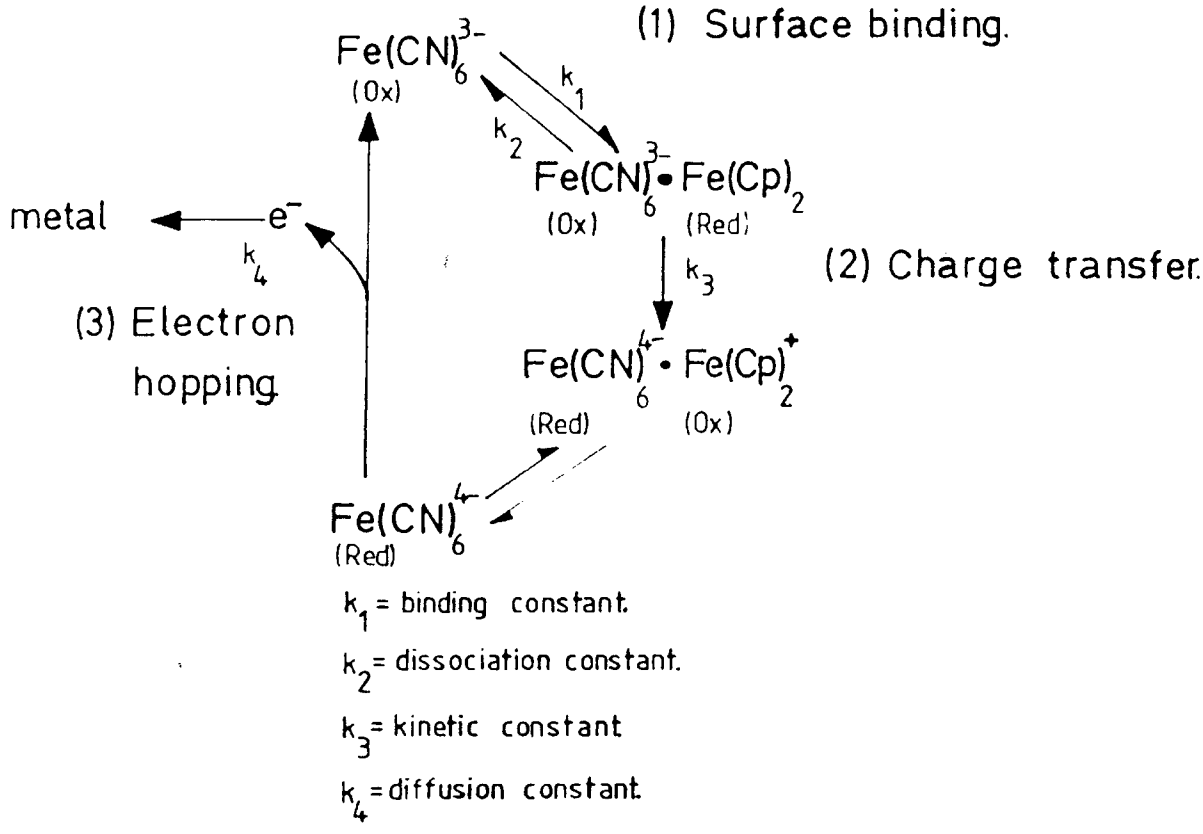

Proposed kinetic model for the oxidation of the ferrocene at the Ni/$Fe(CN)_6^{4-/3-}$ modified electrode.

e^- = an electron, $Fe(Cp)_2$ = the ferrocene, $Fe(CN)_6^{4-/3-}$ = the surface groups present on the modified electrode.

It is important to note, that the diffusion constant, k_4, presented in this model characterises the migration of charge through the surface coat of the modified electrode and should not be confused with the diffusion constant, k_d, which characterises the movement of the redox couple from the bulk solution to the surface of the electrode.

k_3, the kinetic constant, characterises the charge transfer reaction, i.e. the transfer of charge from the solution species to the surface immobilized redox couple.

Fig 9.11. cont'd.

The theoretical basis for the model presented above, as well as that of the kinetic description presented in the text, is analogous to the Briggs and Haldane treatment of enzyme catalyzed reactions (Briggs, G.E. and Haldane, J.B.S. (1925)). As such, the assumptions are similar, i.e. a steady state is assumed such that the concentrations of the number of binding sites and complexed binding sites remain effectively constant over the experimental time scale. As with enzyme catalyzed reactions, the steady state assumption requires that the rate of complex formation should equal its rate of breakdown in any direction.

The implication of equation 3 is that the current observed during the electrochemical experiment can be limited by

i) the rate of electron transfer.

ii) the total number of available "binding sites", N. This in turn can be dependent upon the thickness of the film, i.e. the concentration of surface bound electroactive material, and also the rate at which the electron is transferred from the reduced surface redox couple to the base nickel electrode k_4.

iii) the concentration of electroactive species at the surface of the electrode. $[A]_o$. This is not altogether a trivial statement since it follows that charged solution couples can be electrostatically repulsed from a surface which carries the same net charge. Note that the rate limiting step in the electrochemical oxidation at the Ni/$Fe(CN)_6^{4-/3-}$ modified electrode can either be kinetic, i.e. the rate of electron transfer from the solution couple to the surface bound redox material, or transport limiting, i.e. sluggish electron transport through the surface film. Further experiments, e.g. with rotating disc apparatus, must be carried out to establish which is the case.

Next I looked at the electrochemical oxidation of other ferrocene derivatives at the modified nickel electrode. Bearing in mind the importance of charge as explained above, I used trimethyl-amino-ethyl ferrocene, a positively charged species prepared as described in Materials and Methods, and ferrocene carboxylic acid, a negatively charged ferrocene. The results obtained in this investigation are presented in fig. 9.12. Clearly, for equivalent amounts of material, smaller currents were observed for the oxidation of ferrocene carboxylyic acid than for the other two compounds. This can

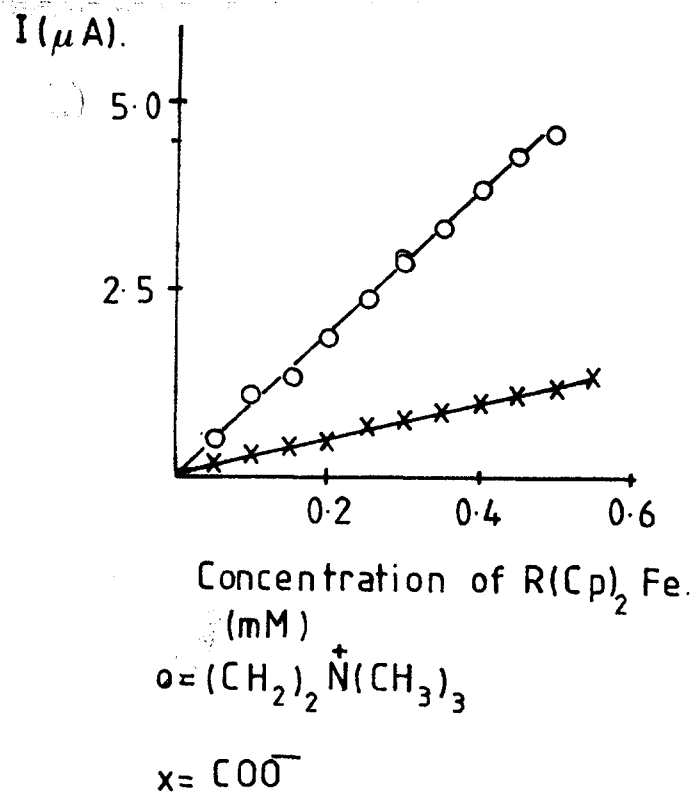

Fig 9.12. Steady state current response as a function of the concentration of different ferrocenes present in the electrochemical cell.

Note the low currents observed for the oxidation of ferrocene carboxylic acid at the Ni/$Fe(CN)_6^{4-/3-}$ modified electrode.

be explained in the light of the model presented above, and by reference to the composition of the surface bound film. It is reasonable to assume that such a surface would present a negative charge to solution species. Consequently, there would be an electrostatic repulsion between it and the ferrocene carboxylic acid which would result in a decrease in the effective concentration of the species at the surface of the electrode, a smaller $[A]_o$ term in equation 3. Furthermore, the effects of the electrostatic repulsion may result in a less favourable interaction between the solution couple and the binding sites on the electrode, i.e. $k_2 >> k_3$. Both instances would result in smaller currents.

It is possible to rule out any kinetic effects by considering the peak oxidation potentials of each of these compounds on gold.

$Fe(Cp)_2 \cdot (CH_2)_2 \cdot \overset{+}{N}(CH_3)_3$	$E_{1/2} = 420mV$ vs SCE
$Fe(Cp)_2 \cdot (CH_2)_2 \cdot N(CH_3)_2$	$E_{1/2} = 350mV$ vs SCE
$Fe(Cp)_2 \cdot COOH$	$E_{1/2} = 275mV$ vs SCE

By inspection it can be seen that ferrocene carboxylic acid is the more powerful reducing agent. It follows that from a purely energetic standpoint the kinetics for the oxidation of ferrocene carboxylic acid at the modified electrode would be more favourable. The least favourable should be for the oxidation of trimethyl-amino-ethyl ferrocene.

Using similar lines of thought it is possible to rule out any steric effects as being the cause of the reduced currents. Simply by inspection it follows that i) has the least bulky side grouping and therefore, from a purely steric standpoint, should give rise to the most favourable surface

binding.

Mediated electron transfer from glucose oxidase to the modified electrode

The stage was now set to see if mediated electron flow in the presence of the ferricinium ion could be observed from reduced glucose oxidase to the Ni/$Fe(CN)_6^{4-/3-}$ modified electrode. From the results presented above it was evident that ferrocene carboxylic acid was not a suitable choice as mediator in this reaction.

Fig. 9.13(a) shows the D.C. cyclic voltammogram of the modified nickel electrode with only dimethyl-amino-ethyl ferrocene and glucose present in the electrochemical cell. Upon addition of glucose oxidase, a striking change occurs in the D.C. voltammogram, fig. 9.13(b). No anodic or cathodic peaks are observed, and a large catalytic current flows at oxidizing potentials. This behaviour is particularly apparent at the slower scan speeds and is indicative of the regeneration of the ferrocene from the corresponding ferricinium ion by glucose oxidase in the reduced form. (Cass, A.G. et al (1984)). The sequence of redox reactions occurring in the electrochemical cell can be represented as;

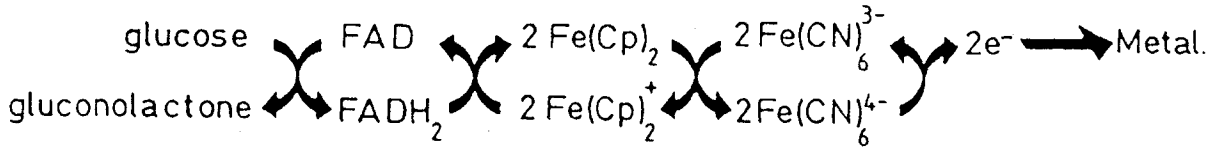

The effects on the steady state current of varying the concentrations of glucose oxidase present in the cell are summarized in fig. 9.14. The loss of linearity at the high enzyme concentrations (> 150 µg/ml) is indicative that the reaction has become rate limiting. If further aliquots of both ferrocene and glucose are added to the cell after the plateau region has been reached there is no observable increase

Fig 9.13.

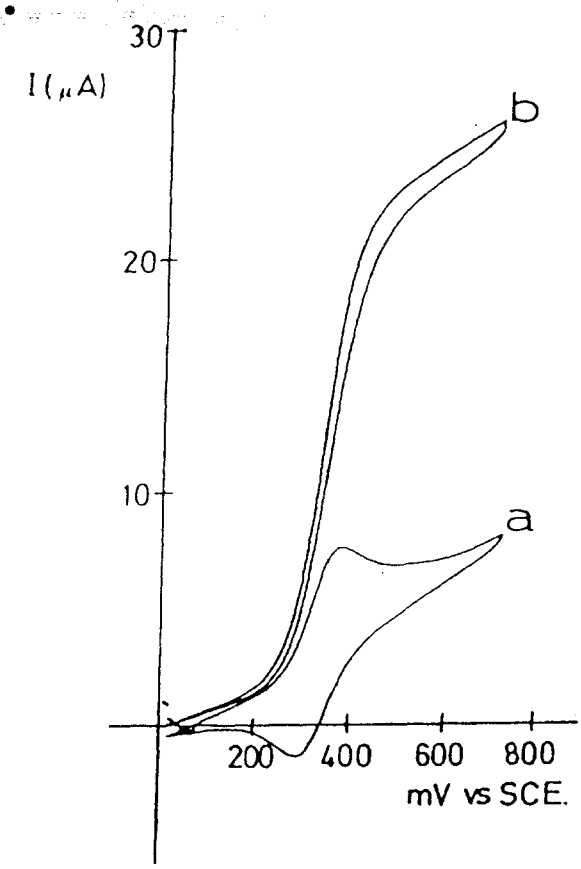

(a) D.C. cyclic voltammogram of the modified nickel electrode in the presence of dimethyl amino ethyl ferrocene (0.5mM) and D-glucose (100mM). The scan rate was $5mVs^{-1}$.

(b) As for (a), but with the addition of glucose oxidase (10μM).

The supporting electrolyte was NaH_2PO_4 (0.1M) pH 7. The experiment was performed in a quiescent solution.

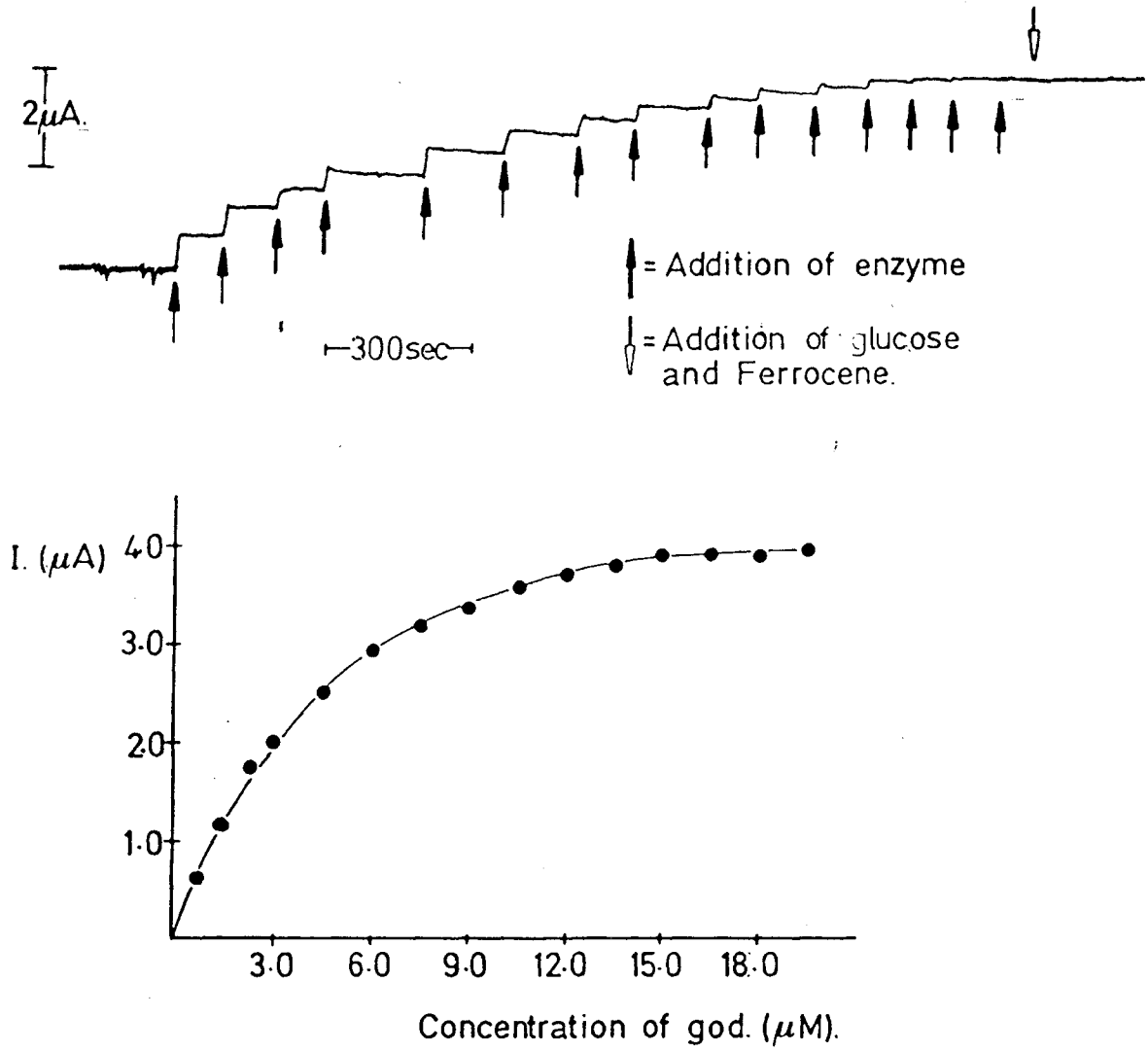

Fig 9.14. Variation in the steady state current as a function of increasing amounts of glucose oxidase present in the electrochemical cell.

The electrolyte was 0.1M sodium phosphate pH 7.0. The modified nickel electrode was potentiostatted at +380mV vs SCE.

Note the hyperbolic nature of the current response curve. Note also, that additions of further aliquots of glucose and ferrocene, arrowed, does not cause any increase in i_{ss} suggesting that both species are not present in rate limiting amounts.

in the observed current. This indicates that the ferrocene and glucose are both present in non rate limiting excess and suggests that the slow step in the overall reaction is attributable to the modified electrode. This observation can again be explained using the saturation model by suggesting that at high enzyme concentrations the role of the enzyme catalysed reaction is faster than the electrochemical reaction performed by modified electrode and consequently becomes rate limiting. Note that this implies that no matter how much enzyme is present in the cell, the overall kinetics of the reaction are controlled by the kinetics of the modified electrode. The analytical implications of this are that, assuming a high enzyme loading, the reaction can be made independent of factors such as loss of enzymic activity from the cell.

Results similar to those presented in fig. 9.13 showed that trimethyl-amino-ethyl ferrocene could also act as a good mediator of reduced glucose oxidase.

Stability of the surface film under conditions of anodic potentiostatting

Having established mediated electron flow from reduced glucose oxidase to the Ni/$Fe(CN)_6^{4-/3-}$ modified electrode, it was now important to investigate the stability of the surface film under conditions of continuous potentiostatting. Although the stability of the modified electrode had already been determined by cyclic voltammetry, it is important to make this distinction since in this instance instability due to potential-dependent-phenomena would be manifest as,

i) Corrosion of the base material. This would be important if there are gaps in the surface film, although it

would not represent too serious a problem with nickel since any corrosion would lead to the formation of a protective oxide.

ii) Reaction of the "immobilisation" bonds, leading to loss of material.

iii) Reaction of the non-resting surface material (i.e. the oxidized form of the surface couple) with species other than the one of interest.

iv) Because the potential is cycled, it is possible that material that is solubilized in, say, the forward sweep can be redeposited in the return sweep and therefore give an incorrect indication of the stability of the surface bound film.

Such phenomena as these would be difficult to observe simply by cyclic voltammetry techniques because of the rapid potential fluctuations involved. This illustrates the inadequacy of characterizing electrode stability simply by stating the number of useable cycles. Murray highlights this point with reference to the decay in the cyclic wave of a ferrocene modified platinum electrode. In this case, the decrease in the peak currents was attributed to the instability of the ferricinium species itself, which was generated by maintaining an anodic potential. (MURRAY, R.W. 1980)

Fig. 9.15 shows two cyclic voltammetric waves obtained from the Ni/$Fe(CN)_6^{4-/3-}$ electrode before and after continuous potentiostatting at +380mV vs SCE for 3 hours in the presence of 50mM dimethyl-amino-ethyl ferrocene. By calculating the area under the anodic (or cathodic) peaks in both a and b, it can be shown that, following the experiment, there is a loss of less than 10% of the surface bound electroactive material from the modified electrode. Although even this slight loss is annoying, in so far as it would lead to irreproducible

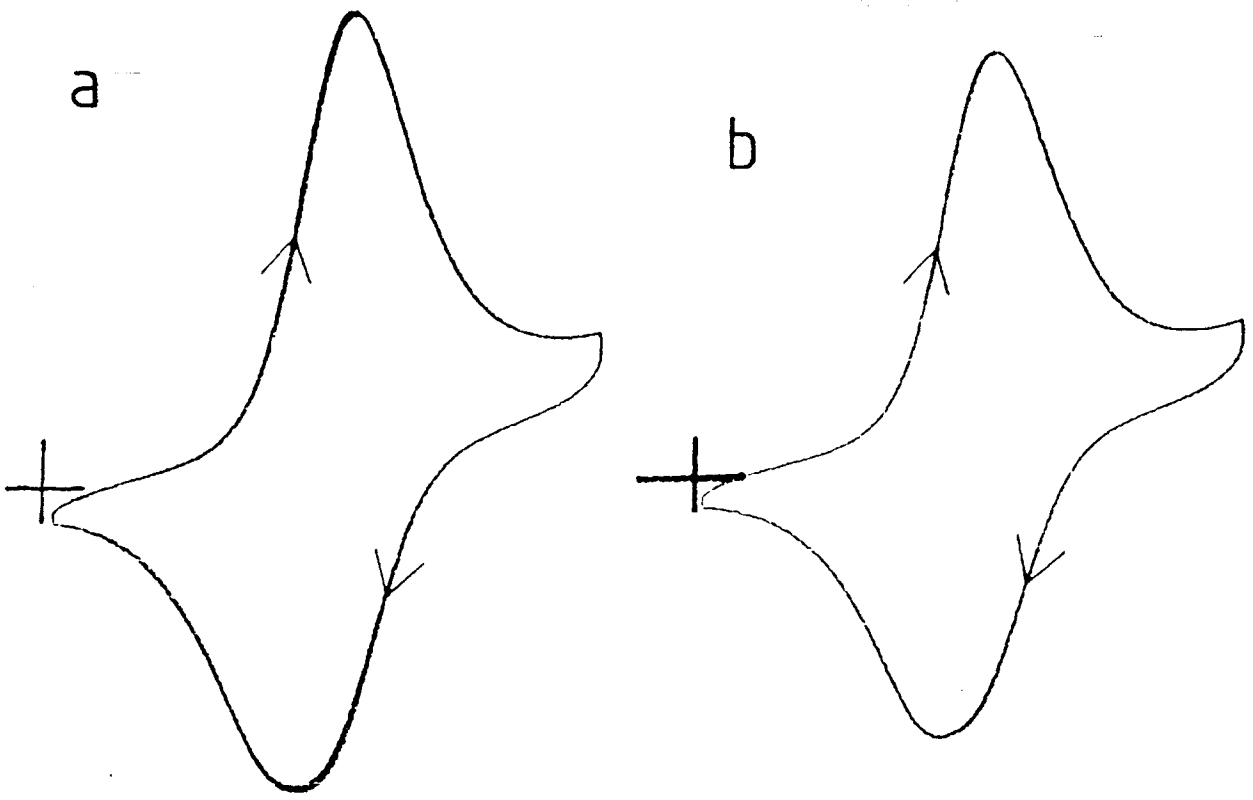

Fig 9.15.

(a) D.C. cyclic voltammogram of a freshly prepared modified nickel electrode.

(b) D.C. cyclic voltammogram of the same electrode after having been used continuously for the oxidation of solution ferrocene. The electrode was potentiostated anodically at 380mV vs SCE.

In both (a) and (b) the electrolyte was NaH_2PO_4 (0.1M) pH 7. The potential was swept at $100mVs^{-1}$. Each cyclic voltammogram represents 20 scans.

The decrease in the peak current recorded in (b) corresponds to a loss of less than 10% of the surface material.

results, it must be pointed out that it does represent three hours continuous usage in a stirred solution. It must therefore be recommended that, for practical uses, the electrode should be held at the anodic potential only for as long as it takes to make the steady state reading and then be returned to the resting state. This simple precaution should, at least in theory, increase the life time and hence usefulness of the surface film.

The reasons for the loss of material are unclear at this stage and require further investigation.

$\underline{Fe(CN)_6^{4-/3-}}$ modified porous nickel electrodes

Returning to the original aim of this investigation, it was now pertinent to see if similar results could be obtained using a porous nickel electrode. These electrodes were constructed as outlined in Materials and Methods.

Because of the high surface areas involved, it was found that good surface coverages could be achieved simply by dipping the electrode in a strong solution of potassium ferricyanide. As with the bulk nickel electrodes, however, it was found that more reproducible surfaces could be obtained electrochemically. Thus, anodic potentiostatting in 100mM potassium ferrocyanide solution was routinely used as the derivitizing reaction.

It was noted that for ideal operation care had to be taken to completely flood the pores of the electrode, thus ensuring that no air pockets remained. This was simply achieved by dripping electrolyte onto the surface of the electrode and allowing the solution to soak into the internal matrix of the electrode. Once "wetted", the electrode was ready for use.

Fig. 9.16 shows a typical D.C. cyclic voltammogram obtained from a $Fe(CN)_6^{4-/3-}$ derivitized porous nickel electrode. The striking feature of this voltammogram is the large currents that are passed during the cyclic potential sweeps. This is simply due to the large surface areas involved, which in turn implies the presence of large amounts of immobilized surface material. Analysis of the waves reveals non ideal behaviour. This is demonstrated by the increase in the peak to peak separation as the scan rate increases and the fact that the $\Delta E_{\frac{1}{2}}$ value is greater than 90mV. The occurrence of complex waves is evident, particularly at the slower sweep rates. The implication of this type of observation has already been discussed. The relationship of the peak current to the scan rate is shown in fig. 9.17.

The derivitized porous nickel electrode shows remarkable stability, as judged by repetitively sweeping the potential from 0 to 800mV vs SCE. The electrode was also found to be stable under conditions of overnight storage.

The oxidation of dimethyl-amino-ethyl ferrocene at the porous electrode is shown in fig. 9.18. As can be seen, the steady state current is not linear over the entire concentration range. As was the case with the modified bulk electrode, the reaction becomes limiting at high substrate concentration. The fact that the porous electrodes gives a linear response over a larger concentration range than the corresponding bulk electrode is simply due to the larger surface area, and hence greater amount of surface material, available to the solution. An important point to note from the results presented in fig. 9.18 is the speed at which the steady state response is obtained. Furthermore, in the time scale involved the steady state

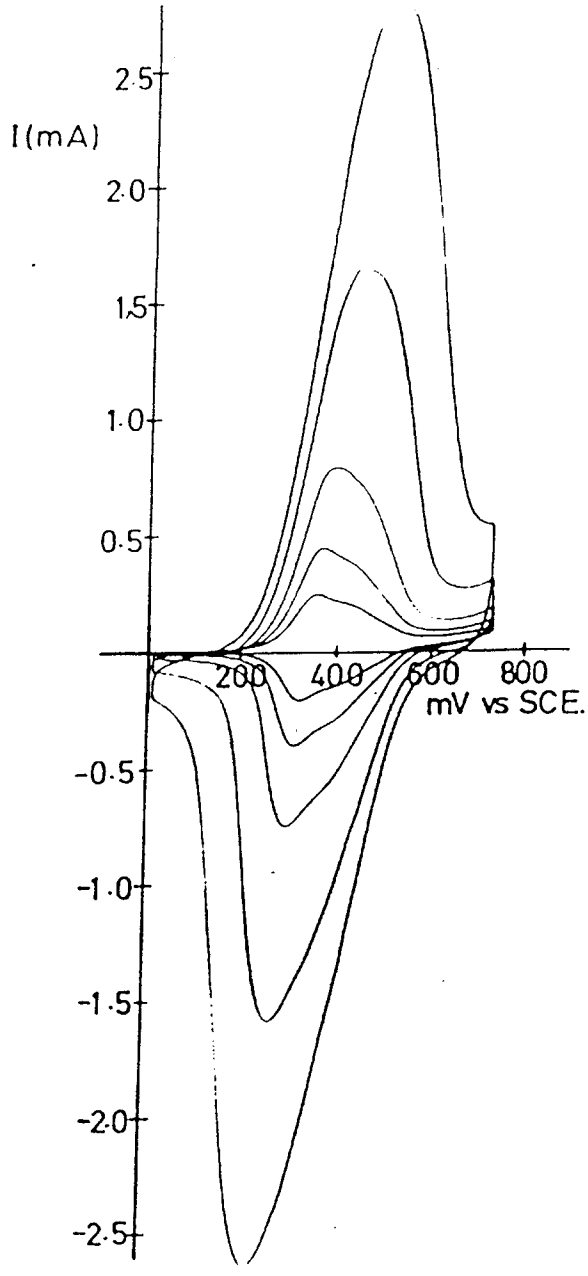

Fig 9.16.

D.C. cyclic voltammogram of the porous Ni/$Fe(CN)_6^{4-/3-}$ electrode in NaH_2PO_4 (0.1M) pH 7 showing the scan rate dependence on the peak current and the peak to peak separation.

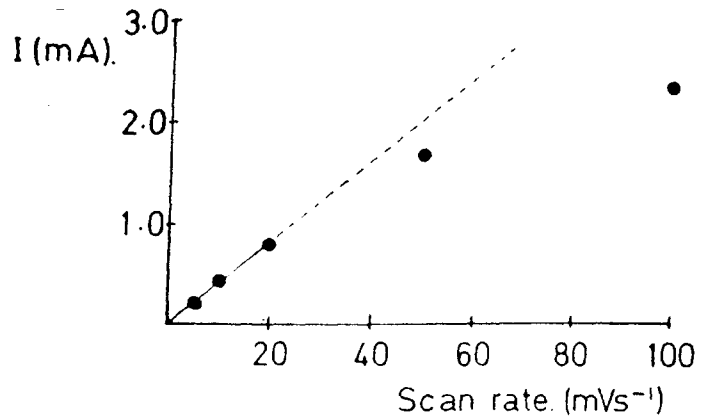

Fig 9.17.
Plot of i_{peak} vs scan rate for the Ni/$Fe(CN)_6^{4-/3-}$ modified porous electrode.

Loss of linearity at scan rates greater than $20mVs^{-1}$ is indicative of diffusion controlled charge transfer in the surface polymer film.

(Note, the data presented above has been corrected for any charging contributions.)

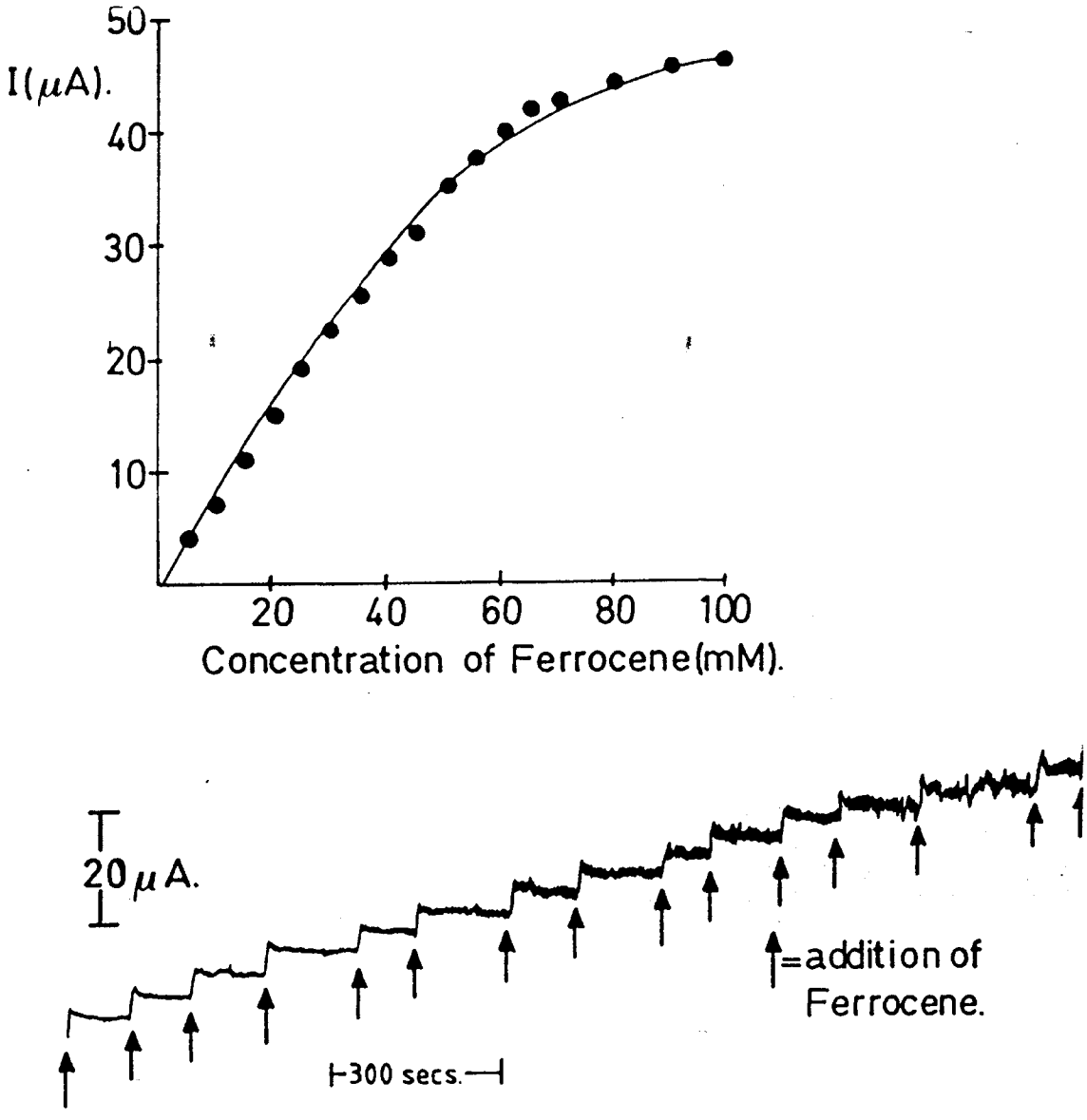

Fig 9.18. Variation in the steady state current as a function of the amount of dimethyl-amino-ethyl ferrocene present in the electrochemical cell.

The electrolyte was 0.1M sodium phosphate pH 7.0.
The recording potential was +380mV vs SCE.

Note that even with the modified porous electrode, the curve loses linearity at the high ferrocene concentrations. The large currents observed and the increased linearity are attributable to the large surface area of the porous electrode.

current response is very stable. The implication of this is that under these conditions the solution redox couple can freely enter the internal matrix of the porous electrode. In other words there appears to be no limitation to the partioning of the solution species.

Fig. 9.19(a) shows a D.C. cyclic voltammogram of the derivitized porous electrode in the presence of dimethyl amino-ethyl–ferrocene and glucose. Figs. 9.19(b) and (c) show the change in the voltammogram that results when glucose oxidase is added to the electrochemical cell. Clearly there is a definite catalytic enhancement of the current when the enzyme is present. By inspection, however, it can be seen that both the anodic, and, to a lesser extent, the cathodic peaks, are still present. Compare this result to the one presented in fig. 9.13(b). The odd shape of the catalytic wave has been rationalized by suggesting that the porous electrode is oxidizing the ferrocene faster than the turn-over rate of the enzyme. As a result, the effective concentration of oxidizable material at the electrode surface becomes depleted, and hence a peak is observed. The sequence of redox reactions occurring in the electrochemical reaction are identical to those presented earlier.

Finally, it was pertinent to compare the responses of both the modified porous and bulk nickel electrodes to various concentrations of glucose, but at the same time keeping the amounts of mediator and enzyme present in the electrochemical cell the same. The results of this investigation are shown in fig. 9.20.

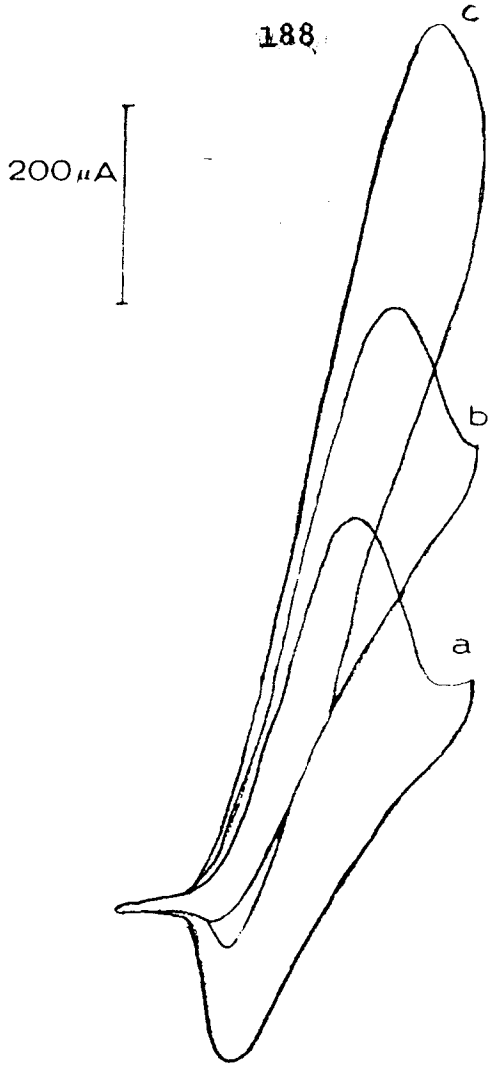

Fig 9.19.

(a) D.C. cyclic voltammogram of the modified porous nickel electrode in the presence of dimethyl amino ethyl ferrocene (0.5mM) and D-glucose (100mM). The scan rate was $5mVs^{-1}$.

(b) As for (a), but with the addition of glucose oxidase (10μM).

(c) As for (a), but with the addition of glucose oxidase (25μM).

Fig 9.13.

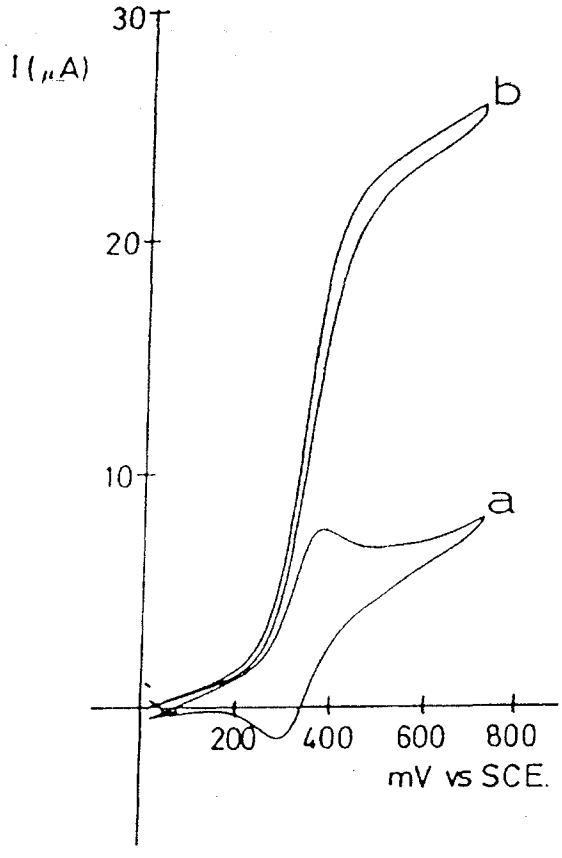

(a) D.C. cyclic voltammogram of the modified nickel electrode in the presence of dimethyl amino ethyl ferrocene (0.5mM) and D-glucose (100mM). The scan rate was $5mVs^{-1}$.
(b) As for (a), but with the addition of glucose oxidase (10μM).

The supporting electrolyte was NaH_2PO_4 (0.1M) pH 7. The experiment was performed in a quiescent solution. (This diagram should be compared with Fig 9.19.)

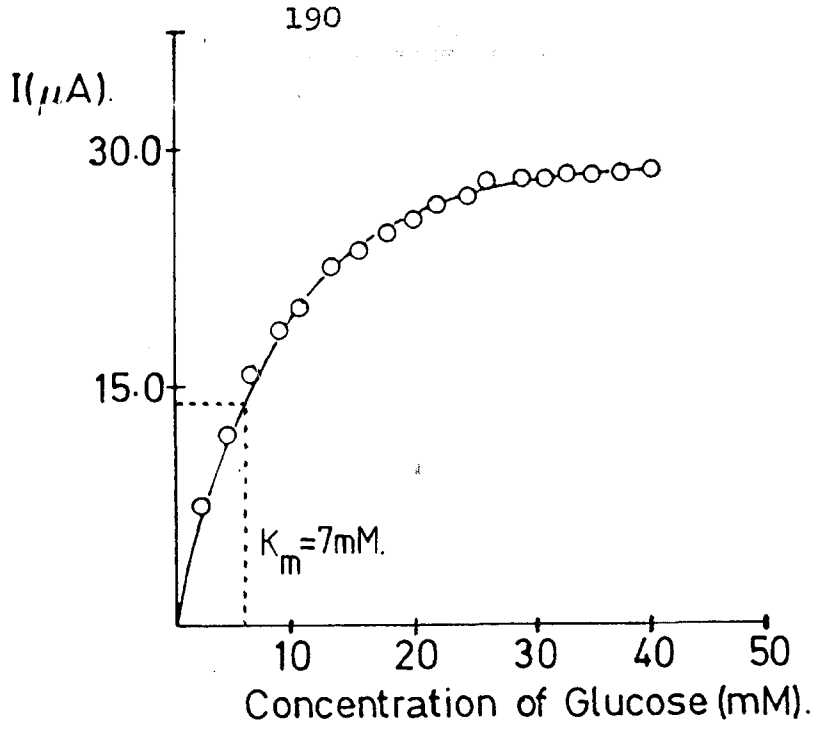

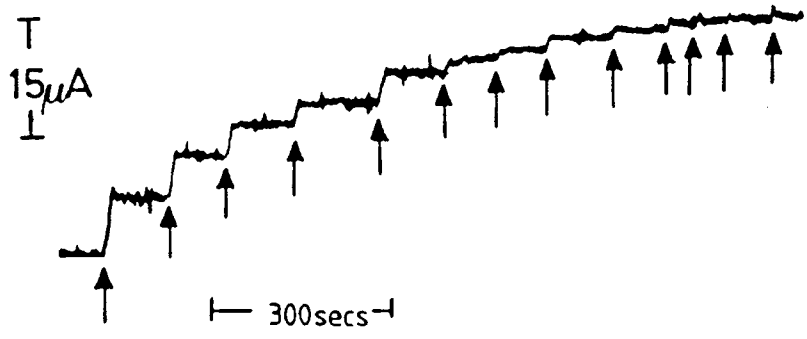

Fig 9.20. Variation in the steady state current as a function of increasing glucose concentration observed with the modified porous nickel electrode.

The electrolyte was 0.1M sodium phosphate pH 7.0.
The concentration of glucose oxidase in the electrochemical cell was 10μM.
The concentration of mediator present in the cell was 1mM.
The recording potential was +380mV vs SCE.

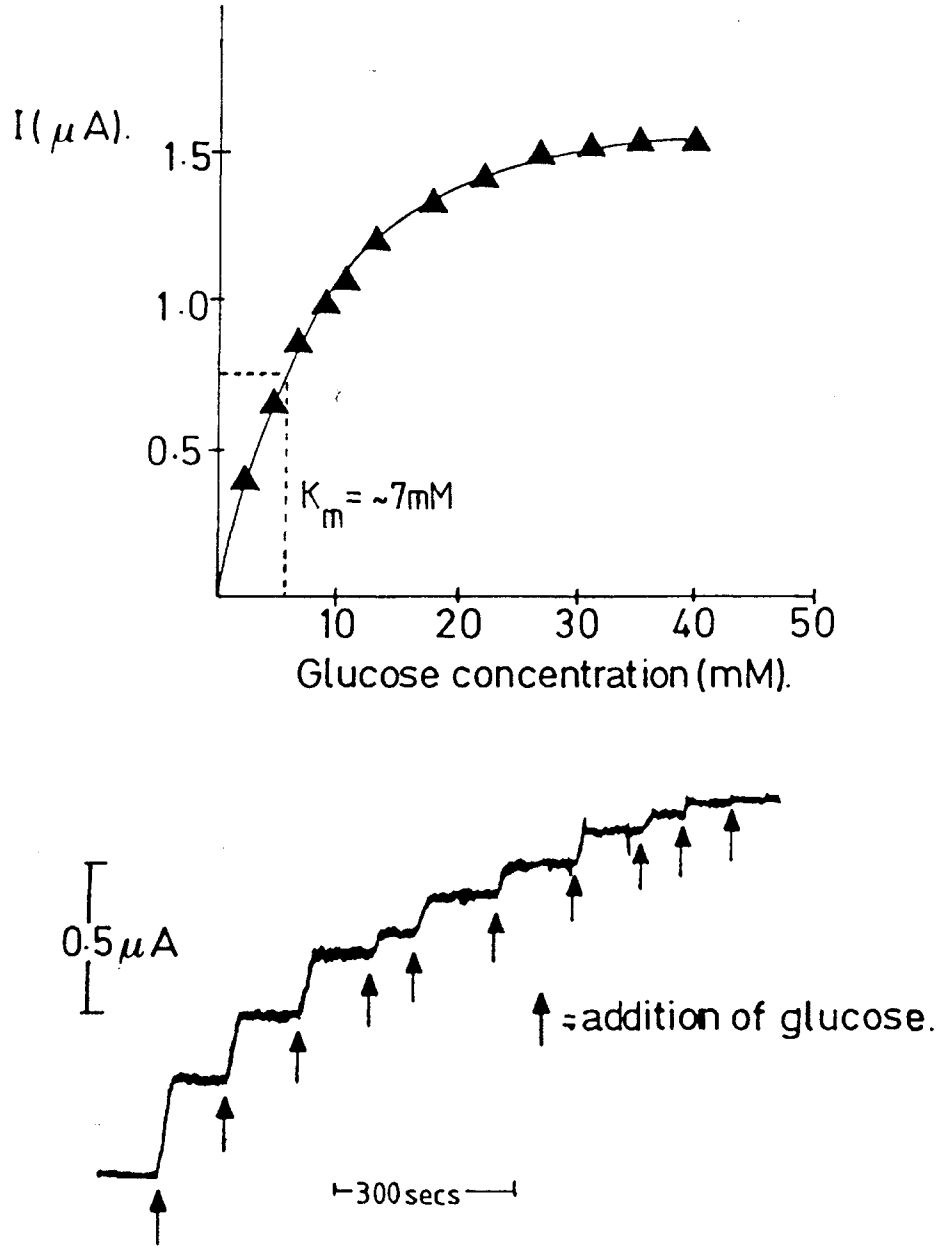

Fig 9.20. Variation in the steady state current as a function of increasing concentrations of glucose present in the electrochemical cell.

The electrolyte was 0.1M sodium phosphate pH 7.0.
The concentration of glucose oxidase in the cell was 10μM.
The concentration of mediator present in the cell was 1mM.

There are two important points to note from this data. The first of these is the large currents that are observed under identical conditions with the modified porous electrode. These large currents can be explained in terms of the large surface areas available with the modified porous electrode. This fact can be better appreciated by considering the following equation;

$$i_{ss} = \frac{nFAXVC}{2K_m}$$

(Adapted from Mell and Malloy 1976)

where i_{ss}=steady-state current, A=effective electrode area, V=enzyme concentration, C=bulk substrate concentration, K_m=Michaelis constant and X=average membrane thickness.(In the above example, this term is not applicable).

From the above equation, it can be appreciated that a large surface area would indeed give enhanced steady state currents.

The second point to note, is that in both cases the K_m' of the electrochemical reactions, i.e. the substrate concentration which gives 1/2 i_{max}, is identical to that obtained under normal assay conditions, i.e. with an oxygen electrode. The implication of this, is that under these conditions, it is the enzyme catalysed reaction which is rate limiting and not the electrochemical process. This idea is in agreement with the proposal of Wilson and Shu (Shu,F.R. and Wilson,G.S. 1976) who suggested that the K_m' can be calculated by amperometric means, if the reaction is catalytically controlled, by the equation;

$$\frac{1}{i_{ss}} = \frac{K_m'}{i_{max}} \frac{1}{C} + \frac{1}{i_{max}}$$

CHAPTER 10

CONCLUSIONS AND DISCUSSION ON SECTION II

The aim of the experiments described above was to see if porous nickel could be used as the base sensor around which an enzyme electrode could be designed. In this respect it was shown that by suitable chemical modification with ferricyanide nickel, a hitherto anodically unstable metal, could be turned into a useful electrode in terms of both its stability and electrochemical reactivity. The presence of a surface bound electroactive material was proved unequivocally by the fact that cyclic voltammetric waves were observed when the electrode was placed into a base electrolyte solution containing no added redox couple. Subsequently, techniques were developed by which porous nickel could be fashioned into an electrode and then be derivitized.

It was found that the kinetic properties of the surface film were influenced by the nature of the supporting solution counterions. Analysis of the cyclic voltammograms obtained from the modified nickel electrode showed that the kinetic behaviour of the surface film was inconsistent with the idea of non diffusive reversible charge transfer. In fact, transport limiting processes were indicated and furthermore, it was found that the surface electroactive layer deposited on both the bulk and porous nickel electrodes was made up of redox species with slightly differing $E_{\frac{1}{2}}$ values. This was explained in terms of the film having been laid down in a non homogeneous manner. This could mean that the surface material is deposited as a series of overlapping layers or may even contain localized areas in which the derivitizing agent has

aggregated. Clearly, SEM analysis of the surface is needed to glean a better understanding of the surface morphology of the electroactive film. Such experiments, however, would only be really applicable to the bulk electrode.

From steady state measurements it was shown that the oxidation of certain solution ferrocenes could be mediated by the redox groups present in the surface layer. However, further studies by rotating disc techniques are required to elucidate the exact mechanism of this reaction.

With the modified electrode mediated electron transfer from reduced glucose oxidase to the porous electrode was observed. The implication of this is that the porous electrode could be used as the base sensor in a mediated glucose sensor. The simplest design would involve trapping the enzyme in the pores of the electrode behind a thin cation exchange membrane and employing a bulk equilibrium assay. The amount of glucose present in an unknown sample could then be calculated from a standard curve. Although this system would work, it does present a number of technical problems, the least of which is the need to add mediator to the sample solution every time a measurement is to be made. To overcome this problem the compound shown below was synthesized as outlined in Materials and Methods for Section II.

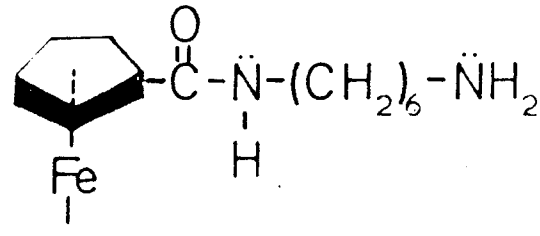

The rationale behind this synthesis is as follows. First, the ferrocene derivative is attached to the surface of the glucose oxidase via the terminal amino group of the hexamethyl arm. This could be done by using carbodiimide or glutaraldehyde chemistry. In either case a stable covalent linkage

would result.

Once anchored onto the surface of the enzyme, it is proposed that because of the flexible arm, the ferrocene moiety will be able to flip between the FAD binding cavity of the glucose oxidase and the surface of the modified electrode. In this fashion the ferrocene will be able to reoxidize the reduced coenzyme and then transfer the charge to the electrode. A diagrammatic representation of this proposal is shown in fig. 10.1.

The analytical advantages of using porous nickel would be;

i) Large enzyme-ferrocene complex loadings.

ii) Large steady state currents, which in turn mean increased sensitivity.

iii) Cheapness of manufacture.

In terms of other possible biosensor uses, it was found that the surface redox groups of the modified electrode did not mediate the oxidation of NADH. Fortunately, this does not mean that the electrode can not be used to monitor the reactions catalysed by NAD^+ linked dehydrogenases. The way around this problem would be to link the oxidation of NADH to the reduction of diaphorase, a flavin containing mitochondrial preparation which uses molecular oxygen to carry out the reaction. It has been shown (Cass, A.G., pers. commun.) that the ferricinium ion can act as an alternative electron sink for reduced diaphorase. It follows from this that by regenerating the ferricinium ion at the modified electrode the reaction catalysed by a particular dehydrogenase can be monitored. Furthermore, it would be possible to trap both diaphorase and the dehydrogenase in the porous nature of the electrode.

It is evident that this work has opened many avenues of possible investigation, both in terms of using the advantageous properties of high surface area electrodes in biosensor designs and looking at the catalytic properties of the $Fe(CN)_6^{4-/3-}$ modified surface.

In the former case it seems logical to continue the work started using the ferrocene derivative. If the enzyme-ferrocene complex is active both in terms of the electrochemistry and the enzymology, then immobilization strategies could then be pursued. Furthermore, this work could be extended to the diaphorase system. In the latter example it is now important to characterize the oxidation reaction of the solution ferrocene at the modified electrode further. If it is found that the reaction is limited by the transfer of charge through the layer, then experiments should be designed to investigate how varying the thickness of the film affects the reaction. By the same token, it would also be important to study the mechanism by which the film grows on the surface of the electrode. For example, does film grow smoothly on the surface of the nickel, or is it deposited in a "patchy" fashion? Do scratches, etc. act as nucleation sites resulting in aggregates? Such studies would be important in developing techniques by which smooth even films of known thickness could be deposited in a reproducible manner onto the surface of the electrode.

APPENDIX I

NICKEL

Nickel was first isolated in 1751 by Axel Cronstedt. Elemental nickel is a strong ductile thermally conductive silvery-white metal. It is ferromagnetic under normal conditions. It is soluble in dilute acids, giving the green aquo $[Ni(H_2O)_6]^{++}$ cation. The metal is soluble in ammonia, its solubility being attributed to the formation of the complex ion $[Ni(NH_3)_6]^{++}$. It is passivated by oxidising agents such as concentrated nitric acid, but is not attacked at ordinary temperatures by moist air. It is resistant to the action of strong alkalis and their fused salts. It is however tarnished in contaminated urban atmospheres due to the formation of NiS. The corrosion resistant properties of nickel have been attributed to the presence of a non porous surface oxide coat.

Nickel makes up about 0.1% of the earth's crust, occurring mainly as the ore pentlanide, $(Ni_9Fe)_9S_8$. It is mined, for the most part, in Canada, South Africa, U.S.S.R. and Finland. It is won by first roasting the ore with silica to give a sulphide melt, or matte, and then converted to the oxide. The oxide is reduced with water gas at 300°C to give crude nickel. Refining is accomplished either by electro-deposition or by treatment with carbon monoxide at 50°C, giving the volatile carbonyl, $Ni(CO)_4$. This is distilled and pyrolysed at 150-180°C, yielding nickel of very high purity.

The main industrial uses of nickel are in plating and alloying. It is used as both a protective and decorative coat, under a much thinner chromium electroplate, on base

metals such as brass and also on diecast zinc or aluminium alloy components. Together with chromium, nickel is used as an additive to iron in the manufacture of stainless steel. Other nickel alloys include cupronickel, which is used in coinage, nichrome, which is used in the manufacture of electric heating elements, and the nimonic, or super alloys, which are used in the manufacture of engine turbine blades.

Nickel, especially finely divided nickel, has the ability to absorb large quantities of hydrogen onto its surface, and therefore special preparations, such as Raney Nickel, have found applications as industrial catalysts in the hydrogenation of fatty acids to give margarine, and the cracking of methane, in the presence of steam, to give methanol.

APPENDIX II

CYCLIC VOLTAMMETRY

In cyclic voltammetry the potential of a stationary working electrode is changed in the sawtooth manner shown below in Figure 1, starting from a potential where no electrode reaction occurs, and moving to potentials where oxidation or reduction of the material being studied, whether in solution or immobilized on the electrode surface, takes place. After traversing the potential region in which one or more electrode reactions take place (the forward sweep), the direction of the linear sweep is reversed and the reactions of the intermediates and products, formed during the forward scan, are often detected.

The time scale of the experiment, controlled by the potential scan rate and the total potential excursion, can be varied. A supporting electrolyte is present to repress migration of charged reactants and products, and ensure good conductivity.

Fig 1.

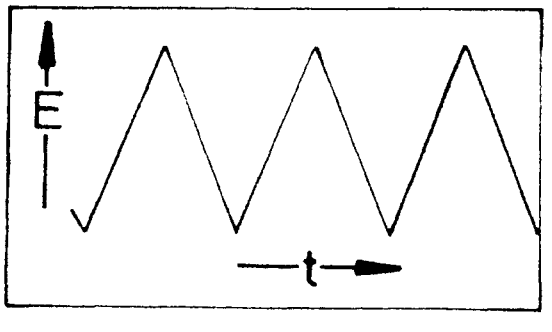

Basic experiment. (The reaction of solution species at an electrode

Cyclic voltammetry is a simple and direct method for measuring the half wave potential of a redox couple when both oxidized and reduced forms are stable during the time required to obtain the voltammogram (current-potential curve).

Consider the cyclic voltammogram (CV) of O_2, Figure 2(A). The forward scan commences at the initial potential of -0.75V

and very little current is obtained until about -1.15V, where oxygen begins to be reduced to the product, the oxygen radical anion or superoxide, as shown below.

$$O_2 + e^- \underset{k_b}{\overset{k_f}{\rightleftharpoons}} O_2^- \quad \text{(equation 1)}$$

The current increases as the rate of reduction increases at more negative potentials, but eventually a maximum is reached, -1.25V, and thereafter decreases steadily. The cathodic peak in the CV, i_{pc}, results from the competition of two factors, the increase in the rate of reduction as the potential is made more negative, and the development of a thickening depletion layer across which reactant must diffuse. At these potentials the reactant concentration distant from the electrode and the current is controlled by the rate of diffusion of reactant through the depletion layer (diffusion controlled current).

The scan direction is reversed at -1.50V (switching potential) and the diffusion-controlled reduction current continues until about -1.25V where net oxidation of O_2^- back to O_2 occurs. The layer from which O_2 has been depleted is an accumulation layer for O_2^- and some of this can diffuse back to the electrode and then be oxidized. An anodic peak in the CV, i_{pa}, is obtained for reasons analagous to those underlying the cathodic peak.

The CV is characterized by several important parameters (see Fig. 2(A)).

i) The cathodic and anodic peak potentials (E_{pc} and E_{pa}).

ii) The cathodic and anodic peak currents (i_{pc} and i_{pa}).

iii) The cathodic half peak potential. ($E_{p/2}$).

iv) The half wave potential. ($E_{\frac{1}{2}}$). The definition of $E_{\frac{1}{2}}$

has been borrowed from classical polarography experiments, according to the equation shown below.

$$E_{\frac{1}{2}} = E^{O} + (RT/nF)\ln(D_r/D_o)^{\frac{1}{2}}. \quad \text{[This implies reversibility]}$$

E^{O} is the formal potential pertaining to the ionic strength of the solution used, D_o and D_r are the diffusion coefficients of the oxidized and reduced forms and n the number of electrons in the half reaction. Because $D_O \quad D_R$, $E_{\frac{1}{2}}$ is usually within a few mV of E^{O} (Svanholm, U. and Parker, V.D. (1975)).

The reduction of oxygen is an example of a reversible reaction. In a reversible process the ratio of surface concentrations of O and R (O_2 and $O_2^{\bar{}}$) as calculated from the Nernst equation for a given potential, differs insignificantly from the actual ratio. In other words, the electron transfer reaction at the electrode is so rapid that equilibrium conditions are maintained even with a substantial net current and a rapidly changing potential. The criteria of reversibility for a freely diffusing solution species are $E_p = E_{pa} - E_{pc} = 57/n$ mV (Nicholson, R.S. and Shain, L. (1964)) which must be independent of scan rate and concentration. Furthermore, the $E_{\frac{1}{2}}$ is situated exactly (within 2/n mV) midway between E_{pa} and E_{pc}.

The reaction of oxygen is diffusion controlled. The citerion for diffusion control is that $i_{pc}/v^{\frac{1}{2}}$ must be a constant (v = sweep rate) (Matsuda, H. and Ayabe, Y. (1955).

Although reversible behaviour for oxygen reduction is observed at 100mV/s, the sweep rate for the reaction in fig. 11.2, the rate constants k_f and k_b in equation 1 are finite,

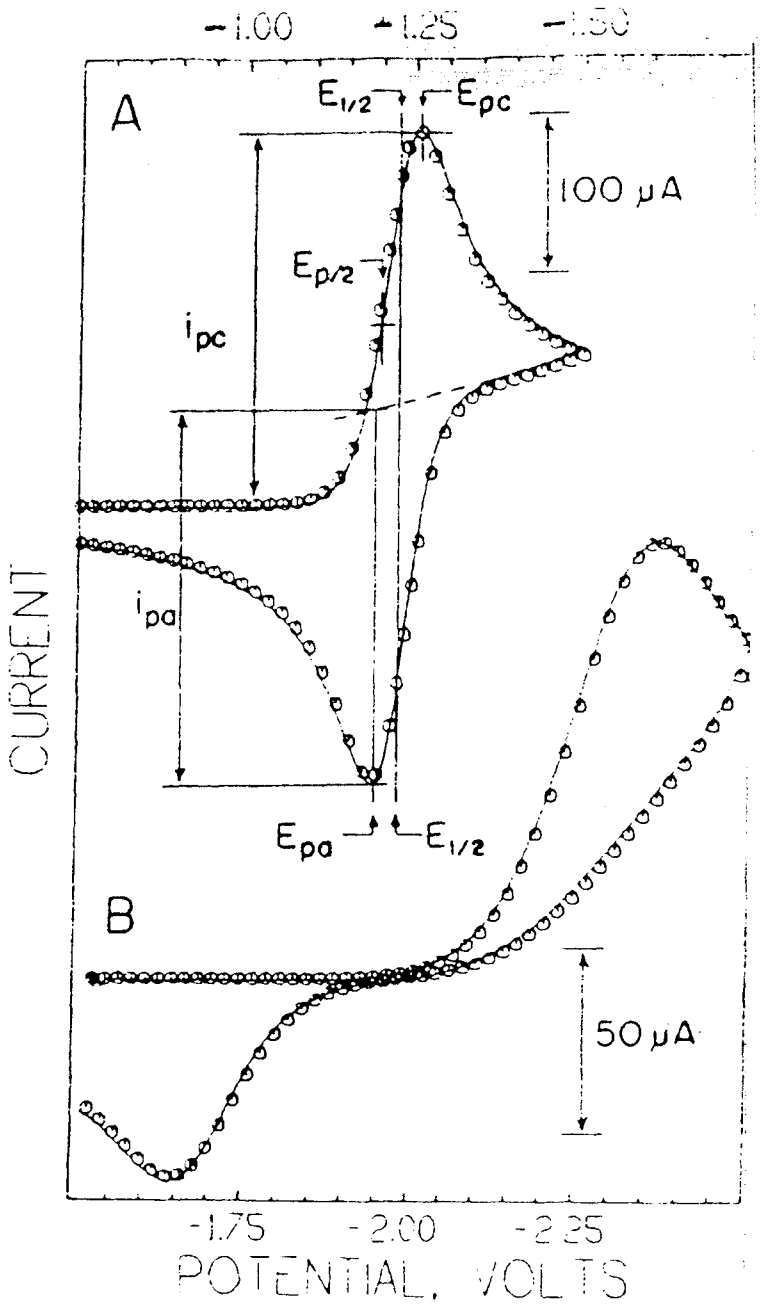

Fig 2. Cyclic voltammograms at a mercury electrode in acetonitrile.

Scan rate: 100mV/s, temperature: 20°C.

Reference electrode: Ag/0.01M $AgNO_3$/0.10M $(C_2H_5)_4NClO_4$ in acetonitrile.

A.cyclic voltammogram of oxygen. (Note, acetonitrile is used to stabilize the oxygen radical anion, the superoxide.)

B.cyclic voltammogram of the reaction of 2-nitropropane.

(Data adapted from Evans,D.H. et al.)

so a higher scan rate will exist, at which the electrode reaction will no longer be able to maintain equilibrium conditions as the potential changes. A reaction is said to be quasi-reversible if k_f and k_b are of the same order of magnitude over most of the potential range or totally reversible if $k_f >> k_b$ for the cathodic peak or $k_b >> k_f$ for the anodic peak.

An example of an irreversible reaction at 100mV/s is shown in Fig. 2(B) which represents the reduction of 2-nitropropane.

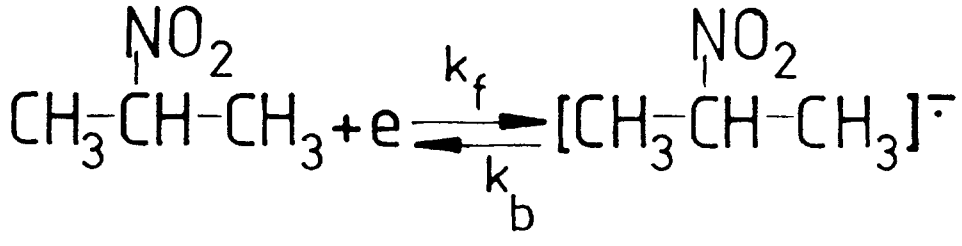

Irreversibility manifests itself through $E_p > 57/n$ mV, E_p increasing with increasing v (Nicholson, R.S. and Shain, I. (1965)).

Cyclic voltammograms from modified electrodes

Peaks are obtained from the oxidation/reduction reactions of surface immobilized species as a result of the interplay between an increase in the electrochemcial rate constant as the potential is swept and the decrease in the concentration of unreacted redox centres as the reaction proceeds. The maximum in the current is represented by the peak height. For redox centres that are anchored in a surface film the peak height is simply proportional to the sweep rate. (Note, not to $v^{\frac{1}{2}}$ as is the case for freely diffusing solution species). This is because the total amount of charge required to change the oxidation state of the layer is independent of

the sweep rate. Hence, a linear variation of peak height and sweep rate is diagnostic of the redox species being attached to the electrode. The area of the peak gives the total amount of charge and hence the number of redox centres. (Nicholson, R.S. and Shain, I. (1964)).

The simple picture assumes that the sweep rate is slow enough and the kinetics of charge transfer fast enough for complete oxidation or reduction in each sweep. If this is not the case and one has a fast sweep rate with slow kinetics, then the peak height will revert to its normal square root dependence on sweep rate. Information can also be obtained from the positions of the peaks on the electrode potential axis. For a simple one-electron redox process taking place in the coat with fast kinetics, then the positions of the anodic and cathodic peaks coincide. If the electrode kinetics are slow or if the sweep rate is too fast, then the positions of the peaks will separate. A series of theoretical papers by Laviron and co-workers has dealt at length with the exact shapes of CVs to be expected from different modified electrodes (Laviron, J. et al (1979, 1980, 1981)).

GLUCOSE OXIDASE

Glucose oxidase from Aspergillus niger is a flavo-protein of M.Wt. 186,000, which catalyses the oxidation of D-glucose to D-gluconolactone which in turn hydrolyses to gluconic acid. (The chemical basis of this reaction is the oxidation of a hemiacetal to a lactone). The reaction sequence is shown below.

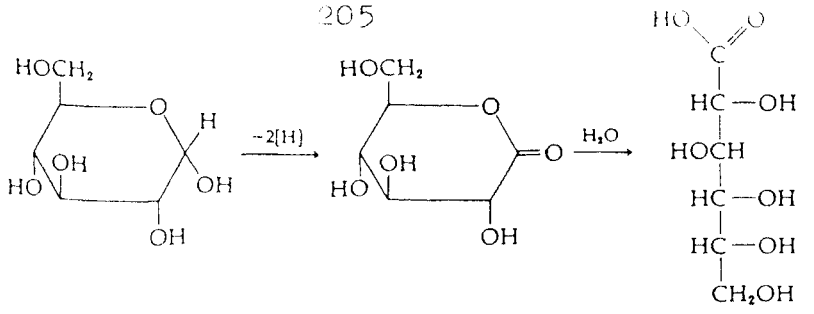

D-Glucose | Lactone of D-gluconic acid | D-Gluconic acid

The reaction of glucose oxidase can traditionally be considered as comprising two half reactions.

1) $E.FAD + D\text{-glucose} \longrightarrow E.FADH_2 + D\text{-gluconolactone}$.

The reductive half reaction.

2) $E.FADH_2 + A_{ox} \longrightarrow E.FAD + A_{red} + 2H^+$

The oxidative half reaction.

The specificity of the enzyme in the reductive half reaction is virtually absolute for D-glucose, whereas a wide range of acceptor molecules are active in the oxidative half reaction. These include the physiological acceptor O_2 as well as several organic, inorganic and organometallic oxidizing agents.

As indicated above, the active cofactor of glucose oxidase is flavine adenine dinucleotide (FAD).

The structure of the FAD moiety is shown below.

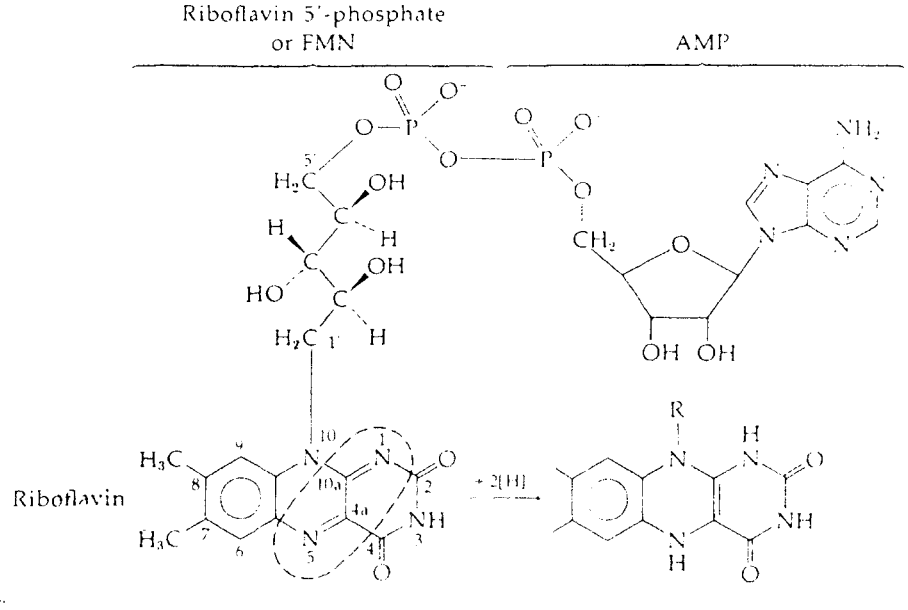

The redox active part of FAD is the isoalloxazine ring which is a two electron acceptor. (Flavin can also participate in one electron reactions).

The FAD cofactor is tightly, but not covalently, bound to the enzyme (Swoboda, B. (1968)) and cycles between reduced and oxidized states whilst attached to the same protein molecule. Furthermore, Swoboda also suggested that the FAD molecule functions to stabilize the structure of the active enzyme.

REFERENCES

A Text Book of Powder Metallurgy, (1967)
Bailey, A.R. ed.
St. Martins Press, N.Y.

Aizawa, M. et al. (1974) Anal. Chim. Acta. 69 p. 431

Albery, J. et al. (1981) J. Am. Chem. Soc. 103 p.3904

Amjad, M. et al. (1977) J. Electrochem. Soc. 124 p. 205

Armstrong, F.A. et al. (1982) FEBS Letters 145 p. 241

Bocarsly, A.B. and Sinna, S. (1982)
J. Electroanal. Chem. 137 p. 158

Bocarsly, A.B. and Sinna, S. (1982)
J. Electroanal. Chem. 140 p. 167

Bourdillon, C. et al. (1979) J. Am. Chem. Soc. 102 p. 4231

Bradford, M. (1976) Anal. Biochem. 72 p. 248

Briggs, G.E. and Haldane, J.B.S. (1925)
Biochem. J. 19 p. 338

Carr, P.W. and Bowers, L.D. (1980)
Immobilized Enzymes in Analytical and Chemical Analysis.
John Wiley and Sons.

Cass, A.G. et al. (1984) Anal. Chem. (in press)

Chibata, I. (1978) Immobilized Enzymes.
John Wiley and Sons.

Cho, Y.K. and Bailey, J.E. (1978) BIOTECHNOL BIOENG. 20 p1651.

Dams, R.A.J. et al. (1982) Inco Technical publication
P.BL. 420

Daum, P. and Murray, R.W. (1974)
J. Electroanal. Chem. 103 p. 286

Delaage, M. and Lazdunski, M. (1968)
Eur. J. Biochem. 4 p. 378

Dubois, J.E. et al. (1981) J. Electroanal. Chem. 117 p. 233

Duke, R.F. et al. (1969) J. Am. Chem. Soc. 91 p. 3904

Eaton, W.A. et al. (1967) J. Phys. Chem. 71 p. 2016

Eddowes, M.J. et al. (1979) J. Am. Chem. Soc. 101 p. 7113

Eddowes, M.J. and Hill, H.A.O. (1979)
J. Am. Chem. Soc. 101 p. 4461

Evans, D.H. et al. (1979) J. Chem. Education 60 p. 290

Fleischmann, M. et al. (1972) J. Chem. Soc. (Perkin Trans. II)
p. 139

Giles, R.D. (1982) Inco Technical publication
P.BL. 419

Goubeau, J. et al. (1954) J. Spectroscopy 58 p. 1078

Guilbault, G.G. and Lubrano; G.J. (1972)
Anal. Chim. Acta. 60 p. 254

Guilbault, G.G. and Montalvo, J.G. (1970)
J. Am. Chem. Soc. 92 p. 2533

Gutmann, G. et al. (1976) Inorg. Chim. Acta. 17 p. 81

Halling, P.J. and Dunnil, P. (1979)
Biotech. Bioeng. 21 p. 393

Heckle, W.A. (1961) Spectrochimica. Acta. 17 p. 600

Hill, R.E. (1964) Physical Metallurgy Principles
D. Van Nostrand Co. N.Y.

Hubaux, A. and Vos, G. (1970) Anal. Chem. 42 p. 849

Ianiello, R.M. and Yacynych, A.M. (1981)
Anal. Chem. 53 p. 2090

Itaya, K. et al. (1982) J. Electrochem. Soc. 222 p. 1498

Itaya, K. et al. (1978) J. Am. Chem. Soc. 104 p. 4761

Kay, G. and Crook, E.M. (1967) Nature 216 p. 514

Katchalski-Katzir, E. and Freeman, A. (1982) TIBS (dec) p. 427

Katchalski-Katzir, E. et al. (1971)
Adv. Enzymol. Relat. Areas. Mol.
Biol. 34 p. 445

Kaufmann, F.B. et al. (1979) J. Am. Chem. Soc. 102 p. 483

Klibanov, A.M. (1975) Anal. Biochem. 93 p. 1

Kuwana, T. et al. (1977) J. Electroanal. Chem. 84 p. 411

Kuwana, T. et al. (1979) J. Electroanal. Chem. 98 p. 345

Kula, M.R. (1979) Applied Biochemistry and Bioengineering. Wingard, L.B. Katchalski-katzir, E. and Goldstein, L. eds. Vol. 2 p. 71

Lancaster, J.E. (1954) J. Chem. Phys. 22 p. 1149

Laviron, E. et al. (1979) J. Electroanal. Chem. 100 p. 263

Laviron, E. et al. (1980) J. Electroanal. Chem. 112 p. 1

Laviron, E. et al. (1980) J. Electroanal. Chem. 115 p. 65

Laviron, E. et al. (1981) J. Electroanal. Chem. 122 p. 37

Matsuda, H. and Ayabe, V. (1955) Electrochem. 59 p. 494

Maugh, T.M. (1984) Science 223 p. 474

Munro, P.A. et al. (1977) Biotech. Bioeng. 14 p. 101

Mell, C.D. and Maloy, J.G. (1975) Anal. Chem. 47 p. 299

Mell, C.D. and Maloy, J.G. (1976) Anal. Chem. 48 p. 1597

Murray, R.W. (1980) Acc. Chem. Res. 13 p. 135

Murray, R.W. and Mosed, M. (1977) J. Electroanal. Chem. 71 p. 393

Nelson, J.M. and Griffin, G.E. (1916) J. Biochem. 39 p. 1109

Nicholson, R.S. and Shain, I. (1964) Anal. Chem. 36 p. 706

Nicholson, R.S. and Shain, I. (1965) Anal.Chem. 37 p. 1351

O'Sullivan, D. (1981) Chem. Eng. News 59 p. 37

Penderson, H.and Horvarth, C. (1981) Applied Biochemistry and Bioengineering. Wingard, L.B. Katchalski-Katzir, E. and Goldstein, L. eds. Vol. 3 p.1

Racine, P. and Mindt, W, (1971) Experentia. Suppl. 18 p. 525

Rigby, P.W.J. et al. (1974) Nature 251 p. 200

Ruckenstein, E. et al. (1982) Biotechnol. Bioen. 24 p. 2357

Shu, F.R. and Wilson, G.S. (1976) Anal. Chem. 48 p. 1679

Smolin, E.M. and Rapoport, L. (1959)
The Chemistry of Heterocyclic Compounds.
Interscience Pub. Inc.

Svanholm, U. and Parker, V.D. (1975)
J. Chem. Soc. Perkin Trans. II p. 75

Swoboda, B. (1968) Biochimica et Biophysica Acta.
175 p. 365

Tracey, V.A. (1965) Powder Metallurgy. Vol 8. p. 241

Updike, S.J. and Hicks, G.A. (1967) Nature 214 p. 986

Wieland, T. et al. (1950) Ann 572 p. 190

Winter, G. et al. (1982) Nature. 299 p. 756

Wrighton, J. et al (1978) J. Am. Chem. Soc. 100 p. 7264.